PALÆO VERTEBRATA

ARTICLE

A new caseid synapsid from the Permian (Guadalupian) of the Lodève basin (Occitanie, France)

Ralf WERNEBURG[a*], Frederik SPINDLER[b], Jocelyn FALCONNET[c], Jean-Sébastien STEYER[c], Monique VIANEY-LIAUD[d], Joerg W. SCHNEIDER[e]

[a]*Naturhistorisches Museum Schloss Bertholdsburg, Burgstr. 6, D-98553 Schleusingen, Germany*
[b]*Dinosaurier Museum Altmühltal, Dinopark 1, 85095 Denkendorf, Germany*
[c]*UMR 7207 CNRS-MNHN-SU-EPHE, Muséum national d'Histoire naturelle, CP 38, 8 rue Buffon, F-75005 Paris, France*
[d]*Institut des Sciences de l'Evolution (UMR 5554 CNRS), cc 064, Université de Montpellier, Place Eugène Bataillon, F-34905 Montpellier cedex 05, France*
[e]*Technical University Bergakademie Freiberg, Institute of Geology, Department of Palaeontology/Stratigraphy, Bernhard-von-Cotta street 2, D-09596 Freiberg, Germany*

**corresponding author: werneburg@museum-schleusingen.de*

Abstract: *Lalieudorhynchus gandi* gen. nov. and sp. nov. is a new caseid synapsid from the Permian of the Lodève Basin, Occitanie, France. This new taxon is represented by a partial but well-preserved postcranial skeleton, and is characterized by the following apomorphies: a transverse section of the sacral and anterior caudal neural spines with a very thin keel-like process anteriorly, a slender dorsal tip of the dorsal and caudal spines, a narrow distal end of the first sacral rib, a fossa on triceps process of metacoracoid, and a very large distal tarsal 1 of same width than the astragalus, with nearly all sides being shallowly concave. The skeleton corresponds to a sub-adult individual that was excavated from the La Lieude Formation dated as Roadian-Capitanian (Guadalupian). A sedimentological and taphonomical analysis of the type locality, together with preliminary osteohistological observations, suggest that this new French caseid was rather aquatic, as already hypothesised for other large forms. A phylogenetic analysis of caseids is performed to test the position of this new taxon and to better understand the evolution of the clade: interestingly, *Lalieudorhynchus gandi* gen. nov. et sp. nov. is closer to the North American "*Cotylorhynchus*" *hancocki* than to the other French caseids *Ruthenosaurus* and *Euromycter* from the Artinskian of the geographically closer Rodez Basin. These two last caseids document the Artinskian radiation of the clade, which remained diverse until Olson's extinction. Caseids survived, as *Lalieudorhynchus* is one of the youngest representatives of the clade, and may have used novel ecological strategies to access their vegetarian food sources.

Keywords: Caseidae, semi-aquatic lifestyle, Guadalupian, France

Submitted 3 February 2021, Accepted 8 April 2022
Published Online 18 July 2022, doi: 10.18563/pv.45.2.e2

INTRODUCTION

The Caseidae were among the first large herbivorous amniotes that have evolved on Pangea. These early synapsids are known from the Pennsylvanian of the USA (*Eocasea* Reisz and Fröbisch, 2014), then in the Permian of the paleo-equatorial belt, from the USA (e.g., *Casea* Willison, 1910) to Russia (e.g., *Ennatosaurus* Efremov, 1956). While the first caseids were small to moderate in size (e.g., Reisz and Fröbisch, 2014; Williston, 1911), later forms acquired a very peculiar body shape, with enormous, barrel-shaped trunks, comparatively tiny triangular skulls with large nares and leaf-like teeth, and massive limbs ending in short digits and powerful unguals (e.g., Romer and Price, 1940; Olson, 1962, 1968). Recently, numerous discoveries (e.g., Berman *et al.*, 2020) and redescriptions (e.g., Reisz *et al.*, 2011) allowed a better understanding of their paleobiodiversity and paleobiology (e.g., Lambertz *et al.*, 2016), but their precise phylogenetic relationships remain discussed since the first analysis of Maddin *et al.* (2008).

Here, we describe the new caseid *Lalieudorhynchus gandi* gen. et sp. nov. from the Permian of France (Lodève Basin), which allows to investigate the evolutionary history of the clade and to reconstruct the living environment of this animal, in the Guadalupian of the Lodève Basin, Occitanie, France.

The first finds (a 60 cm long rib, femora, a vertebra, and bone fragments) of this skeleton were discovered on a private property and in a protected area by one of us (JWS) and Frank Körner in 2001, during geological field mapping in the Lodève Basin. These first fossils have been prepared at the NHMS (Germany) but were returned to France to be legally included in the UM collections, and following the International Research Convention of the Lodève and Saint-Affrique basins (Gand *et al.*, 2000). In parallel, French-German (2004, 2006, 2008) and French (2007, 2009) excavation campaigns have been organized by Georges Gand (UB) and us (JWS, RW, JSS and MVL), with the required field authorizations (see section "Acknowledgements"), to officialise the first discoveries and to find more: in total, about 50 specimens (Tab. 1) have been unearthed, and their taphonomical, sedimentological and stratigraphical context studied in details. Nearly all bones belong to a single large caseid skeleton, with the exception of a small tupilakosaurid vertebral column (Fig. 4H; Werneburg *et al.*, 2007) and few indeterminate enigmatic bones (compare Fig. 17).

The new large caseid skeleton from the Lodève Basin is here described in detail and compared with its Permian relatives, such as *Euromycter rutenus* (Sigogneau-Russell and Russell, 1974) Reisz *et al.*, 2011, and *Ruthenosaurus russellorum* Reisz *et al.*, 2011 from France (Sigogneau-Russell and Russell, 1974; Reisz *et al.*, 2011; JF and JSS pers. obs.), *Martensius bromackerensis* Berman *et al.*, 2020 from Germany (Berman *et al.*, 2020; FS pers. obs.), *Ennatosaurus tecton* Efremov, 1956 from Russia (e.g., Efremov, 1956; Ivakhnenko, 1990; Maddin *et al.*, 2008; Romano *et al.*, 2017a/b; RW pers. obs.), *Alierasaurus ronchii* Romano and Nicosia, 2014 from Italy (Ronchi *et al.*, 2011, Romano and Nicosia, 2014; Romano *et al.*, 2017a), and *Caseopsis*, *Angelosaurus* spp., and *Cotylorhynchus* spp. from the USA (e.g., Stovall *et al.*, 1966; Olson and Beerbower, 1953; Olson, 1962, 1968; Olson and Barghusen, 1962; Romano and Nicosia, 2015; RW + FS pers. obs.). This comparative work also includes recent revisions of formerly enigmatic caseasaurians, such as *Datheosaurus macrourus* Schroeder, 1904 from Poland, *Callibrachion gaudryi* Boule and Glangeaud, 1893 from France (Spindler *et al.*, 2016), and *Phreatophasma aenigmaticum* Efremov, 1954 from Russia (Brocklehurst and Fröbisch, 2017).

GEOLOGICAL SETTING AND AGE

The Lodève Basin belongs to a chain of late Palaeozoic continental basins in southern France, including, from north to south: the Rodez Basin (e.g. Rolando *et al.*, 1988), the Saint-Affrique Basin (e.g. Châteaneuf and Farjanel, 1989; Hübner *et al.*, 2011) and the Lodève Basin. It is situated at the southeastern edge of the Massif Central and east of the Montagne Noire (Fig. 1). The present-day outcrops of the basin cover an area of approximately 150 km^2 (Fig. 1A). The basin was formed as a half-graben structure on the deeply eroded, metamorphosed, folded and faulted remnants of the Variscan orogen, i.e., on metamorphosed Precambrian and Cambrian rocks (Conrad and Odin, 1984; Faure *et al.*, 2009). Its sedimentary fill comprises 1,400 m (not exposed) of Late Pennsylvanian (Stephanian) and about 2,500 m to 3,000 m (well-exposed) of Permian sedimentary rocks (Odin, 1986; Gand *et al.*, 2000; Körner, 2006; Schneider *et al.*, 2006; Lopez *et al.*, 2008). Above an angular unconformity, representing a long erosional hiatus, Middle Triassic Anisian continental clastics were deposited (Lopez, 1992; Bourquin *et al.*, 2011).

The Permian part of the stratigraphic succession of the basin is subdivided into five (e.g., Odin *et al.*, 1987; Lopez *et al.*, 2005, 2008) to six formations (Schneider *et al.*, 2006): sedimentation started during the Asselian (Fig. 1B) with fluviatile clastics and lacustrine black shales of the Usclas–Saint-Privat (160 m thick) and Tuilières–Loiras (350 m thick) formations. In the transition from the upper Tuilières–Loiras Formation to the lower part of the Viala Formation (250 m thick), the facies changes from grey and mainly lacustrine deposits to fluvial-dominated wet red beds. Above a tectonically-induced erosional unconformity ("Saalian movements", Schneider *et al.*, 1995), the Rabejac Formation (280 m thick) starts with fanglomeratic fan deposits at the base, followed by alluvial wet red beds. The alluvial sandstones that dominate the topmost part of the Rabejac Formation exhibit a progressive transition into siltstone-dominated dry playa red beds of the Octon Member (c. 1,150 m thick) of the overlying Salagou Formation. With a sudden increase of coarse silty to fine sandy cm- to dm-thick calcareous strata interbedded in homogeneous vertic siltstones, follows the Mérifons Member (about 625 m thick) of the Salagou Formation (altogether c. 1,750 m thick). Up to decameter-thick conglomerate and pebbly sandstone interbeds at the base of the overlying La Lieude Formation (about 175 m thick, top eroded) herald a drastic facies change from dry playa red beds to the alluvial wet red beds of this unit.

Successive studies have produced increasing temporal resolution for the Permian deposits of the Lodève Basin. First, Doubinger *et al.* (1987) used palynomorphs to date the Usclas–Saint-Privat Formation in the "Late Autunian" (or "Middle-Late Autunian" according to Doubinger and Heyler, 1959), the Tuilières–Loiras Formation in the "Saxonian" and the remaining younger (Viala, Rabejac, Salagou, and La Lieude) formations in the "Thuringian". Based on macroflora, Galtier and Broutin (2008) proposed a late Artinskian-Kungurian age for the Rabejac Formation. Yet more precised biostratigraphic subdivisions started with pioneering investigations of the tetrapod tracks in the Saint-Affrique and Lodève basins by Gand (1986, 1987, 1989, 1993), Gand and Haubold (1984), and Gand *et al.* (2000). Based on a multistratigraphic approach using tetrapod tracks and skeletons (but see e.g. Steyer, 2000 and Werneburg *et al.*, 2020 for a discussion), insect remains, radioisotopic ages of the Viala Formation and the Octon Member of the Salagou Formation, and magnetostratigraphy at the transition between the Salagou Formation and the La Lieude Formation, as well as climate stratigraphy, Körner *et al.* (2003) and Schneider *et al.* (2006: fig. 9) proposed an Asselian-Sakmarian age for the Usclas–Saint-Privat and Viala formations, a late Artinskian age for the Rabejac Formation, a Kungurian-early Wuchiapingian age for the Salagou Formation, and an early Wuchiapingian-middle Changhsingian age for the La Lieude Formation.

The main argument for the placement of the base of the La Lieude Formation within the early Wuchiapingian (Lopingian) was the sudden change from the dry playa red beds of the Salagou Formation to the fluvial wet red beds of the La Lieude Formation. Using a climate-stratigraphy approach, this was correlated with the Zechstein and Bellerophon transgressions in Europe and consequently with facies changes from dry evaporitic red beds in the mega-playa system of the

Figure 1. Location and stratigraphy of the study area and of the type locality of *Lalieudorhynchus gandi* gen. nov. et sp. nov. **(A)** Geology of the southeastern edge of the Massif Central (see inset for the position in France) with the Carboniferous-Permian basins of Rodez, Saint-Affrique, Lodève, and Gabian-Neffiès (from Hübner et al., 2011, modified). **(B)** Stratigraphy of the Lodève Basin correlated with the Standard Global Chronostratigraphic Scale; red stars indicate the isotopic ages of Michel et al. (2015a) (from Schneider et al., 2019, modified). **(C)** Google Earth map 7/10/2018 of the study area; point 1 – outcrop of the c. 13 m thick basal conglomerate of the La Lieude Formation, forming a NE-SW slope edge in the Valos Bas area; point 2 – outcrop of decimetre- to meter-thick coarse basal clastics of the La Lieude Formation; point 3 – cliffs of meter-thick pebbly sandstone-channel deposits of the lower La Lieude Formation (see Fig. 3B); 4 – dashed black line indicate section 2 of the La Lieude Formation of c. 130 m thickness measured mainly by loose blocks and rare outcrops in the Valos Bas area; 5 – continuation of section 2, c. 48 m thick profile of the upper La Lieude Formation measured at the excavation site at the Salagou creek (see Fig. 2B); points 6 to 7 – 101.5 m thick section 1 of the La Lieude Formation measured from its base at point 6 to the top at point 7 (see Fig. 2A). The INPG track site located near La Lieude corresponds to the "*Dalle permienne à empreintes de reptiles de La Lieude*" ("La Lieude Reptiles footprints-bearing Permian slab", JF transl.). This remarkable site has been recorded in 2014 in the "*Inventaire National du Patrimoine Géologique*" ("Geological Heritage National Inventory", JF transl.).

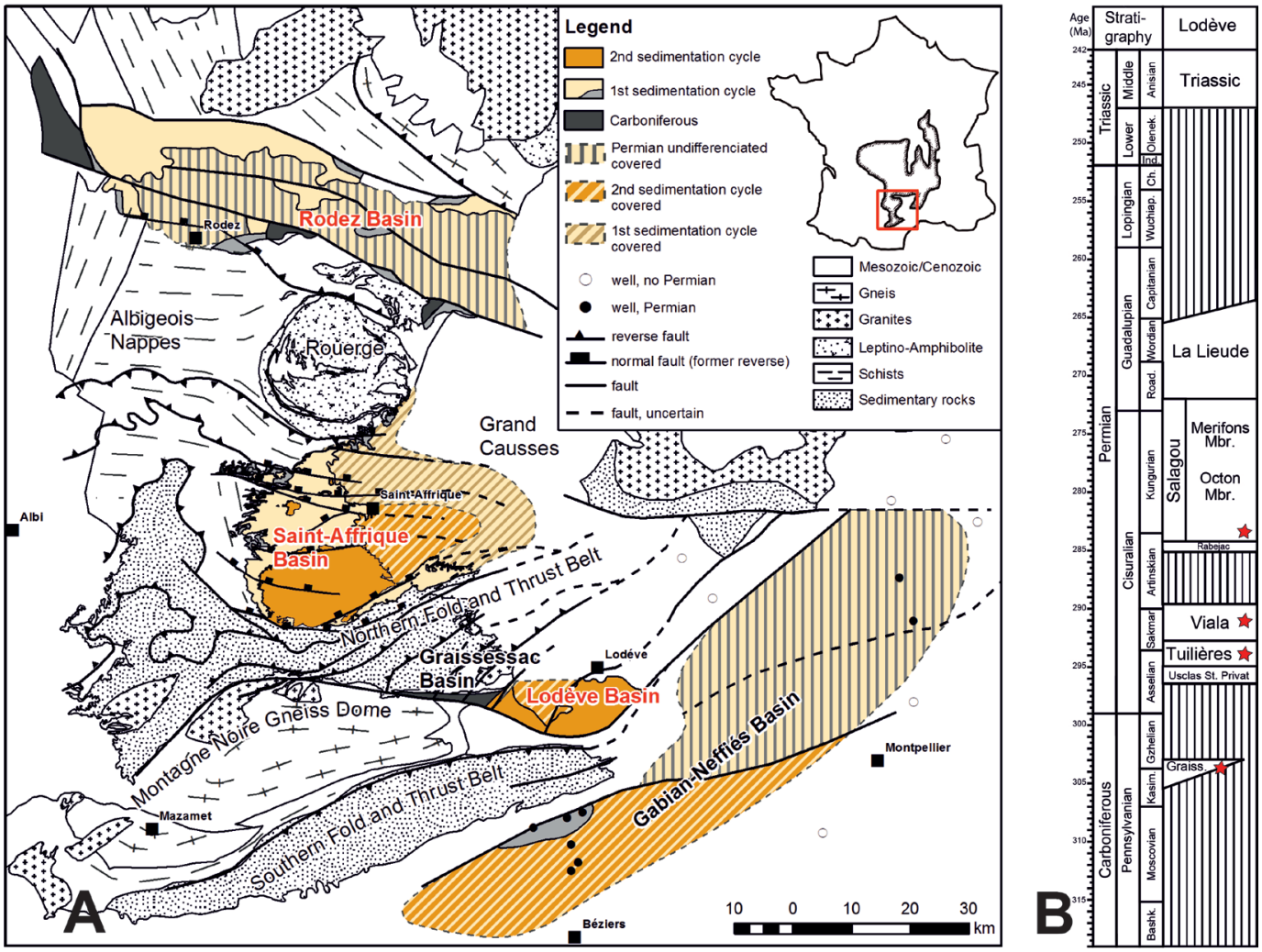
Legend
2nd sedimentation cycle
1st sedimentation cycle
Carboniferous
Permian undifferenciated covered
2nd sedimentation cycle covered
1st sedimentation cycle covered
well, no Permian
well, Permian
reverse fault
normal fault (former reverse)
fault
fault, uncertain
Mesozoic/Cenozoic
Gneis
Granites
Leptino-Amphibolite
Schists
Sedimentary rocks
Rodez Basin
Rodez
Albigeois Nappes
Rouergue
Grand Causses
Saint-Affrique
Saint-Affrique Basin
Albi
Northern Fold and Thrust Belt
Graissessac Basin
Lodève
Lodève Basin
Montagne Noire Gneiss Dome
Montpellier
Gabian-Neffiés Basin
Mazamet
Southern Fold and Thrust Belt
Béziers
10 0 10 20 30 km
A
Age (Ma)
Strati-graphy
Lodève
Triassic
Middle
Lower
Anisian
Olenek.
Ind.
Ch.
Lopingian
Guadalupian
Wuchiap.
Capitanian
Wordian
Road.
Permian
Cisuralian
Kungurian
Artinskian
Sakmar.
Asselian
Carboniferous
Pennsylvanian
Gzhelian
Kasim.
Moscovian
Bashk.
La Lieude
Salagou
Merifons Mbr.
Octon Mbr.
Rabejac
Viala
Tuilières
Usclas St. Privat
Graiss.
B

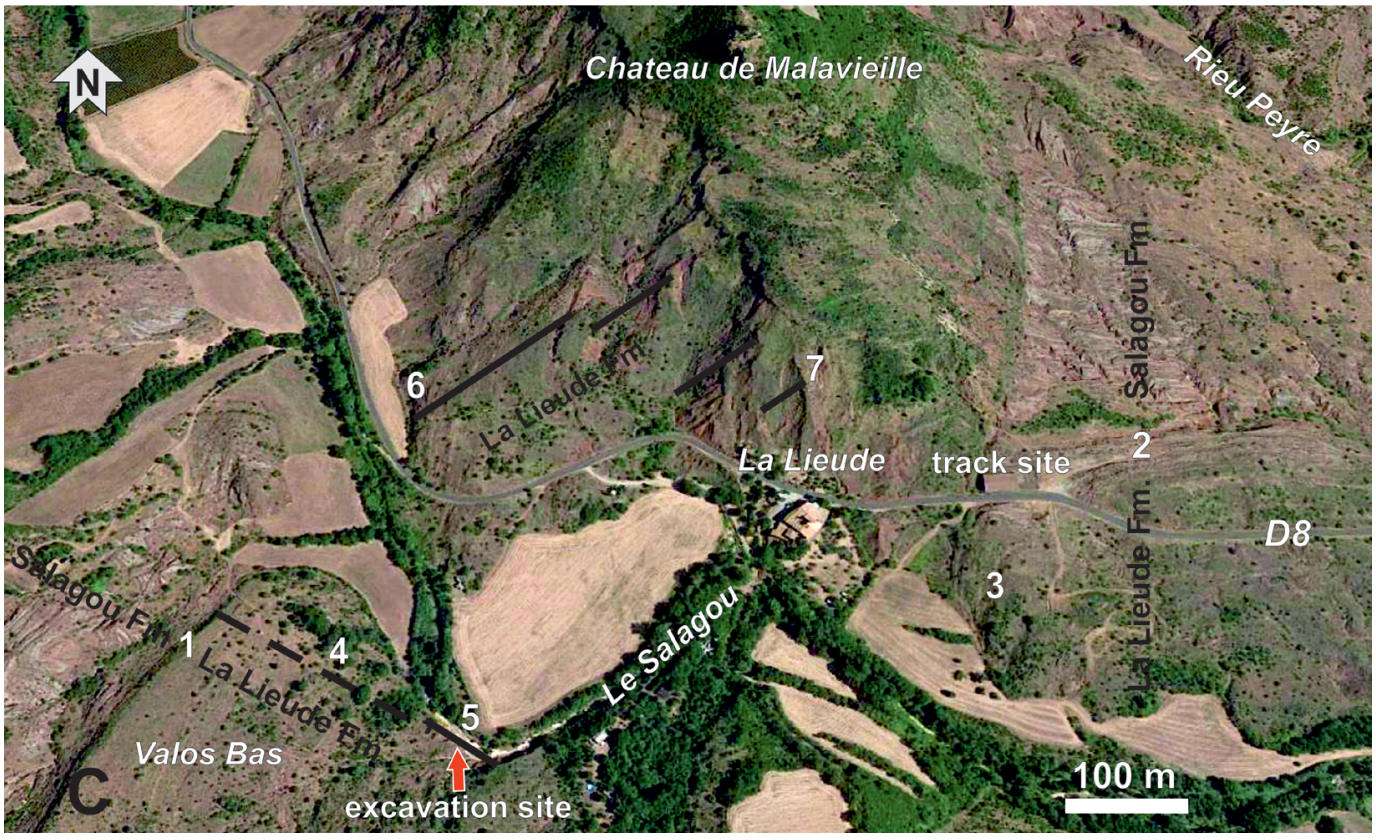
N
Chateau de Malavieille
Rieu Peyre
Salagou Fm.
La Lieude Fm.
6
7
La Lieude track site
2
D8
3
Salagou Fm.
1
La Lieude Fm.
4
Le Salagou
5
Valos Bas
excavation site
100 m
C

Southern Permian Basin to wet red beds in the coastal areas of the Zechstein and Bellerophon seas (Schneider *et al.*, 2006, Roscher and Schneider, 2006). Meanwhile, several new data for the depositional age of the Permian units of the Lodève Basin were produced, especially the high precision CA-ID-TIMS U-Pb zircon ages by Michel *et al.* (2015a, b). Together with biostratigraphic information, especially from tetrapod tracks, the correlation to the Standard Global Chronostratigraphic Scale (SGCS) seems now relatively well constrained (Fig. 1B; Schneider *et al.*, 2020: p. 25).

Nevertheless, because of the scarcity of chronostratigraphic information on the La Lieude Formation, the age of the tetrapod-skeleton-bearing unit must be deduced from that of the underlying Salagou Formation, too. Pyroclastic horizons (tuff no. 1, 2, 9, and 12) in the lower three-fourths of the Octon Member of the Salagou Formation (Fig. 1B) provide an age between 284.40 ± 0.13 Ma and 282.86 ± 0.13 Ma (Michel *et al.*, 2015a, Fig. 7), i.e., latest Artinskian to earliest Kungurian based on the International Chronostratigraphic Chart 2019-05, which is close to the age discussed in Schneider *et al.* (2006). Michel *et al.* (2015a) calculated a duration of sedimentation of 4 My for the whole Salagou Formation but assumed in a conservative approach a duration of about 13.5 My for this formation (ibid, Fig. 2). Consequently, the base of the overlying La Lieude Formation should be situated at roughly 272 Ma, inside the Roadian. Unfortunately, only tuff no. 5 was petrographically investigated by thin sections, indicating that it is most likely a primary ash fall (Schneider *et al.* 2006: fig. 5). Therefore, it remains an open issue if the close age range between the dated tuff beds may be caused by reworked ash falls. Recently, Pfeifer *et al.* (2020), dealing with the depositional environment of the Salagou Formation, question these calculations: they propose a mainly eolian origin for the dominant siltstones of the Salagou Formation. This may change the sedimentation rates and the inferred age of the Salagou Formation.

The minimal age of the La Lieude Formation could be estimated by magnetostratigraphy. Geomagnetic data on the Viala, Rabejac, and Salagou formations obtained during the last decades have indeed been recently compiled and completed by new data on the Octon Member (Haldan *et al.*, 2009) and the La Lieude Formation (Evans, 2012; Evans *et al.*, 2014). From the Viala Formation up into the Octon Member of the Salagou Formation, only reversed polarity was found, indicating deposition during the Permo-Carboniferous Reversed Superchron (PCRS), or Kiaman Superchron (Haldan *et al.*, 2009). The magnetostratigraphy of the La Lieude Formation is a bit more complex: previous reports indeed put the La Lieude Formation either above, below, or included in the Illawarra Reversal (Schiller, 2002; Körner *et al.*, 2003; Legler *et al.*, 2004). The Illawarra Reversal is a global geomagnetic event dated radioisotopically at 266.66 ± 0.76 Ma, i.e. middle Wordian (Hounslow and Balabanov, 2018). In recent studies, the majority of the samples collected in the lower La Lieude Formation exhibit reversed polarity too (Evans, 2012; Evans *et al.*, 2014). In other words, the lower La Lieude Formation would be no younger than the mid-Wordian Illawarra Reversal. However, a sample collected at mid-height of the La Lieude Formation studied section has yielded tentative evidence for normal polarity, therefore indicating the possible proximity of the Illawarra Reversal (Evans, 2012). In this case, the higher La Lieude Formation would have deposited in the Wordian-N (Evans *et al.*, 2014), which may be the GU1n, and the beginning of the succeeding reversed chron GU1r of Hounslow and Balabanov (2018). A minimal latest Wordian–early Capitanian age may therefore be estimated for the upper La Lieude Formation.

The tetrapod ichnofauna of the basal La Lieude Formation includes *Brontopus* and was assigned to Association IV by Gand *et al.* (2000) and Gand and Durand (2006), suggesting a Guadalupian age (Schneider *et al.*, 2019: fig. 2). This is in agreement with the other *Brontopus* occurrences (e.g. Footprint Assemblage 1 of the South African Abrahamskraal Formation, see Marchetti *et al.*, 2019) which are also Guadalupian. This is also in agreement with the skeletal fossil record, which shows that the supposed producers of *Brontopus*, the dinocephalian therapsids, are exclusively Guadalupian and disappear during the end-Guadalupian extinction (e.g., Day *et al.*, 2015; see Fig. 19). Based on radioisotopic ages obtained in the South African Karoo Basin, dinocephalians became extinct shortly after a level dated as 260.259 ± 0.081 Ma, i.e. in the late Capitanian (Day *et al.*, 2015).

The new caseid skeleton described here has been found c. 140 m above the base of the La Lieude Formation: it may have a Guadalupian age based on the biostratigraphic range of other caseids, up to the Roadian/Wordian transition (e.g., Sennikov and Golubev, 2017; Lucas, 2018a; Schneider *et al.*, 2020: fig. 10).

One point remains open. The base of the La Lieude Formation, which is characterised by a strong climatically driven facies change, has so far no known similar and correlative climatic event in the early Guadalupian of other European and North African basins. This could correspond to an important stratigraphic transition, possibly matching a tetrapod turnover between the Cisuralian and the Guadalupian during the Olson's gap (e.g., Lucas, 2018a; Lucas and Golubev, 2019; Schneider *et al.*, 2020).

The Rodez Basin, in the neighbourhood of the Lodève Basin, yielded two caseid taxa from the Permian Grès Rouge Group: *Euromycter*, found near the top of the M1 megasequence, and *Ruthenosaurus*, discovered 120 m higher, in the upper part of the M2 megasequence (Sigogneau-Russell and Russell, 1974; Reisz *et al.*, 2011, JSS pers. obs.). The FII Formation of the underlying Salabru Group has provided "Autunian" palynomorphs and conchostracans (Vetter, 1968; Doubinger, 1974), as well as a tetrapod footprint assemblage that could be correlated with that of the Viala Formation of the Lodève Basin (Gand, 1987; Châteauneuf and Gand, 1989), whose upper part has been dated from the earliest Artinskian (Michel *et al.*, 2015). Compared to the Saint-Affrique and Lodève basins, unfortunately, the Grès Rouge Group of Rodez has only produced scarce, poorly preserved plants and ichnites besides these caseids, which render them delicate to date based on biostratigraphy alone (Reisz *et al.*, 2011). Magnetostratigraphic data indicate that the whole Grès Rouge Group exhibited a reverse polarity (Diego-Orozco *et al.*, 2002), which may suggest a correlation with the PCRS. In this case, the Grès Rouge Group would be no younger than the Illawarra Reversal, which is middle Wordian (Hounslow and Balabanov, 2018). A late Artinskian to early Wordian age may thus be estimated for the entire Grès Rouge Group from these data. Based on Bourges *et al.* (1987), Rolando *et al.* (1988), Hübner *et al.* (2011) and personal observations (JWS), these M1 and M2 megasequences are equivalents of the Combret Member of the Saint-Pierre Formation of the Saint-Affrique Basin and of the Rabejac Formation of the Lodève Basin (Fig. 1B). Based on the radioisotopic age of the Octon Member (see above), the underlying Rabejac Formation and the correlative the M1 and M2 megasequences of the Grès Rouge Group may be of latest

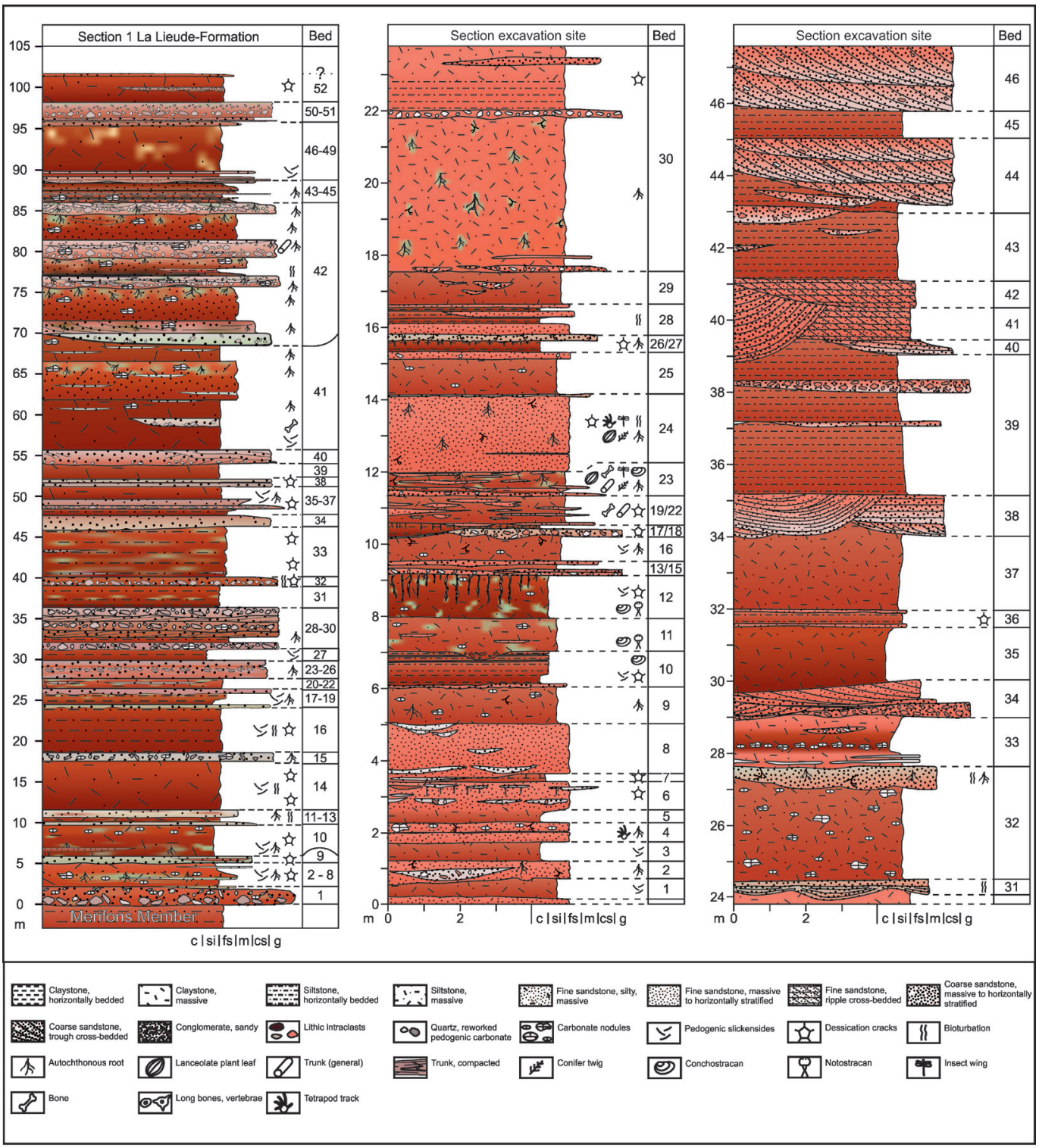

Figure 2. Lithology and fossil content of the La Lieude Formation and of the type locality of *Lalieudorhynchus gandi* gen. nov. et sp. nov. **(A)** Section 1 at the southern slope of the Château de Malavieille hill (between points 6 and 7 in Fig. 1C) of 101.5 m thickness; best exposed profile of the formation at the type locality. **(B)** Section in the excavation area at the Salagou creek (point 5 in Fig. 1C); because of missing marker beds, this section is not directly correlated to section 1 though regarded as the upper continuation of it. Colours refer approximately to the rock colours in the outcrops.

Artinskian age: this is compatible with the stratigraphic data mentioned above. Finally, in Italy, the alluvial plain deposits of the Cala del Vino Formation (Sardinia) yielded the huge caseid *Alierasaurus*. Based on Ronchi *et al.* (2011), Romano *et al.* (2018), and personal observations (JWS), this Cala del Vino Formation resembles the wet red beds of the La Lieude Formation and may also be of Roadian to earliest Capitanian age, as discussed above. The occurrence of the tetrapod track *Merifontichnus* in both the basal La Lieude Formation and the Cala del Vino Formation (Citton *et al.*, 2019) supports this assumption.

SEDIMENTOLOGY AND TAPHONOMY

The following informations are presented here to better understand the taphonomy and paleoecology of the new caseid from the La Lieude Member (e.g., Odin *et al.*, 1987; Lopez *et al.*, 2005, 2008) or La Lieude Formation (Schneider *et al.*, 2006; and this paper).

Sedimentology of the La Lieude Formation. Two hundred-seventy metres east of the farmhouse La Lieude at the flank of the valley of the creek Rieu Peyre, directly north of the road D 8 (Fig. 1C, point 2), the upper part of the M**é**rifons Member of the Salagou Formation and the basal conglomerates of the La Lieude Formation are well exposed. Here, the basal conglomerate starts with decimetre- to meter-thick coarse clastic beds interfingering with M**é**rifons Member-type siltstones and mudstones (Körner *et al.*, 2006). In this part of the section, the famous tetrapod tracksite in a pond deposit of the La Lieude Formation is situated about 170 m east of La Lieude farmhouse (Gand *et al.*, 2000). Located under a shelter, along the road D8, this site is officially known as the "*Dalle permienne à empreintes de reptiles de La Lieude*" (Fig. 1C, INPG tracksite). In the area immediately south to the road D8 at the shelter, above the basal conglomerates approximately meter-thick, large-scale, low-angle, trough bedded, pebbly sandstone-channel deposits are exposed in isolated cliffs (Fig. 1C, point 3; Fig. 3B). The transition to the southwest, towards the caseid remains-bearing section at the Salagou creek (Fig. 1C, point 5), is unfortunately covered by Holocene deposits. However, northwest to north of the La Lieude farmhouse, uphill to the ruins of the Ch**â**teau de Malavieille, the completely exposed section 1 of the La Lieude Formation, starting from its base, was measured with dm-resolution over a thickness of 101.5 m (Fig. 1C, points 6 to 7; Fig. 2A). Section 2 of c. 130 m thickness was measured perpendicular to the strike from the boundary between the Salagou and La Lieude formations in the area of Valos Bas in the west, up to the excavation site at the Salagou creek in the east, but with a lower resolution due to poor exposures, soil, and vegetation cover (Fig. 1C, points 1, 4, 5). Both sections differ in the thickness of the basal conglomerate, which is about 2 m in section 1 in the north (Fig.1C, point 6; Fig. 2A) and 13 m in section 2 in the south (Fig. 1C, point 1). Generally, the reddish-brown basal conglomerate is matrix- to clast-supported and indistinctly stratified at dm-scale (Figs. 2A, 3C). Matrix content varies between 20-80%. The majority (70%) of clasts in section 2 are angular-subrounded, dark grey and brownish-reddish limestone and dolostone pebbles (6-25 cm diameter), with subordinate components (15%) of subrounded-rounded quartzite and metamorphic quartz pebbles (2 cm diameter). In places, rip-up sediment clasts (up to 15%, up to 15 cm diameter) are sourced from the underlying M**é**rifons Member of the Salagou Formation. The pebble size in the northern section is generally lower and decreases in both sections upward to between 5 cm and 2 cm. The units that overlie the conglomerate (>170 m) consist of irregular, dm-to-6-meter-thick interbeds of red-brown, partially clayey or fine sandy siltstones and silty claystones intercalated with 1-2 m-thick (in average), fine- to coarse-grained, partially pebbly channel sandstones (Figs. 2A, B; 3A). In places, 1-3.5-m-thick, poorly sorted, matrix-supported conglomerates with 1-2 cm pebble-sized clasts are present.

Facies pattern and depositional environment of the La Lieude Formation. The basal conglomerate, especially in the southern Valos Bas section (section 2; Fig. 1C, point 4), has denser, larger, and more immature clasts with a higher proportion of Cambrian limestone composition (Fig. 3C) compared to conglomerates higher in the section. Indistinct internal bedding caused by changing matrix-content is characteristic. The clast content is likely derived from the Montagne Noire in the west (Fig. 1A; Körner, 2006; Pfeifer *et al.*, 2016), so the coarse clastics are interpreted as distal fan deposits in a braided river system distal to the La Tour-sur-Orb coarse clastic fan deposits at the border of the Montagne Noire (Körner, 2006; and pers. comm. Körner, 2020). The thickness of the basal conglomerate decreases from 13 m to 2 m, parallel to the strike, over a distance of 250 m from the southern Valos Bas area (section 2; Fig. 1C, point 1) to the northern Ch**â**teau de Malavieille exposures (section 1; Fig. 1C, point 6). East of La Lieude (Fig. 1C, point 2) in the direction of sediment transport in a distance of ~700 m from the base of section 1, the basal conglomerate is reduced to only dm-to-m-thick beds, and is interbedded with M**é**rifons-type sediments. This implies that the southern area (section 2) belongs to the main channel system, and the northern area (section 1) to side channels at the start of the deposition of the La Lieude Formation. Up section, the conglomerates are mostly matrix-supported with subrounded extraclasts of 2 cm average diameter only and have a higher maturity (mainly quartz). Sandy to silty matrix content is usually very high, with a mean of 70% to 80%. In the highest exposed part of the La Lieude Formation, the section of the Salagou creek at the excavation site (Fig. 1C, point 5; Fig. 2B), 20 cm to 30 cm thick and laterally several meters to decametres traceable fanglomeratic beds are typical (Figs. 3F, 4A, 5D-F). The clast content is dominated by mm- to cm-sized reworked pedogenic carbonate nodules and cm-sized siltstone and claystone intraclasts; quartz extraclasts have only mm-sizes. All these features point together with the bad organisation of the channel sediments to braid plain deposits as well as to debris flows generated by sporadic heavy rainfalls. Root traces (Fig. 4B), rhizoconcretions, and greenish leaching patches indicate a pedogenic overprint.

The fine clastics in the section 1 (c. 50% of the whole thickness; Fig. 2A) are mainly poorly sorted sandy or clayey siltstones. Because of the facies architecture, i.e. the interbedding with coarser clastic channel deposits, they are interpreted as fluvial overbank deposits. Common features are different types of paleosols. Through the whole section, a general overprint by vertisol and calcic-vertisol formation is observed, indicated by destruction of primary horizonation by shrink-swell pedoturbation, blocky fracturing, randomly-oriented slickensides (Fig. 3G), cm- to several dm-deep desiccation cracks (Fig. 3E), common root traces (Fig. 4B), calcitic rhizoconcretions, and pedogenic carbonate nodules of mm- to cm-size (Schneider *et al.*, 2006; Körner, 2006). Michel *et al.* (2015a) classified the latter as stage II through stage IV pedogenic carbonate accumulations after Machette (1985). Additionally, and in contrast to the dry playa red beds of the Salagou Formation, invertebrate burrows of the *Scoyenia*-ichnofacies (Buatois and Mángano, 1995) are commonly observed.

In conclusion, these features fit well with the wet red beds as characterised by Schneider *et al.* (2010, 2015). Wet red beds are indicative of a subhumid to semiarid climate with seasonal wet and dry conditions, causing the vertisol formation. Additionally, evaporation is higher than precipitation, allowing the formation of calcic soils. These conditions were present

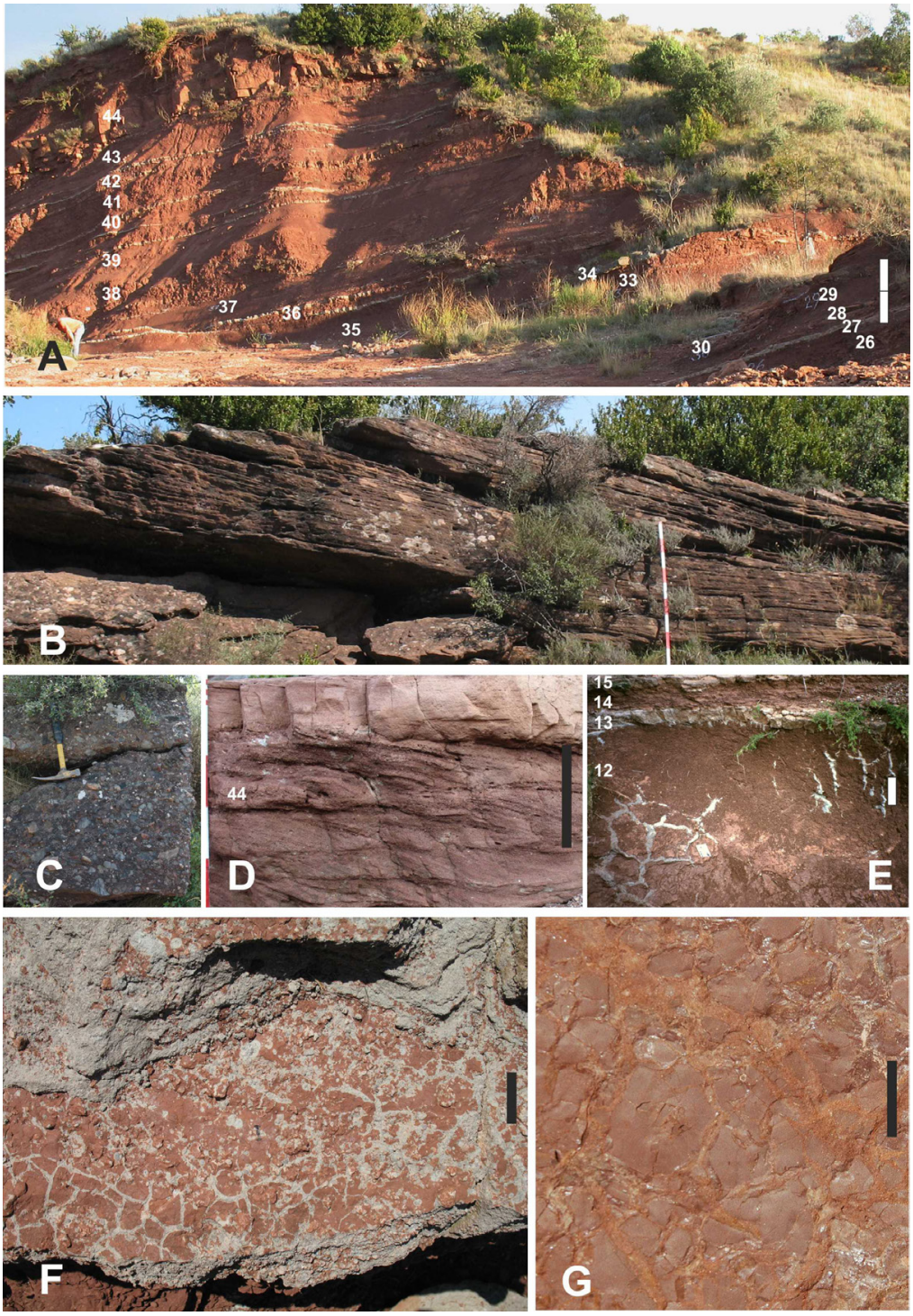

Figure 3. Sedimentology of the La Lieude Formation and of the type locality of *Lalieudorhynchus gandi* gen. nov. et sp. nov. **(A)** Beds above the bone bearing horizon (bed numbers refer to the excavation site section, see Fig. 2B); the section is dominated by pedogenic overprinted braid plain siltstones with intercalated pebbly debris flows (e.g. bed 27) and sandy, partially pebbly minor channels (e.g. beds 34, 38, 40, 42); the top of the section (beds 44 - 46) is formed by stacked pebbly channel sandstones of a c. 4.5 m thick major channel system; scale bar is 4 m. **(B)** Part of the large-scale low-angle trough bedded pebbly sandstone channels above the basal conglomerate of the La Lieude Formation, south of road D8 at the "*Dalle permienne à empreintes de reptiles de La Lieude*" (Fig. 1C, point3); scale bar is 90 cm. **(C)** Coarse fanglomeratic basal conglomerate of the La Lieude Formation in the Valos Bas area (Fig.1C, point 1); clast content consist of angular-subrounded, dark grey and brownish-reddish limestone and dolostone pebbles (6-25 cm diameter), with subordinate components (15%) of subrounded-rounded quartzite and metamorphic quartz pebbles (2 cm diameter); hammer for scale is 30 cm. **(D)** Part of the up to 5 m thick stacked fluvial channel deposits of bed 44 in (A), trough cross-bedded medium- to coarse-grained, and, in places, pebbly sandstone; pebbles are mainly intraclasts (reworked carbonate nodules and siltstone) and partially quartz; scale bar is 20 cm. **(E)** Desiccation cracks (up to 90 cm deep) in pedogenic (vertic) overbank siltstones of bed 12 c. 2 m below the bone-bearing bed 23 in Fig. 2B; bed 13 is a sandy-pebbly debris flow (mainly intraclasts); bed 15 is a medium- to coarse grained, indistinctly planar to horizontal bedded medium to coarse sandstone with single horizontal to sub-vertical *Scoyenia*-like burrows (0.5 cm diameter); scale bar is 20 cm. **(F)** Typical debris flow of pebbly medium to coarse grained sandstone with mainly reworked pedogenic carbonate clasts; desiccation cracks on bedding planes indicate multistoried deposition; scale bar is 5 cm. **(G)** Typical claystone bed in the top of debris flows with desiccation cracks and vertisol overprint causing the blocky fracturing (bed 23/7 in Fig. 2B); scale bar is 1 cm.

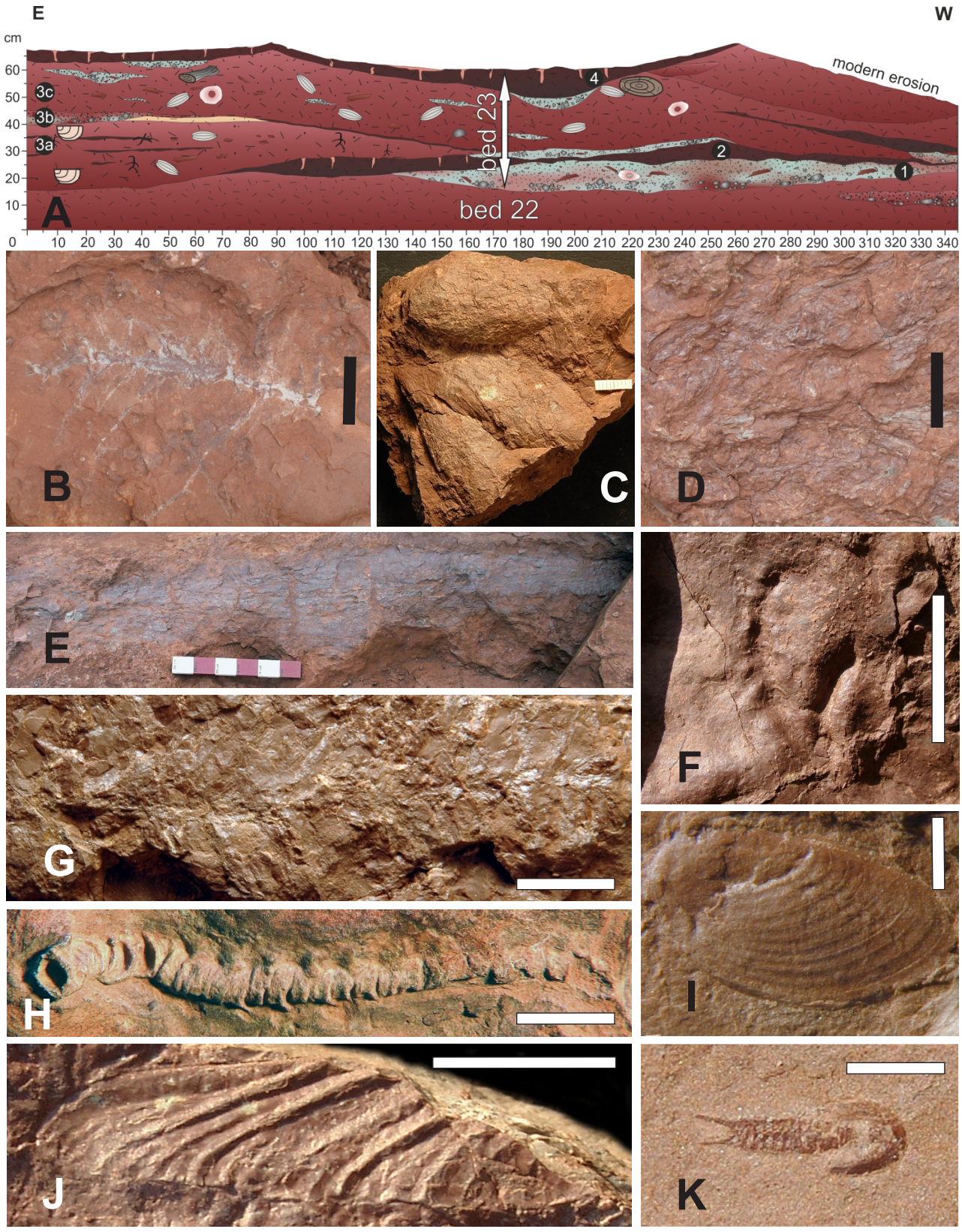

Figure 4. Fossil content of the La Lieude Formation and of the type locality of *Lalieudorhynchus gandi* gen. nov. et sp. nov. **(A)** Detail of bed 23 (see Fig. 2B) with the bone bearing stacked distal debris flow horizons 23/1 to 23/3c; for legend, see Fig. 2. **(B)** Branched root from bed 24, typical for the rooting in silty beds; scale bar is 2cm. **(C)** Aggregation of ovoid to lanceolate leaves of most likely *Plagiozamites*, common in bed 23; FG 691/1 scale bar is 1 cm. **(D)** Plant detritus of cm- to dm-size in silty parts of the debris flow bed 23; scale bar is 5 cm. **(E)** Part of a minimally 1.50 m long and 0.25 m wide (compressed) tree trunk in bed 23; scale bar is 30 cm. **(F)** *Dromopus* tetrapod track from bed 24; scale bar is 2 cm. **(G)** Indeterminable plant leaf from bed 23; scale bar is 1 cm. **(H)** Tupilakosaurid temnospondyl vertebral column (from Werneburg et al., 2007: fig. 2) from bed 22; UM-LIE 01; scale bar is 1 cm. **(I)** Lioestheriid conchostracan, occurring in beds 23 and 24; FG 691/2 scale bar is 1 mm; **(J)** Fragment of an odonatan insect wing from bed 24; scale bar is 1cm. **(K)** Juvenile triopsid from a puddle deposit at base of bed 11; FG 691/3; scale bar is 1 mm.

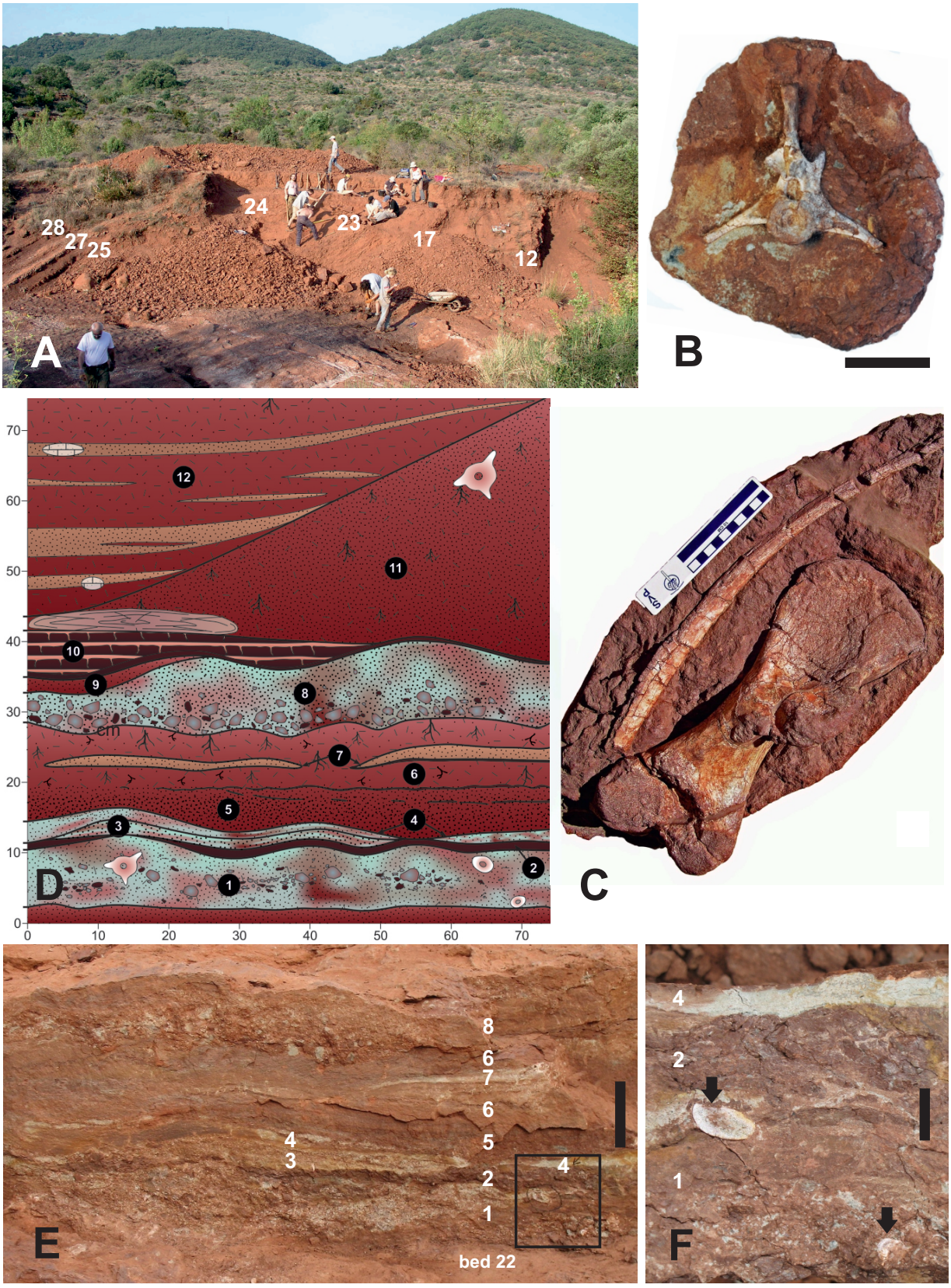

Figure 5. Type locality of *Lalieudorhynchus gandi* gen. nov. et sp. nov. south of the Salagou creek (see Fig. 1C, point 5) with details of the bone-bearing bed 23 and skeletal remains as an example. **(A)** Excavation site in 2006, bed numbers refer to Fig. 2B; **(B)** First sacral vertebra with its ribs, UM-LIE 15, found in bed 23/11 in (D); scale bar is 10 cm; **(C)** Left femur and mid-dorsal rib, UM-LIE 05 and UM-LIE 06, from bed 23; scale bar is 10 cm. **(D)** Lithology and fossil content of the stacked distal debris flow unit bed 23; most of the bones come from bed 23/1, and single only from 23/11; the single coarser distal debris flows as bed 23/1 and 23/8 are covered by pure claystones settled down from suspension load in standing water bodies (beds 23/2, 23/9); rooting in the silty distal debris flow beds indicate that some time may have elapsed between each debris flow event; for legend, see Fig. 2. **(E)** Photo of the top of bed 22 and beds 23/1 to 23/8 shown in (D); scale bar is 10 cm. **(F)** Close up of the frame in (E) with two bone fragments; scale bar is 2 cm.

in the paleo-equatorial belt during the later Cisuralian and the Guadalupian in the biome 2 of Ziegler (1990), when the Lodève Basin was situated at about 10° North and influenced by a monsoonal climate (Körner *et al.*, 2003, 2006).

As pointed out by Schneider *et al.* (2006) based on sedimentology and geochemistry and supported by Michel *et al.* (2015a) by paleosol investigations (but see also Pochat and Van Den Driessche, 2011, 2015, and reply by Michel *et al.*, 2015b), the change from the dry (partially evaporitic) playa red beds of the Salagou Formation to the wet alluvial plain red beds of the La Lieude Formation marks a rapid climatic change to higher precipitation rates. The up-to-13-m-thick basal fanglomerates of the La Lieude Formation are interpreted as the result of the mobilisation and transport into the basin of accumulated debris already generated in the time of the Salagou Formation at the Montagne Noire paleo-elevation. They share the same provenance as the wind-blown detritus of the Salagou Formation (Pfeifer *et al.*, 2016, 2020). This basal low maturity debris of angular to subrounded and up to dm-size clasts originated from physical weathering under the dry semiarid to arid climate of the Salagou Formation (Körner, 2006; Michel *et al.*, 2015a) and were transported from the La Tour-sur-Orb area in the west (about 10 km from La Lieude) by the higher transport capacity of braided rivers caused by increased precipitations at the start of deposition of the La Lieude Formation.

Facies pattern and taphonomy of the type locality. The excavation site of the caseid is situated southwest of La Lieude, on the southern bank of the Salagou creek (GPS coordinates available by asking to JSS) about 120 m to 140 m above the base of the La Lieude Formation (Fig. 1C, point 5). A direct correlation with the well exposed section 1 (Fig.1C, points 6-7) at the Château de Malavieille is not possible because of missing correlative marker beds. Yet an approximate correlation is given here based on the thickness of both sections: in this regard, the excavation site section (Fig. 2B) may represent the upper continuation of section 1 (Fig. 2A).

As mentioned above, most of section 2 in the Valos Bas area is badly exposed. Directly at the excavation site, the upper parts of the La Lieude Formation in this area are well exposed (deeping 30°, 140° SE) and were measured with cm- to dm-resolution over a thickness of c. 48 m (Fig. 2B). Generally, the facies pattern compares to the somewhat monotonous alluvial plain deposits of interbeds of coarser channels with pedogenically overprinted siltstones as described above for section 1 (Fig. 2A). In more detail, beds 1 to 39 of section 2 (Fig. 2B) with a thickness of c. 39 m represent a long-lasting deposition of mainly silty overbank deposits of a braid plain. Characteristic are rooted calcic-vertisols (e.g., beds 4, 9, 11-12, 16, 24-26, 32-33). Intercalated are small, approximately 10-20 cm thick and 1-3 m wide sandy channels (e.g., in beds 2, 6, 8, 11, 17, 19-22, 29, 31, 33) and dm-thick debris flow deposits (e.g., beds 13, 17, 23, inside 30, base 34, inside 39). The channel fill consists mainly of a medium- to coarse-grained, and, in places, pebbly sandstone. Pebbles are mainly intraclasts of red claystone and/or siltstone of up to cm-size as well as mm-sized pedogenic carbonate nodules; in addition, quartz and metamorphite extraclasts of only mm-size may occur. The debris flows contain in an unsorted sandy matrix mostly reworked carbonate nodules and/or clay- and siltstone intraclasts, and, in places, extraclasts (Fig. 3F, 4A, 5D-F) as described above for the channel fills. Because of the 20° SE-dip, deep excavations up to 3.5 m in section 2 have focused on beds 17 to 24 (Fig. 5A). Beds 20 to 23 contain the tetrapod remains. They form a distinct sequence of c. 1.4 m thickness. Most of the bones come from debris flow horizons (Fig. 4A, beds 23/1 to 23/3; Fig. 5D-F, beds 23/1 to 23/8), and some from mudflows (e.g. bed 23/11 in Fig. 5D). The debris flows are irregularly wavy bedded, in places with or without an erosive base (Figs. 4A, 5D, E). The bones are buried parallel as well as inclined to the bedding planes depending on the cohesivity of the sediment flows. These debris flows also contain common plant axes of cm- to dm- diameter (Fig. 4E) as well as, in places, very common lanceolate, somewhat curled up plant leaves of 5 to 11 cm length (Fig. 4C) which are of ?noeggerathialean, most likely *Plagiozamites* affinity (pers. comm. DiMichele and Galtier, 2020). Less common are *Podozamites*-like coniferophyte remains (pers. comm. DiMichele and Galtier, 2020) as well as *Supaia*-like fragments. The coarse debris are covered by red-brown pure claystones of 1 -7 cm thicknesses that follows the irregular relief of the debris flows and somewhat compensates for it in places (Fig. 4A, bed 23/2 and 4; Fig. 5D-F, beds 23/2 and 19). The beds in between the coarse debris flows consist of small-scale irregular interbeds of only cm-thick medium- to coarse grained silty sandstone, with mm- to cm-sized intra- and extraclasts (see above), as well as intercalated mm-thick claystone layers (Fig.4A; Fig. 5D-F). The sandy beds are finely rooted (root-diameter 1 mm).

In total, an area of about 68 m^2 has been excavated during each of the up-to-10-day campaigns from 2004 to 2009 (e.g. Fig. 5A). But, the highest concentration of bones was found in an area of only 18 m^2 in a nearly west-east extension. To the south of this area, the bone-containing coarser beds pinch out or are eroded by a roughly west-east oriented younger channel. The same is observed to the north, but not so clearly because of modern erosion of the SE-deeping Permian beds. Rare tree trunks of up to 2 m in length and 0.15-0.20 m in width (Fig. 4E), as well as smaller plant axes in bed 23, also show this west-east orientation.

Taphonomic conclusions. Altogether, the sequence of beds 20 to 23 is interpreted as stacked debris flow deposits of different intensities and grain sizes from pebbly sandy flows to siltier mud flows. Rooting between the flows indicates that this was not a single depositional event (Fig. 4A, bed 23/3a; Fig. 5D, bed 23/7). Instead, we assume that these flows represent different seasons in a seasonally dry/wet, subhumid to semiarid climate. Claystone beds of 0.5-10 cm thickness and common desiccation cracks on the top of the debris flows of bed 23 indicate depositions from suspended loads in temporary standing water bodies of puddles and pools (Figs. 4A, 5D-F). Because of strong pedogenic slickensides, no fossils were preserved in these claystone beds (Fig. 3G). Mudflows above these claystones (e.g. Fig. 4A, bed 23/3a, b) contain, besides claystone rip-off clasts, plant remains (Figs. 4C, F) and conchostracans (Fig. 4I) - the latters lived in standing water bodies and were incorporated in these mudflows by reworking.

As inferred from their irregular lateral and vertical distributions in the section, the bones were reworked and redeposited several times. Because of the lack of distinct rounding-off traces, the transport distance was yet relatively short. The skeleton remains were not exposed for several years to the strong seasonal climate, which would have caused the brecciating of the bones. In fact, no bone chips have been found. On the contrary, especially the well-preserved, unfractured 0.60 m long ribs (Figs. 10C1 and D) indicate that collagen was still present, in agreement with fast burial (Behrensmeyer, 1978),

as also observed on the other caseid remains from the Italian Cala del Vino Formation (Ronchi *et al.*, 2011; Romano *et al.*, 2018). Scavenging traces such as bite marks on the bones were not found. Nevertheless, scavenging could not be completely excluded, as the isolated ilium (Fig. 12) may indicate.

Based on the La Lieude tetrapod ichnoassociation, large (several metres long) synapsids were the probable producers of the ichnotaxon *Brontopus*, including *Planipes* with which it was synonymized (footprint length up to 0.40 m) (Gand *et al.*, 2000; Marchetti *et al.*, 2019). These synapsids may have been dinocephalian therapsids, or even large caseids (Gand, 1987; Gand *et al.*, 2000; Gand and Durand, 2006; Marchetti *et al.*, 2019). The latter group may fit with our bodyfossil discoveries. Recently, the detailed revision of *Brontopus* has nevertheless confirmed that dinocephalian likely produced the two ichnospecies known in La Lieude (Marchetti *et al.*, 2019). In contrast, the comparative anatomy of various synapsids indicates that the shape and anatomy of large caseids (represented by *Cotylorhynchus romeri*) make them a much better fit for *Dimetropus osageorum* (Sacchi *et al.*, 2014; Romano *et al.*, 2016). At the excavation site, indistinct tetrapod tracks were found (Fig. 4F): they are unfortunately indeterminable (pers. comm. Marchetti, 2020).

Based on their size-range, the caseid bones belong most probably to a single individual. Their sporadic distribution in the 1.4 m thick sequence of beds 19 to 23 of different lithologies with a concentration in a roughly 40 cm thick part of bed 23, requires an explanation: we proposed that the dead animal decayed in a vegetated area (bones are associated with common terrestrial plant remains), alternatively sub-aquatically because of common claystone intraclasts in the bone-bearing debris flows. The co-occurrence of the caseid bones with a vertebral column of an aquatic tupilakosaurid temnospondyl (Fig. 4H) may support this hypothesis (Werneburg *et al.*, 2007).

The supposed semi-aquatic and possibly hippopotamid-like lifestyle of largest caseids (Lambertz *et al.*, 2016) requires a minimum water depth of about 1 m. In the entire section of the La Lieude Formation are different potential aquatic habitats, e.g. the 0.15-1.80 cm thick, partially silty claystone beds in the excavation site section (Fig. 2B, beds 3, 5, 7, lower 10, inside 18, 26, inside 28, basal 33, 35). Those beds originate from suspension-sedimentation in standing water bodies after stronger flood events. Aquatic arthropods adapted to temporary standing waters, such as conchostracans and triopsids (Figs. 4I, K), were also found in some of these beds, but rarely due to strong pedoturbation. Another potential habitat could have been larger river channels that occur in the La Lieude Formation with thicknesses up to 3.5 m of conglomerate and/or up to 5 m of stacked sandstone fills (Figs. 2A, B). However, multistoried fills and rooting indicate that they might not have been year-around filled with flowing water in the seasonal climate of the La Lieude Formation. But standing water bodies may have exist in abandoned channels as well as in floodplain lakes and ponds also during the dry season to enable the survival of the aquatic temnospondyl tupilakosaurid. Common rooting of the sediments and in places common macro-plant remains (Figs. 4C, D, G), among them up to 0.20 m width compressed tree trunks (Fig. 4E), are evidence of food-sources of this new large herbivorous caseid. The frequent leaves of ?*Plagiozamites* (Fig. 4C), and the co-occurrence with (rare) *Podozamites*-like coniferophyte remains as well as *Supaia*-like fragments are interpreted in synthesis with sedimentological evidence as a flora adapted to a seasonally dry climate. Submersed water plants are not preserved at La Lieude, as it is mostly the case in Permian localities. Yet non-calcareous macroalgae, even rarely well preserved, have been described from several late Pennsylvanian and Permian basins (e.g. Steyer *et al.* 2000; Krings *et al.*, 2007; Barthel, 2009). In contrast, the calcareous characean algae could be common in many late Paleozoic temporary lakes and ponds (e.g. Gebhardt and Schneider, 1985; Lucas, 2018b).

MATERIAL AND METHODS

The about 50 caseid bones were collected in 2001, and 2004 up to 2008. Their preparation was carried out mechanically by Georg Sommer (NHMS) and Suzanne Jiquel (UM). The specimens are housed in the paleontological collections of the Université de Montpellier, in the collection UM-LIE; some casts are stored in the NHMS and FG (see Table 1). A thin section of the thoracic rib (Fig. 10H) has been realized at the FG, it is in the collection UM-LIE 03b. Photographs of this thin section were made at FG with a digital microscope KEYENCE VX-5000 under cross-polarized light.

Institutional Abbreviations. **AMNH**, American Museum of Natural History, New York, USA; **CNRS**, Centre National de la Recherche Scientifique, France; **FG**, Technical University Bergakademie Freiberg, Saxony, Germany; **MNHN**, Muséum national d'Histoire naturelle, Paris, France; **NHMS**, Naturhistorisches Museum Schloss Bertholdsburg, Schleusingen, Thuringia, Germany; **OMNH**, Oklahoma Museum of Natural History, Norman, Oklahoma, USA; **UB**, Université de Bourgogne, Dijon, France; **UM**, Université de Montpellier, Hérault, France.

SYSTEMATIC PALEONTOLOGY

SYNAPSIDA Osborn, 1903

CASEASAURIA Williston, 1912

CASEIDAE Williston, 1911

***Lalieudorhynchus gandi* gen. nov. et sp. nov.**

Figures 5B-C, 6-13, 16B, D

Holotype. A disarticulated and partial postcranial skeleton consisting of the bones UM-LIE 02-37, UM-LIE 39-41, UM-LIE 45 and UM-LIE 47 (see Table 1) and belonging to a single individual (see below).

Etymology. The genus name is a combination of La Lieude, located close to the type locality, and the New Latin 'rhynchus', from the Greek 'rhynchos' ('nose'), sometimes used for caseids. The species name honours Georges Gand (UB) who has been working on the Lodève Basin for decades, including the La Lieude INPG track site, and co-organized and promoted our excavation campaigns.

Type horizon and age. Beds 20–23, La Lieude Formation, c. 140 m above the base; Roadian/Wordian to early Capitanian, Guadalupian, Permian.

Type locality. Southwest of the La Lieude farmhouse, at the southern bank of the Salagou creek (GPS coordinates available by asking to JSS), approximately 15 km south of Lodève, Hérault, Occitanie, France (Fig. 1).

Table 1. List of the excavated bones from La Lieude and surroundings (Holotype material in bold. The specimens with cast stored in NHMS & FG have an X).

Number	Anatomy	Taxonomy	Cast	Reference	Figure	Remarks
UM-LIE 01	vertebral column	Tupilakosauridae indet.	X	Werneburg et al., 2007 this paper	2, 3A 4H	
UM-LIE 02	posterior dorsal rib	*Lalieudorhynchus gandi*	X	this paper	10C	l = 60 cm
UM-LIE 03	short part of large rib	*L. gandi*	X	this paper		l = 30 cm
UM-LIE 04	right femur	*L. gandi*	X	this paper	13B, D	
UM-LIE 05	left femur	*L. gandi*	X	this paper	5C, 13A, C	on a block with UM-LIE 06
UM-LIE 06	mid-dorsal rib	*L. gandi*	X	this paper	5C	on a block with UM-LIE 05
UM-LIE 07	3rd sacral vertebra	*L. gandi*	X	this paper	8B	
UM-LIE 08	2nd caudal rib	*L. gandi*	X	this paper	10G	
UM-LIE 09	21th rib with robust head	*L. gandi*		this paper	10D	
UM-LIE 10	proximal caudal vertebra	*L. gandi*		this paper		
UM-LIE 11a	partial haemapophysis	*L. gandi*		this paper		
UM-LIE 11b	partial haemapophysis	*L. gandi*		this paper		
UM-LIE 12	astragalus	*L. gandi*		this paper	14A	
UM-LIE 13	partial phalanx	*L. gandi*		this paper		
UM-LIE 14	partial non-ungual phalanx	*L. gandi*		this paper	15D	
UM-LIE 15	1st sacral vertebra + ribs	*L. gandi*	X	this paper	5B, 8A	
UM-LIE 16	partial neural arch	*L. gandi*	X	this paper	7A	
UM-LIE 17a	~18th vertebra, centrum	*L. gandi*	X	this paper	7B	correspond to UM-LIE 17b
UM-LIE 17b	~18th vertebra, neural arch	*L. gandi*	X	this paper	7B	correspond to UM-LIE 17a
UM-LIE 18	4-5th caudal vertebra with left rib	*L. gandi*	X	this paper	8E	
UM-LIE 19	1st caudal vertebra with left rib	*L. gandi*	X	this paper	8D	
UM-LIE 20	~17th caudal vertebra	*L. gandi*	X	this paper	9A	
UM-LIE 21	30th – 35th caudal vertebra	*L. gandi*	X	this paper	9C	
UM-LIE 22	caudal praezygapophysis	*L. gandi*	X	this paper		
UM-LIE 23	head of anterior dorsal rib	*L. gandi*	X	this paper	9B	
UM-LIE 24	head of rib	*L. gandi*	X	this paper	10A	
UM-LIE 25	head of anterior dorsal rib	*L. gandi*	X	this paper		
UM-LIE 26	head of mid-dorsal rib	*L. gandi*		this paper		
UM-LIE 27	rib	*L. gandi*	X	this paper		l = 30 cm
UM-LIE 28	~22nd dorsal rib	*L. gandi*	X	this paper	10E	l = 21 cm
UM-LIE 29	rib	*L. gandi*	X	this paper		l = 20 cm
UM-LIE 30	rib	*L. gandi*	X	this paper		
UM-LIE 31	non-ungual phalanx	*L. gandi*	X	this paper	15C	
UM-LIE 32	middle phalanx (ph1.1)	*L. gandi*	X	this paper	15B, E, 16D	
UM-LIE 33	first metatarsal (mt 1)	*L. gandi*	X	this paper	15A, 16B	
UM-LIE 34	large tarsal (?t 1)	*L. gandi*	X	this paper	14, 15E	
UM-LIE 35	small tarsal remain	*L. gandi*	X	this paper		
UM-LIE 36	probable left ilium	*L. gandi*	X	this paper	12	
UM-LIE 37	right scapulocoracoid	*L. gandi*	X	this paper	11	50 cm in height
UM-LIE 38	?epipterygoid or ?hyoid or …?	?Caseidae	X	this paper	17	
UM-LIE 39	small rib head	*L. gandi*		this paper		
UM-LIE 40	large rib head	*L. gandi*		this paper		
UM-LIE 41	neural arch portion	*L. gandi*		this paper		
UM-LIE 42	small, flat bone in sediment	?Caseidae		this paper		
UM-LIE 43	rib fragment	Tetrapoda		this paper		Château de Malavieille hill
UM-LIE 44	bone pebble	?Caseidae		this paper		
UM-LIE 45	~25th dorsal rib	*L. gandi*		this paper	10F	
UM-LIE 46	indeterminate flat bone	?Caseidae		this paper		
UM-LIE 47	proximal half of a mid-dorsal rib	*L. gandi*		this paper	10B	
UM-LIE 48	indeterminate flat bone	?Caseidae		this paper		
UM-LIE 49	indeterminate flat bone	?Caseidae		this paper		
UM-LIE 50	indeterminate flat bone	?Caseidae		this paper		

Diagnosis. A caseid synapsid that can be distinguished from all other known members of this family by the following unique features:

1) Transverse section of the neural spines of sacral and anterior caudal vertebrae with abrupt narrowed anterior outline partly caused by a very thin keel-like process starting above the prezygapophyses and running upwards along the entire vertical edge to the top of the neural spine.
2) Dorsal tip of dorsal and caudal spines slender (instead of showing lateral thickening).
3) First sacral rib narrow in its distal end (lacking a strong widening).
4) Fossa on triceps process of metacoracoid.
5) Very large distal tarsal 1 of same width as that of the astragalus, with nearly all sides being shallowly concave.

The new caseid is characterized by the combination of the following features, which differ from certain caseids:

6) Neural spine straightly erected, in contrast to *Ruthenosaurus,* but shared with other caseids.
7) Long mid-caudal centra, elongated below their postzygapophyses, but with low neural arches, in contrast to *Alierasaurus*.
8) Three sacral and most anterior caudal centra short and transversely very broad, shared with *Ruthenosaurus*, but in contrast to *Cotylorhynchus romeri.*
9) Neural spine of the first sacral and first caudal vertebrae greatly elongated dorsally, in contrast to *Cotylorhynchus romeri* and *Ruthenosaurus*, but shared with "*Cotylorhynchus" hancocki.*
10) Supraglenoid foramen present, opening laterally in supraglenoid fossa and medially in dorsal portion of the subscapular fossa, shared with "*Cotylorhynchus" hancocki* .
11) Scapular blade with a wide shaft, much wider than that in *Alierasaurus* (pers. inf. Romano, 2016).
12) Process-like bulged anteromedian margin of the scapula, in contrast to *Cotylorhynchus romeri* and *Alierasaurus,* but shared with "*Cotylorhynchus" hancocki*, "*C." bransoni*, and *Angelosaurus romeri.*
13) Two parts of the glenoid fossa with an angle of about 130°, shared only with "*Cotylorhynchus" bransoni*.
14) Femur with posterior condyle much more distal than the anterior one, in contrast to *Ruthenosaurus*.
15) Popliteal area of the femur relatively wide with robust furrows, in contrast to *Cotylorhynchus romeri*.
16) Proximal head of the femur very massive in dorsoventral view, in contrast to *Cotylorhynchus romeri*.
17) Femur with large pronounced internal trochanter and little fourth trochanter in its distal half, in contrast to *Cotylorhynchus romeri*, *Angelosaurus dolani*, *Casea broilii* and *Ruthenosaurus,* but shared with "*Cotylorhynchus" hancocki*, *A. romeri* and *A. greeni.*
18) Very wide intercondylar fossa of the femur; therefore with narrow posterodorsal condyle, in contrast to *Cotylorhynchus romeri* and *Ruthenosaurus*.
19) Astragalus nearly as broad as long, in contrast to most other caseids, but shared with "*Cotylorhynchus" hancocki.*
20) Robust and enlarged metatarsal I, shared only with *Alierasaurus*.

(Further morphometric and discrete autapomorphic characters are given below).

Comparative description.

The holotypic skeleton is composed of about 50 well-preserved but disarticulated bones (Fig. 6): nearly 10 vertebrae and 15 ribs posterior to the cervical region (Figs. 7-10), the large (h c. 50 cm) and complete right scapulocoracoid (Fig. 11), the dorsal branch of the left ilium (Fig. 12), both femora (Fig. 13) and bones of the pes (Figs. 14-16). The total body length of *Lalieudorhynchus gandi* gen. nov. et sp. nov. is estimated at 3,75 meters (Fig. 6).

Vertebrae. The nearly spool-shaped centrum is deeply amphicoelous but without a notochordal canal. Its suture with the neural arch is well developed in the dorsal, sacral, and anterior caudal vertebrae, but not in the middle caudal ones (see 'ontogenetic stage' below). The centra are relatively short and similar in length as those in *Cotylorhynchus romeri* (Stovall *et al.*, 1966) or *Ruthenosaurus* (Reisz *et al.*, 2011). The longest centrum is located in the mid-dorsal region (Fig. 7B2, not fully complete). A slightly shorter centrum occurs in the anterior caudal region (Figs. 8E3 and 9A2) and the shortest centra are in the sacral region (Fig. 8C). A ventral median

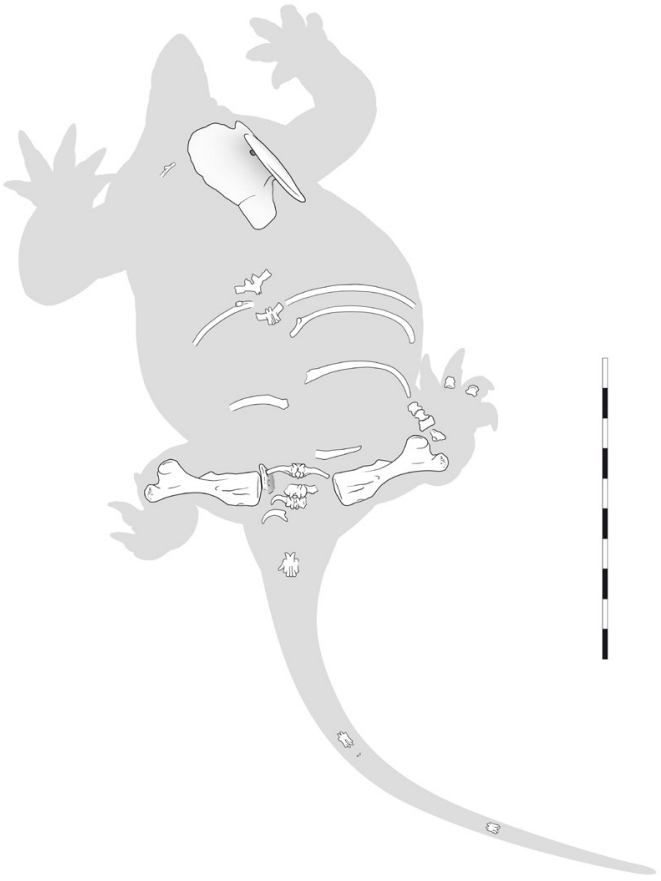

Figure 6. Chosen inventory of *Lalieudorhynchus gandi* gen. nov. et sp. nov., holotype, with skeletal elements of nearly certain anatomical positions, omitting fragmentary ribs and further pieces. Based on proportional comparisons with *Cotylorhynchus romeri* (e.g. OMNH 01673), *Lalieudorhynchus* differs in having a longer and slender femur, smaller sacral vertebrae, and smaller phalanges. Scale bar 1m; reconstructed total length of *Lalieudorhynchus gandi* about 3.60 m.

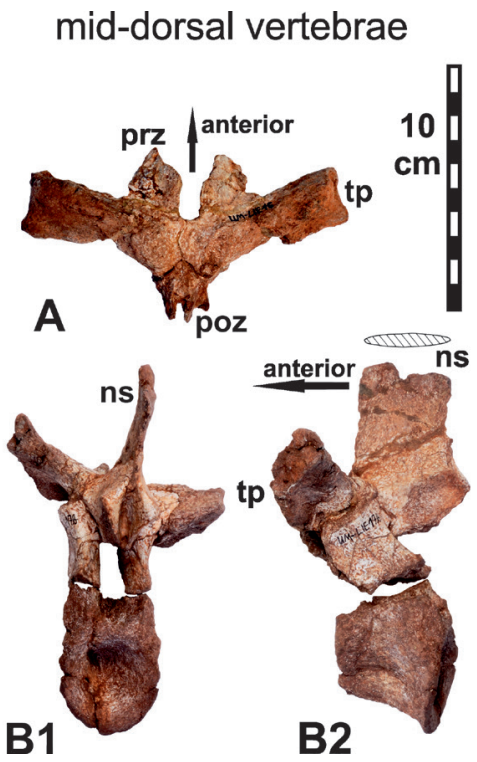

Figure 7. Mid dorsal vertebrae, *Lalieudorhynchus gandi* gen. nov. et sp. nov., holotype. **A**, neural arch of mid dorsal vertebra (ca. 16th presacral), UM-LIE 16, in ventral view; **B**, mid dorsal vertebra (ca. 18th presacral), UM-LIE 17, in posterior **(B1)** and left lateral **(B2)** views. **Abbreviations: ns,** neural spine; **poz**, postzygapophysis; **prz**, prezygapophysis; **tp**, transverse process.

ridge or keel on the convex ventral centra may be present in the mid-dorsal region (Fig. 7B, but deformed). A pair of flat ridges are developed in the sacral and caudal regions, as in *Cotylorhynchus romeri* (Stovall *et al.*, 1966: fig. 3).

The shape of the neural arches varies along the vertebral column. The transverse processes are very elongated in the mid-dorsal region (Fig. 7). Their lateral extension is equal to the height of the neural spine. These transverse processes are relatively straight laterally but with a slight up- and forward extension, as in *Cotylorhynchus romeri* (Stovall *et al.*, 1966: 5). On their anteroventral margin, a robust ridge gives them a triangular profile (Fig. 7A). A curved suture is visible in the same vertebra between both parts of the neural arch in ventral view. The probable 18th vertebra has a very broad transverse process in posteroventral view (Fig. 7B), as in "*Cotylorhynchus" hancocki* (Olson, 1968: fig. 11K). The neural spine of this vertebra is very wide in lateral view, with a very thin-oval transverse section. The postzygapophysis is enlarged compared to the elongation of the neural spine. This neural spine is straightly erected in the mid-dorsal vertebrae and up to the anterior caudal ones (Figs. 7-8), as in *Cotylorhynchus romeri* (Stovall *et al.*, 1966: fig. 1), but in contrast to *Ruthenosaurus* (Reisz *et al.*, 2011: 232, fig. 3) which typically shows anteriorly tilting neural spines with diamond-shaped transverse sections. In *Lalieudorhynchus*, a hyposphene is developed below the postzygapophyses in the dorsal to caudal vertebrae (Figs. 7B, 8D2, 8E2), as in *"Cotylorhynchus" hancocki*. It is missing in all other caseids.

The three sacral and most anterior caudal vertebrae have the largest centra. These centra are short and very broad (Fig. 8C), as in *Ruthenosaurus* (Reisz *et al.*, 2011: fig. 3), but not in *Cotylorhynchus romeri* (Stovall *et al.*, 1966: fig. 3) where they are much narrower. In *Lalieudorhynchus*, these centra are especially thickened in their antero- and posteroventral ends (Fig. 8C), as in the caudal vertebrae of *Alierasaurus* (Romano and Nicosia, 2014: fig. 2). The neural spine of the first sacral and first caudal vertebrae is also very dorsally expanded (Figs. 8A, D), much more than that of *Cotylorhynchus romeri* (Stovall *et al.*, 1966: fig. 1) or of *Ruthenosaurus* (Reisz *et al.*, 2011: fig. 3), but similarly than the neural spine of the large "*Cotylorhynchus" hancocki* (Olson, 1962: plate 8A-C). The outline of the transverse section of the sacral and anterior caudal vertebrae is unique in *Lalieudorhynchus*: it is triangular or narrow oval in its posterior part (Figs 8A and 8E3), whereas it is abrupt and narrowed in its anterior part because of a very thin keel-like process above the prezygapophyses and up to the top of the neural spine (Figs. 8E2, 3). This is a drastic difference with the robust diamond-shaped transverse section in both *Ruthenosaurus* (Reisz *et al.*, 2011: fig. 3B) and *Cotylorhynchus romeri* (compare mounted skeletons OMNH 01673 and AMNH FR 7517). The sacral vertebrae are identified by the configuration of their ribs (see below).

The caudal centra are elongated, especially in their posterior part below the postzygapophyses (Fig. 9). The mid-caudal centra have the same proportions than those of *Cotylorhynchus hancocki* (Olson, 1968: fig. 12O-P) and of *Cotylorhynchus romeri* (specimen "auf rotem Grund" AMNH FR 7517, FS pers. obs., but not in Stovall *et al.*, 1966: fig. 3). The mid-caudal centra with low neural arches of *Alierasaurus* (Romano and Nicosia, 2014: fig.2) are short and without an elongated part below the postzygapophyses, in contrast to the others.

Ribs. Ribs are preserved in the anterior, mid-, posterior dorsal and anterior caudal regions (Fig. 10). The longest one (60 cm) is regularly curved, suggesting a barrel-like thorax or trunk (Fig. 10C) as typical for large caseids. This large rib also shows a relative short distance between its capitulum and tuberculum: as it does not fit with the elongated transverse process of the mid-dorsal vertebrae (around the 18th position, Fig. 7B), it may be more posteriorly located, around the 20th position, as seen in *Cotylorhynchus romeri* which has ribs with a shelf-like flange directed towards the tuberculum (Stovall *et al.*, 1966: fig. 5). Mid-dorsal ribs have indeed very elongated transverse processes with the capitulum very distant from the tuberculum, as seen in many caseids such as *Cotylorhynchus romeri* (OMNH 04188, pers. obs. FS), *Angelosaurus romeri* (Olson and Barghusen, 1962: fig.7C) and *Alierasaurus* (Romano and Nicosia, 2014: fig.3A-B). In *Lalieudorhynchus*, the head of the ribs also shows cup-like tubercles (Figs. 10C, E).

Interestingly, the thoracic rib has been cut to reveal its microstructure and to obtain preliminary information on bone histology: its histological thin section (Fig. 10H) shows a very developed spongiosa (c. 99% of the surface of the section), a very thin outer cortica, and no medulla. The cortica is not sharply defined on the whole perimeter of the section. The small poorly preserved portions of this cortica show bone tissue, which is rather fibrolamellar than lamellar-zonal, unfortunately without any visible growth mark. The subcircular outline of this section and the partial preservation of this cortica suggest a moderate post-mortem transport of the bone. The extremely extended spongiosa consists of very large anastomosed trabeculae in the central region of the section, the average diameter of which decreases relatively progressively towards periphery. These numerous trabeculae suggest a highly vascularized spongiosa, and are secondarily filled by the sedimentary matrix. This extended osteoporotic

spongiosa, the thin cortica, and the absence of a medulla is a typical pattern of aquatic tetrapods (e.g., Steyer *et al.* 2004). The fact that this spongiosa covers most of the surface of the section even suggests a quasi-permanent aquatic way of life of the animal, but this hypothesis is to take into caution because it is based on a single bone section only, and it must be tested on more material using quantitative and statistical comparisons (using for example the software Bone profiler, Girondot and Laurin, 2003). The anterior dorsal rib UM-LIE 03 may be the 5th compared with those of *Cotylorhynchus romeri* (Stovall *et*

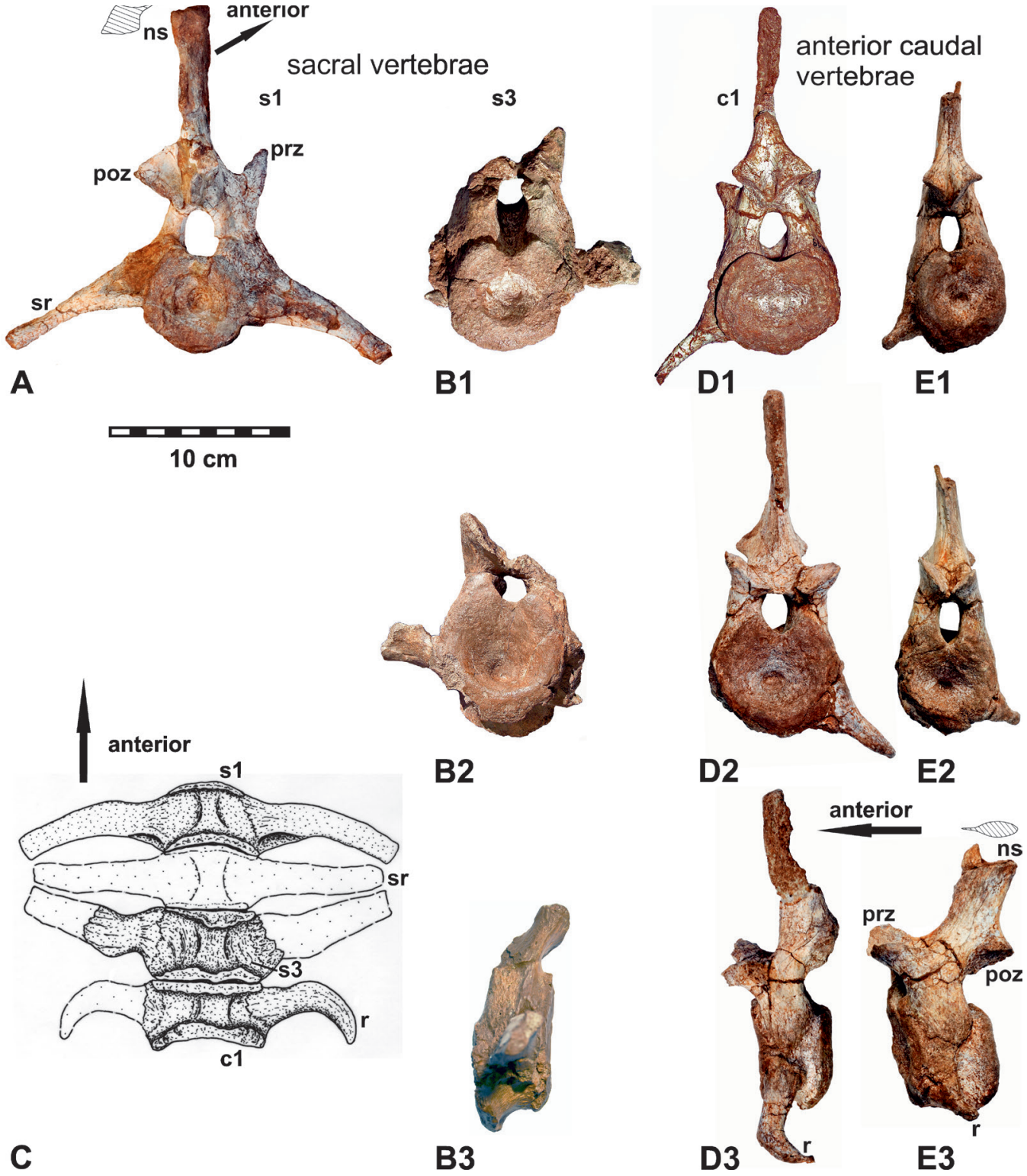

Figure 8. Sacral and anterior caudal vertebrae of *Lalieudorhynchus gandi* gen. nov. et sp. nov., holotype. **A,** first sacral vertebra in posterior view, UM-LIE 15; **B**, third sacral vertebra in posterior **(B1)**, anterior **(B2)** and right lateral **(B3)** views, UM-LIE 07; **C**, reconstruction of the three sacral and first caudal vertebrae in ventral view; **D,** first caudal vertebra in posterior **(D1)**, anterior **(D2)** and left lateral **(D3)** views, UM-LIE 19; **E**, anterior caudal vertebra (4th–5th), in posterior **(E1)**, anterior **(E2)** and left lateral **(E3)** views, UM-LIE 18. **Abbreviations: cv,** caudal vertebra; **ns**, neural spine; **poz**, postzygapophysis; **prz**, prezygapophysis; **r**, rib; **sr**, sacral rib; **sv**, sacral vertebra.

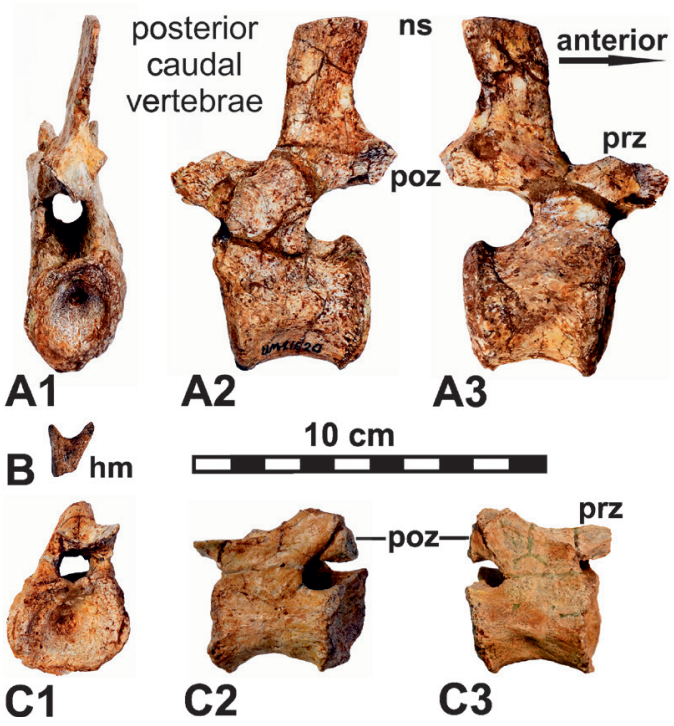

Figure 9. Mid and posterior caudal vertebrae and haemapophysis of *Lalieudorhynchus gandi* gen. nov. et sp. nov., holotype. **A**, mid caudal vertebra (ca. 17th), in posterior **(A1)**, left lateral **(A2)** and right lateral **(A3)** views, UM-LIE 20; **B**, haemapophysis in ?posterior view, UM-LIE 23; **C**, posterior caudal vertebra (30th–35th), in anterior **(C1)**, left lateral **(C2)** and right lateral **(C3)** views, UM-LIE 21. **Abbreviations: hm**, haemapophysis**, ns**, neural spine; **poz**, postzygapophysis; **prz**, prezygapophysis.

al., 1966: fig. 4). The rib UM-LIE 03 shows a robust proximal head and is similar to the 21st of *Cotylorhynchus romeri* (Stovall *et al.*, 1966: fig. 5). The same comparison is possible for the 22nd, 25th (posterior dorsal rib) and the two first caudal ribs (Figs. 8C, 10F-H).

The sacral ribs are also interesting: the first left one shows a rather dorsal suture with the first sacral vertebra - the later being completely preserved and, together with the second sacral vertebra, of similar length than those of *Cotylorhynchus romeri* (Figs. 8A, C). The first right sacral rib is negatively preserved by the imprint of its narrow distal end, and does not show the typical widening usually visible in all other caseids. Both left and right first sacral ribs are clearly curved posteriorly. The second sacral ribs are missing. The right third sacral rib forms a wide proximal half branch, which is typically anteriorly curved and more narrow distally (Figs. 8B, C). This sacral rib sutures anteroventrally the vertebra by a crest (Figs. 8B2, C).

Scapulocoracoid. The scapulocoracoid of *Lalieudorhynchus gandi* gen. nov. et sp. nov. is a huge bone, about 50 cm tall, made from three elements (Fig. 11): the scapula and two coracoids, here identified as the procoracoid and the metacoracoid following the homology proposed by Vickaryous and Hall (2006). Here, these bones appear tightly fused together. Only a part of the dorsoventrally directed suture uniting the metacoracoid to the procoracoid remains discernible ventral to the glenoid fossa (Figs. 11D-F). The rest of the suture, which would have been located onto the glenoid fossa (Romer and Price, 1940: fig. 22), has been obliterated, as has been the other sutures (see ontogenetic stage).

The scapulocoracoid is L-shaped, composed of a tall and thin scapular blade separated from a lower and thicker coracoid plate by a large glenoid fossa, as in all early synapsids (e.g., Romer and Price, 1940: figs 22-24). The shape of the scapulocoracoid of *Lalieudosaurus gandi* gen. nov. et sp. nov. is very similar to that of other giant caseids, and most especially *Cotylorhynchus* (Stovall *et al.*, 1966: fig. 7; Olson, 1968: fig. 14A, B; Romano and Nicosia, 2015: Appendix S6, pl. I, fig. B-D, pl. II, fig. A-B), to the point that the following description could essentially apply to the latter genus.

The scapulocoracoid of *Lalieudorhynchus gandi* gen. nov. et sp. nov. is anteroposteriorly wide, but dorsoventrally short, which results in a large but robust structure. Its general outline resembles that of *"Cotylorhynchus" hancocki*, "*Cotylorhynchus*" *bransoni*, and *Angelosaurus romeri* (Romano and Nicosia, 2015: Appendix S6, pl. I, figs A-D, pl. II, figs A-B2, pl. III). The scapular blade itself is wide but relatively low, consisting essentially in a thin blade of bone thickening posteriorly into a robust, rounded shaft. Dorsal to the glenoid, the scapular blade expands then flares posteriorly, close to the top, leaving two distinct inflections on its posterior margin. Dorsal to this level, the posterior margin becomes progressively thinner. The anterior two-thirds of its dorsal margin are subhorizontal, whereas the remaining third is strongly recurved posteroventrally.

On its lateral surface, the scapulocoracoid exhibits anteriorly two shallow but distinct depressions: a dorsal one, on the scapula, for the origin of the scapular deltoid muscles and a ventral one, on the scapula and procoracoid, for the origin of the scapulohumeralis anterior and supracoracoideus muscles as recognized in other Palaeozoic tetrapods (Romer, 1922; Holmes, 1977). These two depressions are separated by a low ridge running from the lateral supraglenoid ridge to the anterodorsally margin of the scapula, where it ends as a gently rounded scapular process, also seen in sphenacodontids and more especially in *Edaphosaurus* and large caseids (Romer and Price, 1940: fig. 22-24; Olson, 1968: fig. 14; Romano and Nicosia, 2015: Appendix S6, pl. I-III). Although there is no such structure in smaller caseids (Olson, 1968: fig. 14C-D, G-H) or in *Alierasaurus* (RW, pers. obs.), there is a distinct scapular process in each species of *Cotylorhynchus* and in *Angelosaurus romeri* where it even projects dorsally to delimitate a notch in some specimens (Olson, 1968: fig. 14A-B, E-F; Romano and Nicosia, 2015: Appendix S6, pl. I, fig. B-D, pl. II, fig. A-B, pl. III). Such differences could be related to the poor preservation of some *Cotylorhynchus* and *Angelosaurus* specimens, but ontogenetic variations may also be accounted for (see Ontogenetic stage). In any case, the exquisite preservation of UM-LIE 37 indicates that the moderate development of such a scapular process and the absence of a dorsal notch are genuine in *Lalieudorhynchus gandi* gen. nov. et sp. nov.

The scapular blade and the coracoid plate form in posterior view an angle of about 135° (Figs. 11B, E), comparable to that of 135°-150° seen in *Cotylorhynchus* (Romano and Nicosia, 2015: appendix S6, pl. I, fig. A, pl. II, fig. A-B). However, this angle may vary considerably because the scapulocoracoid is prone to post-mortem distortion and deformation, especially in caseids where it is particularly huge and fragile (RW and JF, pers. obs.).

The glenoid fossa has the typical helical shape seen in early synapsids, with posterior, median, and anterior areas that are respectively facing dorsolaterally, laterally, and posteroventrally (e.g., Romer and Price, 1940: figs 22-24). However, the glenoid appears remarkably broad, robust, and concave in *Lalieudorhynchus gandi* gen. nov. et sp. nov., as in

the largest caseids (Romano and Nicosia, 2015: pl. I, figs B, D, pl. II, figs A, B). The glenoid fossa is orientated anterodorsally, at about 50° from the horizontal plane in lateral view, resulting in a rather oblique surface compared to other early synapsids, in which this angle ranges from 20° to 50° (e.g., Romer and Price, 1940: fig. 22-24; Olson, 1968: fig. 14; Romano and Nicosia, 2015: pl. I-III).

The supraglenoid buttress is robust, gently rounded and delimitates a wide, shallow and triangular supraglenoid fossa which is orientated posterolaterally. In other caseids and varanopids, the supraglenoid fossa is also shallow but orientated more posteriorly (Campione and Reisz, 2010: fig. 10; Romano and Nicosia, 2015: Appendix S6, pl. II, fig. A-B, pl. III, fig. A). In other synapsids, however, the same fossa becomes either

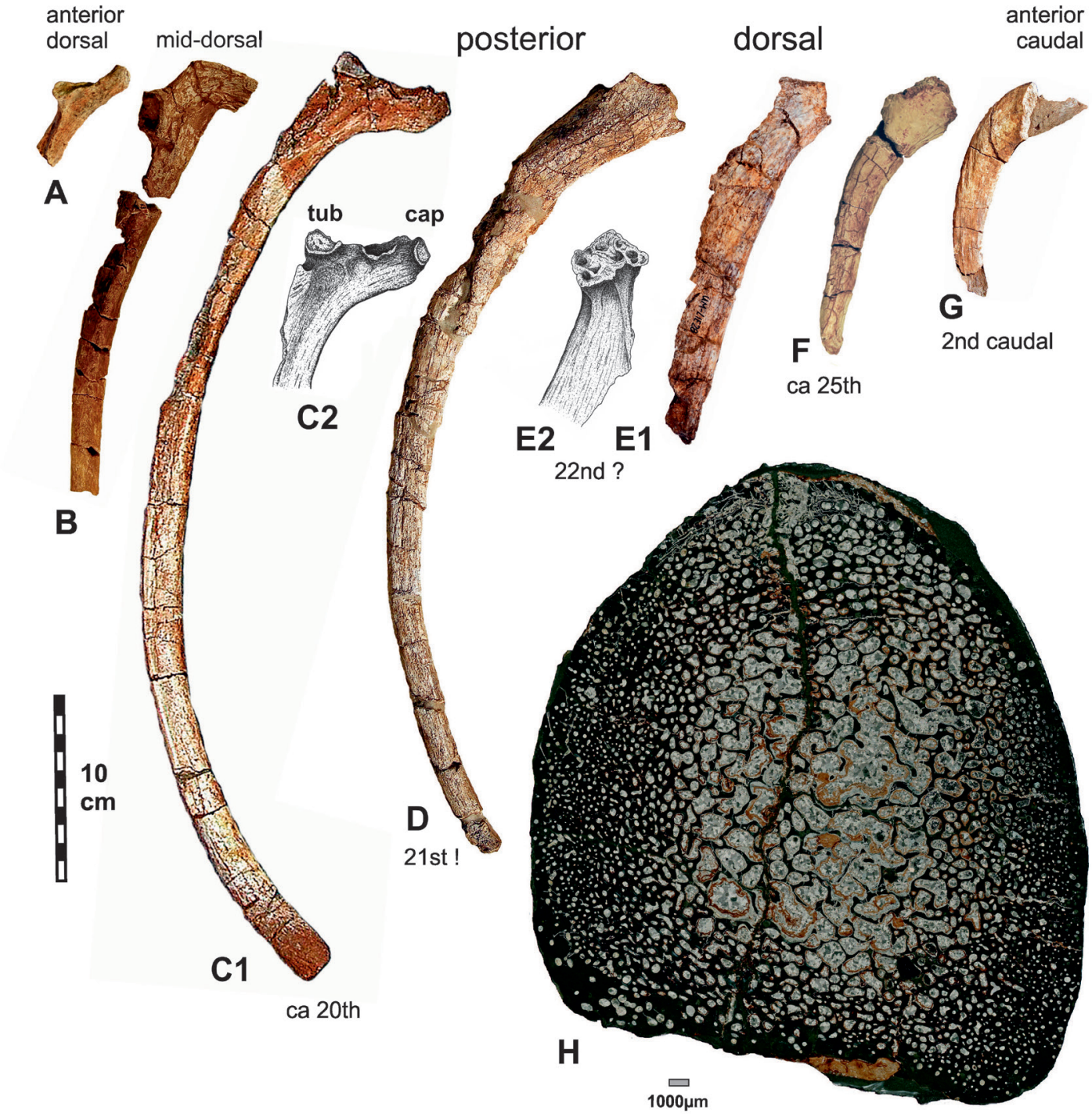

Figure 10. Ribs of *Lalieudorhynchus gandi* gen. nov. et sp. nov., holotype. **A**, left posterior cervical rib (ca. 5th presacral), in posterior view, UM-LIE 24; **B**, left mid-dorsal rib, in posterior view, UM-LIE 47; **C**, left posterior dorsal rib **(C1)** with drawing of the proximal part **(C2)**, in posterior view, UM-LIE 02; **D**, right posterior dorsal rib (21st presacral), in posterior view, UM-LIE 09; **E**, right posterior dorsal rib (probably 22nd presacral), in anterodorsal view **(E1)** with drawing of the proximal part in ventral view **(E2)**, UM-LIE 28; **F** left posterior dorsal rib (ca. 25th presacral), in posterior view, UM-LIE 45; **G** left anterior caudal rib (2nd), in dorsal view (compare Fig. 6C), UM-LIE 08; **H**, cross section UM-LIE 03b of dorsal rib UM-LIE 03a (compare Fig. 6C), showing the very limited cortica and extended spongiosa (see text). **Abbreviations: cap**, capitulum; **tub**, tuberculum.

deeper, as in ophiacodontids, shallower and more laterally orientated in edaphosaurids and sphenacodontids, and even disappears with the supraglenoid buttress in therapsids (Benson, 2012: Appendix S1, #178, fig. A6).

The longitudinal infraglenoid fossa marks the boundary of the anteroventral margin of the glenoid fossa. Just anteriorly lies the supracoracoid foramen, located dorsally within an expanded, oval-shaped lateral external opening of about

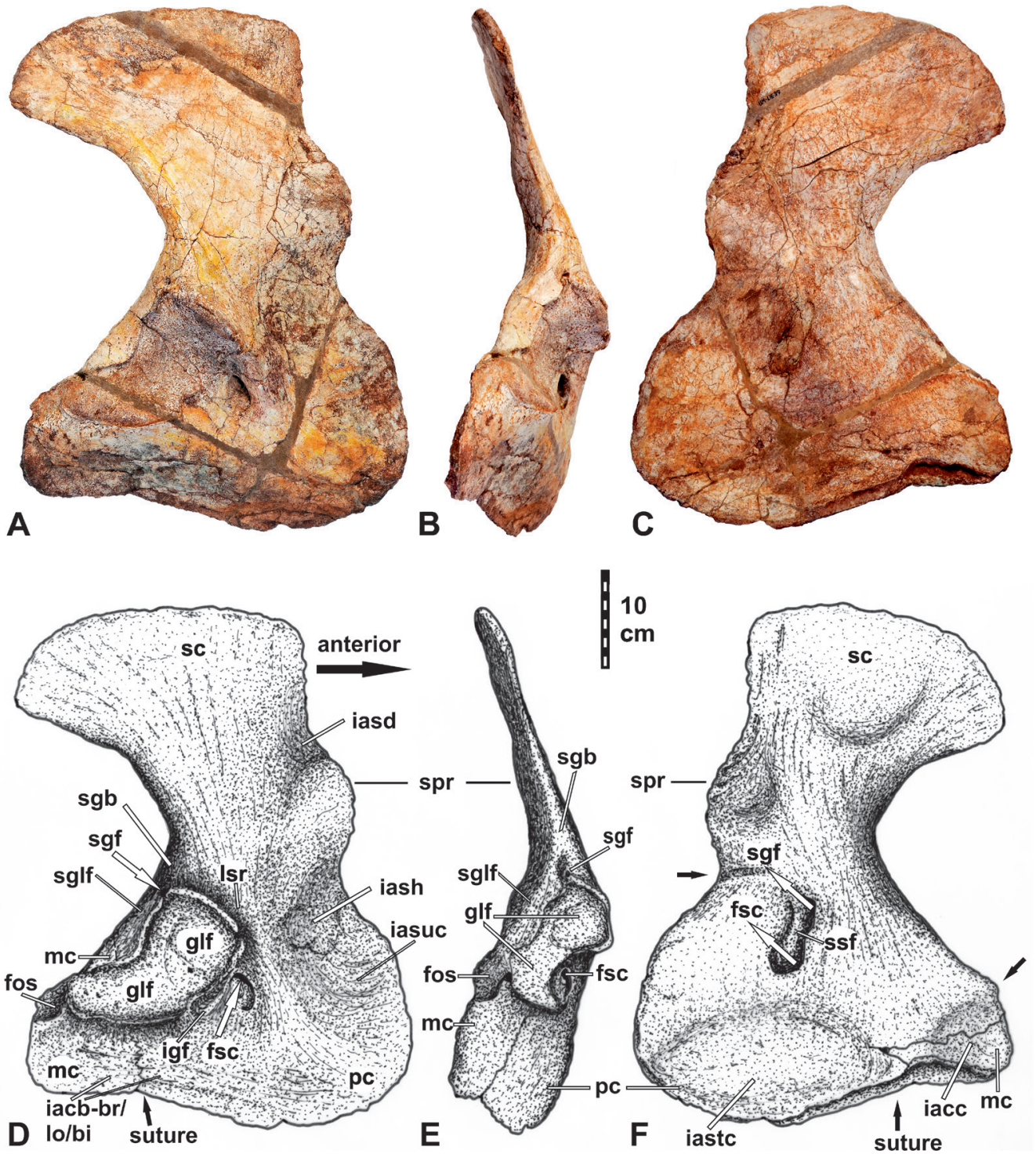

Figure 11. Right scapulocoracoid, *Lalieudorhynchus gandi* gen. nov. et sp. nov., holotype, UM-LIE 37. **A, D,** lateral view; **B, E,** posterior view; **C, F,** medial view; **Abbreviations: fos,** fossa; **fsc,** foramen supracoracoideus; **glf**, glenoid fossa; **mc,** metacoracoid; **iacb-br/lo/bi,** origin area for the coracobrachialis brevis, longus and biceps; **iacc,** insertion area for the costocoracoideus; **iasd,** origin area for the scapular deltoids; **iash,** origin area for the scapulohumeralis anterior; **iastc,** insertion area for the sternocoracoideus; **iasuc,** origin area for the supracoracoideus; **igf,** infraglenoid fossa; **lsr** lateral supraglenoid ridge; **mc**, metacoracoid; **pc**, procoracoid; **spr**, scapular process; **sc**, scapular blade; **sgb**, supraglenoid buttress; **sgf**, supraglenoid foramen; **sglf**, supraglenoid fossa; **ssf**, subscapular fossa.

3.5 cm in height. The lower part of this external opening ends in two small fossae whereas its upper part is pierced by the large, anterodorsally directed supracoracoid foramen, which appears as a elongated oval of about 2 cm in diameter. Medially, the supracoracoid foramen opens in the lower part of the subscapular fossa, which extends 9 cm in an elongated, narrow oval depression (Figs. 11C, F). While the presence and position of this foramen are in agreement with the anatomy of other caseids (Williston, 1911a: pl. XIX, fig. 1-3; Stovall *et al.*, 1966: fig. 7; Olson, 1968: fig. 14), that of a supraglenoid foramen is much more unusual. Absent even in adequately known taxa (Olson, 1968; Reisz *et al.*, 2011; Sumida *et al.*, 2014), such a foramen has been recently identified in a specimen of "*Cotylorhynchus" hancocki* for the first time in a caseasaur (Benson, 2012: Appendix S1, #179; Romano *et al.*, 2017 a). In "*Cotylorhynchus" hancocki* and *Lalieudorhynchus gandi*, the supraglenoid foramen is located on the eponym fossa, as in *Edaphosaurus* spp., *Ophiacodon* spp., and some varanopids (e.g., Williston and Case, 1913: p. 50; Romer and Price, 1940: p. 277, pl. 38; Modesto and Reisz, 1992: fig. 6) – a condition similar to that of diadectomorphs (Williston, 1911b) and thus possibly plesiomorphic for amniotes. In non-caseasaur synapsids, in contrast, the supraglenoid foramen is either on the lateral supraglenoid ridge or anterior to it (Romer and Price, 1940: pl. 27, 44; Langston and Reisz, 1981: fig. 14A; Campione and Reisz, 2010: fig. 10).

The coracoid plate appears relatively low, especially posteriorly (Figs. 11A, C, D, F), compared to those figured by Stovall *et al.* (1966: fig. 7) and Olson (1968: fig. 14), a difference, likely due to the heavy crushing suffered by the specimens they used for their reconstructions. Better preserved scapulocoracoids show that the coracoid plate of *Lalieudorhynchus gandi* is as low as those of *Cotylorhynchus* and *Angelosaurus* (Romano and Nicosia, 2015: Appendix S6, pl. I, figs A-D, pl. II, figs A-B, pl. III). The area located posterior to the glenoid serves as the origin of the coracoid head of the triceps muscle in a variety of Palaeozoic tetrapods (e.g., Romer, 1922: pl. XXXIII, fig. 1-6). In *Lalieudorhynchus gandi*, there is a low and rounded triceps process, just as in *Cotylorhynchus hancocki* and *Cotylorhynchus bransoni* (Romano and Nicosia, 2015: Appendix S6, pl. I., figs A-D, pl. II, figs A-B2). A rounded, but more prominent triceps process has been reconstructed by Stovall *et al.* (1966: fig. 7) for *Cotylorhynchus romeri* using several specimens. In the same article, however, Stovall *et al.* (1966: 15) themselves described it as showing little development, because it is indeed not as broad nor as prominent as in some varanopids, edaphosaurids, and sphenacodonts (e.g., Romer and Price, 1940: fig. 22-24). In a drawing published later by Olson (1968: fig. 14f), however, the triceps process of *Cotylorhynchus romeri* appears as low as in the other species of *Cotylorhynchus* mentioned above. Whether these differences are due to taxonomic, ontogenetic, or taphonomic variations in these caseids remains poorly understood at the moment. In any case, the triceps process of *Lalieudorhynchus gandi* is noteworthy because its lateral surface bears a small, shallow, and rounded fossa (Fig. 11), whose rugose surface likely marks the origin of the coracoid head of the triceps muscle. While the development and shape of the triceps process vary quite a lot in Paleozoic tetrapods (e.g., Romer, 1922: pl. XXXIII, fig. 1-6), the presence of such a lateral fossa is unheard of, as far as we know. The very prominent triceps process of sphenacodontids bears a foramen on its medial surface, visible in posteroventral view (Benson, 2012: Appendix S1, #184-185, fig. A6C-E, Appendix S2), but its shape, location, and supposed function differ clearly from those of the fossa observed on *Lalieudorhynchus gandi*. Ventral to the glenoid is an anteroposteriorly elongated depression on the metacoracoid for the insertion of the coracobrachialis brevis and longus and the biceps muscles (Romer, 1922; Holmes, 1977). The coracoid symphysis, located on the medioventral margin of the entire metacoracoid and the posterior half of the procoracoid, is deeply concave (see Ontogenetic below).

The medial surface of the scapulocoracoid bears fewer identifiable features than the lateral one. The most striking is the subscapular fossa in which both the supraglenoid and supracoracoid foramina open, as described above. Also notable is the massive, rounded scapular torus, which starts from the posterior scapular margin, at the level of the glenoid, then extends obliquely to reach the anterodorsal corner of the scapula. From this scapular torus diverge two branches. The first branch is a rounded ridge that forms the posterior margin of the scapula and delimitates with the scapular torus a wide, shallow, dorsal depression. The second branch is a low ridge that separates a small, shallow, anterior depression from the subscapular fossa. These depressions likely serves for the attachment of muscles, but the configuration of this area is unclear when compared to better known amniotes (e.g., Romer, 1922; Holmes, 1977). Ventrally, the scapulocoracoid bears two other depressions whose respective role is better understood. The sternocoracoideus muscle thus inserted onto an oval, anteroposteriorly elongated depression located on the ventral half of the procoracoid while the costocoracoideus muscle inserted on a smaller, more rounded depression located on the posteroventral corner of the metacoracoid (Romer, 1922; Holmes, 2003). Regarding other caseids, the medial surface of the scapulocoracoid remains has been poorly described and illustrated. The available litterature nevertheless suggests that this region differs little between "*Co." hancocki*, *Co. romeri*, *Angelosaurus romeri*, and *Lalieudorhynchus gandi* gen. nov. et sp. nov. (Stovall *et al.*, 1966: fig. 7; Romano and Nicosia, 2015: Appendix S6, pl. I, figs. A1, C1, pl. II, figs. A1, B1, pl. III, figs. A1, B1).

***?Ilium*.** This blade like bone (15.7 cm length) looks like an ilium. It is anteroposteriorly short but relatively extended dorsally, with a narrow shaft. It is narrow transversally except at the level of its extremities which are thickened (Fig. 12). Its surface is striated and the striations widen towards the bone margin. This bone is tentative interpreted as the left iliac blade. Alternatively, it could be an ischium (with the upper outline being the surface for the acetabular in this case) but this hypothesis is rejected because its thicken extremity fits better with the acetabular region of an ilium, and the striations are also typical for an ilium.

This probable ilium has a narrow blade compared to that of *Cotylorhynchus romeri* (Stovall *et al.*, 1966: fig. 8), "*C." hancocki* and *Angelosaurus* (Olson, 1968: figs 19G-I). Here, the probable anterodorsal iliac process is very poorly developed in contrast to that of *Cotylorhynchus romeri* (Stovall *et al.*, 1966: fig. 8) and *Ruthenosaurus* (Reisz *et al.* 2011: fig. 7). The probable posterodorsal iliac process is partly preserved and may be slightly larger than the anterodorsal one: this is also the case in *Ennatosaurus* and *Cotylorhynchus romeri,* but not in *Ruthenosaurus* where the posterodorsal process is much larger than the anterodorsal one. In *Lalieudorhynchus*, the anteroventral part of the probable iliac blade is swollen and may indicate the near margin of the acetabulum. An anteroventral directed narrow fossa lies below the posterodorsal process and nearby a little foramen may be present (Figs. 12B, D). A little

longitudinal area for muscle attachment is preserved at the top of the medial surface of the probable iliac blade. Rounded, flat depressions on the upper part of the probable inner iliac blade may fit with the contact of the first and second sacral ribs, which is similar in *Ruthenosaurus.* The general shape of the probable ilium is very similar to that of the small caseid *Ennatosaurus* (Olson, 1968: figs. 19E, 22L, M) or *Caseopsis* (Olson, 1968: fig. 19F).

Femur. Both left and right femora are preserved, with lengths of about 35.5 cm (Fig. 13). It is only surpassed in large individuals of "*Cotylorhynchus" hancocki* (Olson, 1968: tab. 3a). The anatomical nomenclature for this bone follows mostly Romer and Parson (1983). The femur is a straight and relatively short bone with broad heads. It is shorter and more robust than in *Cotylorhynchus romeri* (Stovall *et al.*, 1966: fig. 11). The proximal head has nearly the same width as the distal one.

The posterior distal condyle is much more distally extended than the anterior one, in contrast to *Ruthenosaurus* (Reisz *et al.*, 2011: fig. 8). The articular surfaces for the tibia are well developed ventrally on both condyles, while the articular surface for the fibula is situated on the posterodistal part of the posterior condyle (Figs. 13D1, D2, D4). The popliteal area is rounded, relatively wide with robust furrows, and much larger and deeper than that of *Cotylorhynchus romeri* (Stovall *et al.*, 1966: fig. 11).

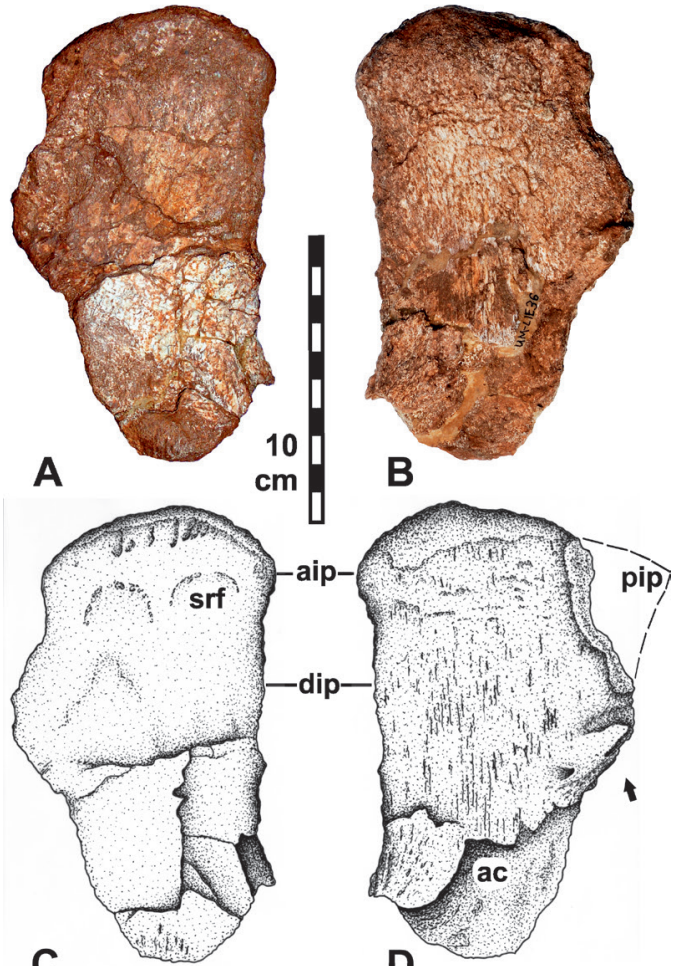

Figure 12. Probable left ilium of *Lalieudorhynchus gandi* gen. nov. et sp. nov., holotype, UM-LIE 36. **A, C,** medial view; **B, D,** lateral view; **Abbreviations: ac**, probable region of the acetabulum fossa; **aip**, anterodorsal iliac process; **dip**, dorsal iliac process; **pip**, posterodorsal iliac process; **srf**, sacral rib facet.

In *Lalieudorhynchus*, the proximal head of the femur is convex rounded with a rugose area that indicates the presence of a cartilaginous cap. This proximal area for articulation with the girdle is very well developed dorsoventrally (Figs. 13B3, D3), in contrast to that of *Cotylorhynchus romeri* (Stovall *et al.*, 1966: fig. 11). The intertrochanteric fossa is very large and deeply convex because its surrounding posterior intertrochanteric ridge and internal trochanter are high. This intertrochanteric fossa reaches almost the mid-length of the bone; it is therefore much more elongate compared to that in most other caseids.

The internal trochanter is relatively robust in shape, starting in the proximal second quarter of the bone length and ending in its distal half. But it is smaller in size than those of *Cotylorhynchus romeri*, *Ruthenosaurus*, *Angelosaurus dolani* or *Casea broilii.* The fourth trochanter lies at the mid-length of the femur and is much smaller than the internal trochanter. A variation between the left and the right femur is visible on their ventral ridges: in the left femur, a trough-like neck seems to separate the small, knob-shaped fourth trochanter from the large internal trochanter (Figs. 13A, C). Yet in the right femur these trochanters seem confluent, with blurred distinctions. The fourth trochanter is nearly missing in *Cotylorhynchus romeri*, *Angelosaurus dolani* or *Casea broilii*. It is reduced in *Ruthenosaurus*, but well visible in *Dimetrodon* (Romer and Parson, 1983), ophiacodontids, sphenacodonts (Stovall *et al.*, 1966), *"Cotylorhynchus" hancocki*, *Angelosaurus romeri* and *A. greeni* (Olson, 1962: plates 3K, 4H, I, 9F).

The attachment structures for the ischiotrochanteriscus and puboischiofemoralis internus muscles are well preserved dorsally on the proximal femoral head; they appear as small ridges and fossae on the dorsal side of the proximal region of the femur (Figs. 13B2, D2). Two large distinct rugose ridges for these muscles are also recorded in this femoral region in *Cotylorhynchus romeri*. In *Lalieudorhynchus*, the intercondylar fossa is much wider than the posterodorsal condyle.

This is the opposite in *Cotylorhynchus romeri* and *Ruthenosaurus* where the intercondylar fossa is narrower than the posterodorsal condyle. In *Lalieudorhynchus*, longitudinal ridges are present on the posterodorsal condyle, as in *Cotylorhynchus romeri*. A fossa, visible in posterior view only, is also developed on the posterior side of the posterior condyle, between its dorsal part and the posterior articular surfaces for the tibia.

Pes. An astragalus, two tarsal elements and five phalanges have been found closed to each other but not articulated: based on their respective sizes, they may belong to the hind foot of the same individual (Figs. 14-16). The **astragalus** is nearly as broad as long. It has a pronounced head-like structure with a flat facet for the fibula and a large flat bony plate without special developed facet for the tibia. A typical arterial notch is visible on the medial side of the bony plate to the neighbouring calcaneum. This is also the case in *Cotylorhynchus romeri* (Stovall *et al.*, 1966: 24 and fig. 16). The shape of the astragalus of *Lalieudorhynchus* differs from that of most other caseids, but is very similar to that of *"Cotylorhynchus" hancocki* (Olson, 1962: fig.12A).

A very large distal **tarsal 1** (5-6 cm wide and 4-5 cm long) has also been found (Figs. 14B, 15E), with nearly all its sides typically concave. It fits in size and articulation with the distinct metatarsal I (see description below). This tarsal 1 is of the same width than the astragalus, therefore extraordinary large in comparison with that of other caseids. This width also

correlates with that of the extraordinary wide metatarsal I (Fig. 15E). Another tarsal element, small in size (24 x 11-16 x 7 mm) and subrectangular in shape, remains unidentified (UM-LIE 35).

The **metatarsal I** is very robust, and as long (40 mm) as wide (38-39 mm, measured at the level of its heads) (Figs. 15A, 15E, and 16B). The diameter of its subcircular shaft is 22 mm in dorsal view and 19 mm in lateral view. Its proximal head is very large, expanded dorsoventrally, and flat to convex, with a large ventrodistally directed bulge. This head is dorsoventrally much more elongated than the flat-concave distal surface of the tarsal 1 (25 mm). Therefore, it draws a marked flexion in ventral direction. Its distal head is expanded, but less dorsoventrally than proximally (25 mm). Its dorsoventral length is yet few millimeters more than that of the concave proximal head of the first following phalanx (22 mm). This also draws a marked flexion in ventral direction. The articular surfaces of the metatarsal I form an angle of about 110 degrees with the long axis (Figs. 16A3, 16B3). The same shape is also known in the metatarsal I of *Alierasaurus* where it is slightly

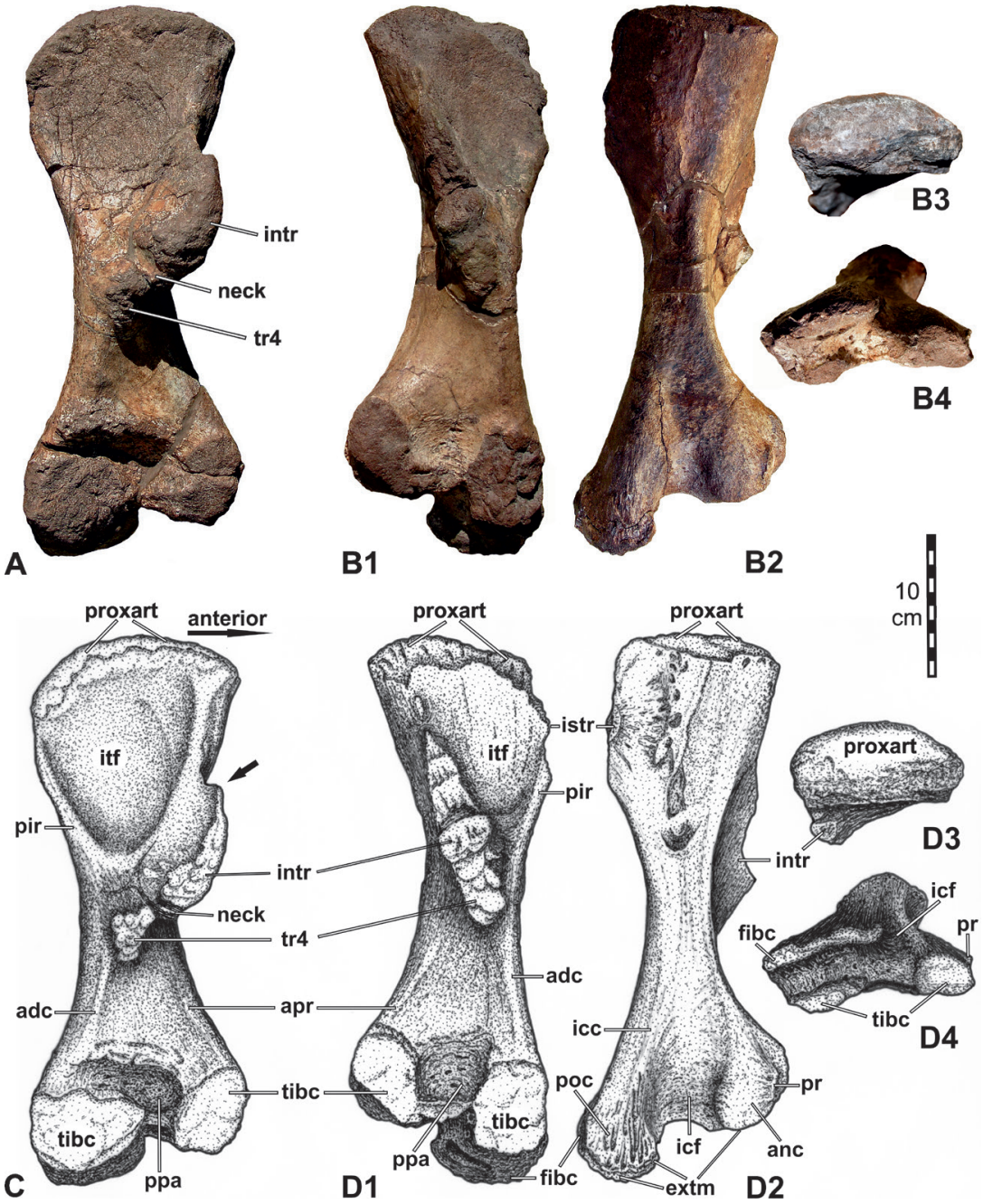

Figure 13. Femora of *Lalieudorhynchus gandi* gen. nov. et sp. nov., holotype. **A, C,** left femur in ventral view, UM-LIE 05; **B, D,** right femur, UM-LIE 04, in ventral (**B1**, **D1**), dorsal (**B2, D2**), proximal (**B3, D3**), and mostly distal and slightly dorsal (**B4, D4**) views. **Abbreviations: adc,** adductor crest; **anc,** anterior condyle; **apr,** anterior popliteal ridge; **extm,** area of extensor muscles; **fibc,** articular surface for fibula; **icc,** intercondylar crest; **icf,** intercondylar fossa; **intr,** internal trochanter; **istr,** insertion area for ischiotrochantericus muscle; **itf,** intertrochanteric fossa; **pir,** posterior intertrochanteric ridge; **poc,** posterior condyle; **ppa**, popliteal area; **pr**, process for the ligament of the knee on anterior condyle; **proxart,** proximal area for articulation with pelvic girdle; **tibc,** articular surface for tibia; **tr4,** fourth trochanter.

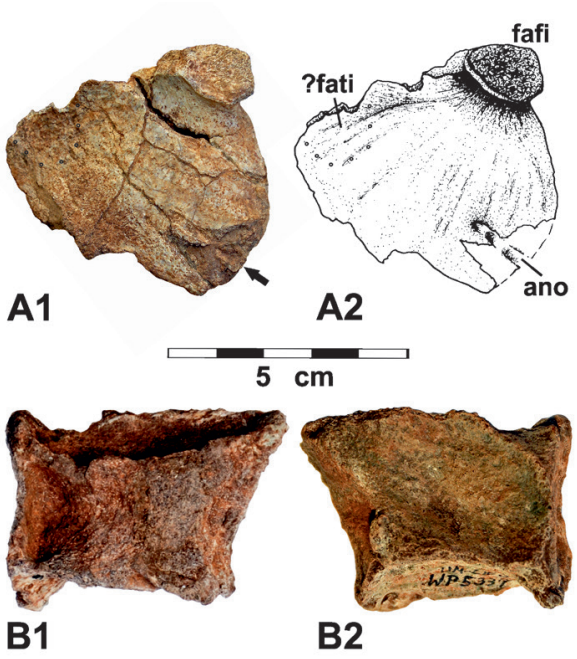

Figure 14. Tarsus of *Lalieudorhynchus gandi* gen. nov. et sp. nov., holotype. **A**, left astragalus, UM-LIE 12, in anterodorsal view; **B**, distal tarsal (?1), UM-LIE 34, in dorsal **(B1)** and ventral **(B2)** views. **Abbreviations: ano,** arterial notch; **fafi,** facet for the fibula; **fati,** facet for the tibia.

longer and wider in lateral view (Romano and Nicosia, 2015: figs 6A-C). In other pelycosaurian synapsids, these proportions of the metatarsal I are unknown, although this bone is wider proximally in *Casea broilii* (Williston 1910), *Angelosaurus dolani* (Olson, 1968: fig. 18D) and *Dimetrodon milleri* (Reisz, 1986: fig. 33A).

As all non-ungual phalanges, the **first phalanx of the first axis** is also typically short (40 mm) and wide (39 mm, measured at the level of its heads) (Figs. 15B, E, and 16D). The width of its shaft is 29 mm in dorsal view and only 11 mm in lateral view. Its concave proximal head is of 22 mm in dorsoventral dimension and has ventrodistally directed triangular facets in its lateral ends. The distal head consists of a bilobed articular surface, which is ventrally oriented. A pair of dorsodistal directed concave facets is located in its lateral end. The other recorded phalanges are of similar shape but smaller in size (Figs. 15C, D, and UM-LIE 13). These phalanges are also known in *Alierasaurus* where they are more elongated, or in *Cotylorhynchus romeri* (Stovall *et al.*, 1966) where they are in general smaller.

ONTOGENETIC STAGE

Despite its large size, the skeleton of *Lalieudorhynchus* shows an interesting mix of immature and mature features.

Axial skeleton. In most preserved vertebrae, the anterior and posterior surfaces of the centra are unfinished and slightly rugose (Figs. 7B, 8A, E1) to strongly rugose (Fig. 8E2). A more ossified condition is present in the middle caudal centra (Figs. 9A, C), where these surfaces are rather smooth, almost finished. This ambiguous association of both immature and mature features is best seen in the sacral III (Figs. 8B1-2) whose anterior and posterior articular surfaces are respectively smooth and rugose, both from the lips to the bottom of the notochordal pit (see below). The zygapophyseal surfaces are similarly rugose in dorsal (Fig. 7B) and anterior caudal vertebrae (Fig. 8E), but smooth in the sacral (Figs. 5B, 8A) and middle caudal ones (Fig. 9A).

The neurocentral suture of the dorsal vertebrae is open, with concave, unfinished pedicels (Fig. 7A-B), leaving the neural arches separated from their respective centra. In sacrals (Fig. 8A-B) and anterior caudals (Fig. 8E), however, the same suture is closed, though still not obliterated, with a junction covered with a slightly to strongly rugose surface. The neurocentral suture is faint but still discernible in a middle caudal vertebra (Fig. 9A), before disappearing in the more posterior vertebrae (e.g., Fig. 9C). The sacral (Figs. 5B, 8A) and anterior caudal vertebrae (Fig. 8D, E) also display a distinct costoneurocentral suture, which forms a triple junction underlined by its spongious surface and orientation. The left ribs of the same anterior caudals (Figs. 8D, E) have been found firmly attached to their respective vertebra, a mature trait. Their right ribs, however, detached after death, perhaps because their suture with their respective vertebra was looser on the left side. Damages suffered by the left flank of the body, before or during burial, may have also been responsible for this difference. Regardless, the costoneurocentral suture was certainly still loose in anterior caudals, as the second caudal rib (Fig. 10G) was found separated from its vertebra. A paired neurocentral suture is surprisingly visible in the caudal vertebrae of the posterior half of the anterior region (UM-LIE 10), the middle region (Fig. 9A), and the posterior caudal region (Fig. 9C) – a sign of immaturity (e.g., Romer and Price, 1940).

The two sacral ribs I (Fig. 8A) may have been separated from the ilium (Fig. 12A, C) between the death of the animal and its final deposition: this may have happened because the iliocostal suture was still free, as in immature individuals, in contrast with the tight costovertebral suture occurring between the sacral ribs I and their vertebra (Fig. 8A). There is no evidence of suturation nor fusion between successive sacral ribs or sacral centra, as reported in *Cotylorhynchus romeri* (Stovall *et al.*, 1966) or *Angelosaurus romeri* and *An. dolani* (Olson and Barghusen, 1962). The co-occurrence of an anterior smooth and a posterior rugose articular surfaces in the sacral III nevertheless suggests a more rapid anterior ossification, a possible first step toward the co-ossification of the sacrals II and III.

These features suggest that the sequence of ossification and co-ossification of neural, central, and costal elements followed the plesiomorphic posterior to anterior direction seen in many other tetrapods including non-mammalian synapsids (e.g., Romer and Price, 1940; Brochu, 1996; Irmis, 2007). The persistence of the neurocentral and neurocentrocostal sutures in caudal vertebrae is typical of young individuals. The more posterior the sutures are, the younger is the individual (JF pers. obs.). Here, the presence of sutures in anterior middle caudal vertebrae and open sutures in sacral and anterior caudal vertebrae confirms that this skeleton corresponds to a late juvenile or an early adult individual.

Appendicular skeleton. The scapulocoracoid (Fig. 11) has a smooth surface showing only a faint suture on its lateral surface, distinguishing the metacoracoid from the procoracoid. There is no trace of a suture between the scapula and the coracoids. In early amniotes, this condition is seen in young adults, in which the scapula and the procoracoid suture then fuse together earlier during ontogeny than with the metacoracoid (e.g., Romer and Price, 1940; Holmes, 1977; Currie, 1981;

Reisz, 1981). In caseids, no suture between these three elements has been observed, to the point that the presence of two coracoids in these synapsids has long remained conjectural (e.g., Olson, 1968). *Ruthenosaurus*, *Callibrachion* and now *Lalieudorhynchus* possessed two coracoid ossifications (Reisz *et al.*, 2011; Spindler *et al.*, 2016; this paper), a classical synapomorphy of the amniote clade (Laurin and Reisz, 1995). This suggests that the scapula and coracoids ossified and co-ossified relatively early during ontogeny, hence the absence of sutures even in specimens identified as young individuals (e.g., Williston, 1910; Olson, 1968). This condition may be related to a more prominent role of the forelimbs for locomotion and/or foraging in caseids, compared to other synapsids. An alternative explanation is that previously described specimens were too poorly preserved and/or prepared to identify such sutures, as many specimens ascribed to *Cotylorhynchus*, *Angelosaurus*, *Ennatosaurus* and others suffered from heavy crushing (e.g., Olson, 1962, 1968).

Although the scapulocoracoid is remarkably ossified as a whole, some areas in particular are not. The surface of the glenoid fossa, for instance, is still covered with unfinished bone. More striking, however, is the deeply concave dorsal

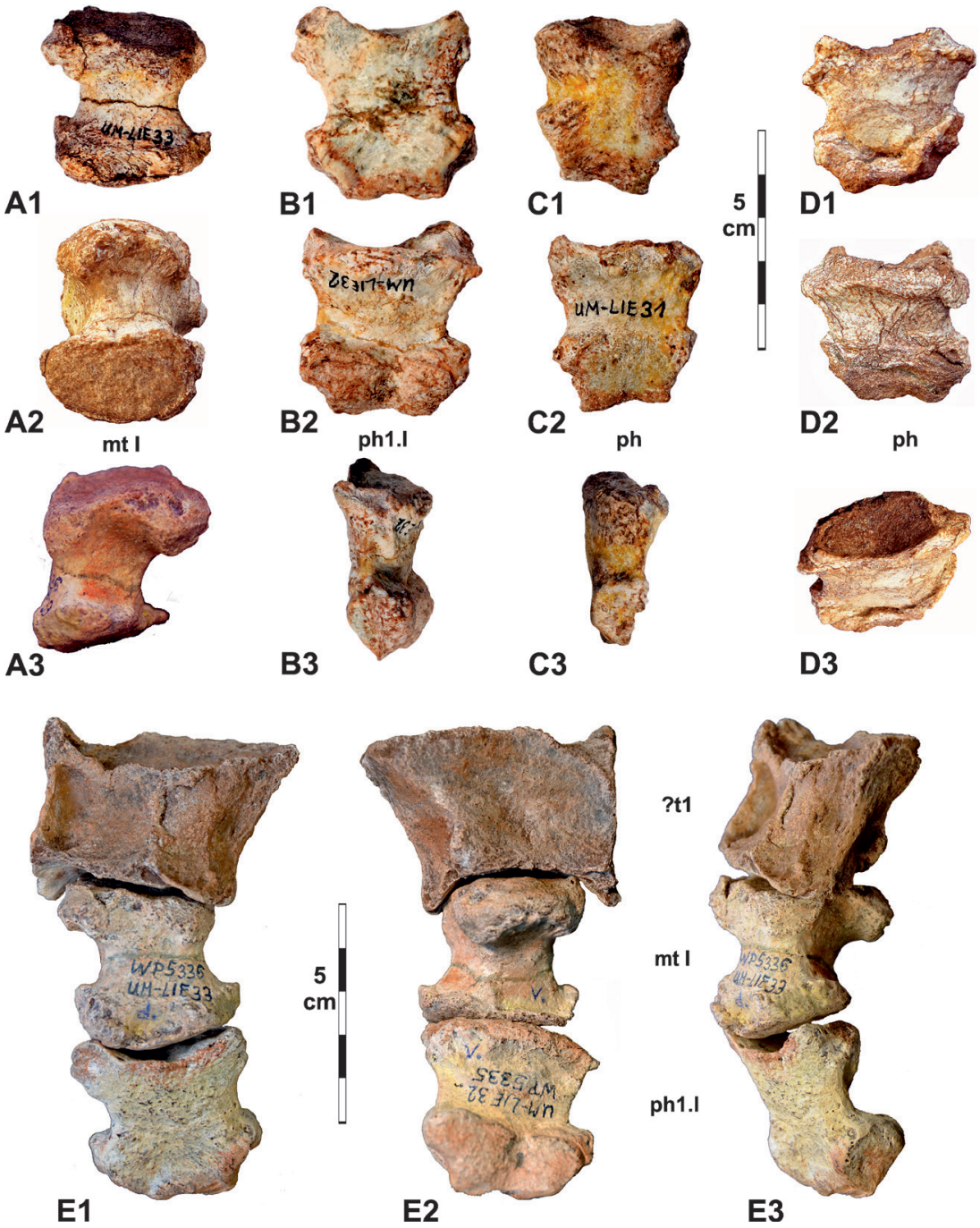

Figure 15. Pes of *Lalieudorhynchus gandi* gen. nov. et sp. nov., holotype. Metatarsal **(A, E),** phalanges **(B–E),** and tarsal (**E**). **A,** right metatarsal I, UM-LIE 33, in dorsal **(A1),** ventral **(A2),** and medial **(A3)** views; **B**, phalanx 1 of pedal digit 1, UM-LIE 32, in dorsal **(B1)**, ventral **(B2)**, and medial **(B3)** views; **C–D**, non-ungual phalanges, UM-LIE 31 (**C**) and UM-LIE 14 (**D**), in dorsal **(C1, D1)**, ventral **(C2, D2)**, medial or lateral **(C3)**, and dorsoproximal **(D3)** views; **E**, reconstruction of tarsal 1 with pedal digit 1, UM-LIE 32, 33, 34, in dorsal **(E1)**, ventral **(E2),** and dorsomedial **(E3)** views. **Abbreviations: mt**, metatarsal; **ph**, phalanx; **t**, tarsal.

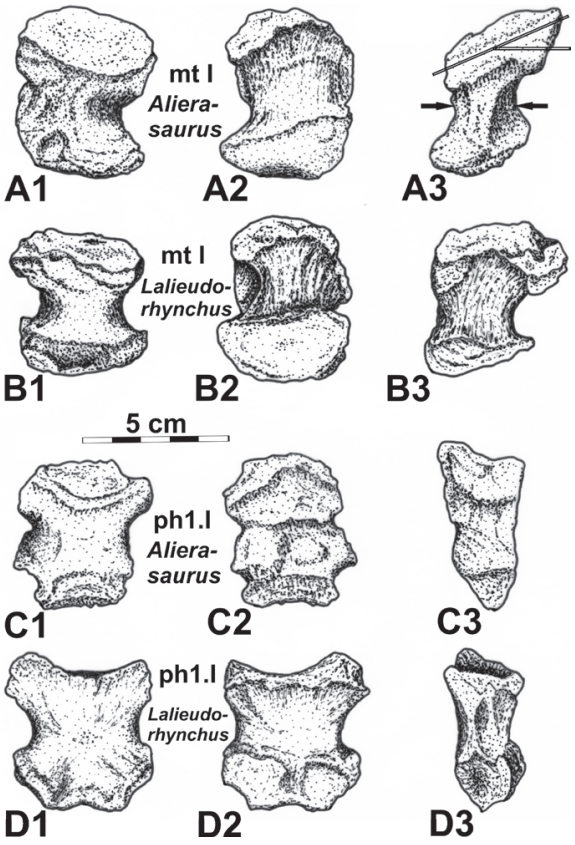

Figure 16. Comparison of metatarsals I and phalanges 1-I of *Alierasaurus*, and *Lalieudorhynchus*. Metatarsal I (**A–B**); phalanx 1 of digit I (**C–D**), in dorsal (column **1**), ventral (column **2**), and lateral (column **3**) views. **A**, **C**, *Alierasaurus ronchii*. **A**, MPUR NS 151/6, redrawn from Romano and Nicosia (2014: fig. 6A–C). **C**, MPUR NS 151/4, redrawn from Romano and Nicosia (2014: fig. 8A–C). **B**, **D**, *Lalieudorhynchus gandi* gen. nov. et sp. nov., holotype. **B**, drawing from UM-LIE 33. **D**, drawing from UM-LIE 32. **Abbreviations: mt**, metatarsal; **ph**, phalanx.

Figure 17. Indeterminate bone of Tetrapoda indet., UM-LIE 38, from the type locality of *Lalieudorhynchus gandi* gen. nov. et sp. nov., but probably not belonging to the holotype of *L. gandi.*

end of the scapular blade and the coracoid symphysis. These two features indicate that these areas were still covered with cartilage, a typical immature feature.

Contrary to the scapulocoracoid, the possible ilium (Fig. 12) was found isolated, possibly because it was still free. In any case, the medial surface of the iliac blade is made of smooth, finished bone while its lateral surface is covered with rugosities and scars. This is confirmed by the very poor ossification and shallow concavity of the acetabulum. These observations are all congruent with the fact that the ilium and the sacral vertebrae were found separately and not sutured nor even fused together, as it should have been the case in a fully mature synapsid (e.g., Romer and Price, 1940), and even more the caseid *Angelosaurus*, in which the sacrum incorporated up to four sacral vertebrae and their ribs (Olson and Barghusen, 1962; Olson, 1968; LeBlanc and Reisz, 2014).

In contrast, the right femur (Figs. 13B, D) appears to be mature, with its smooth, finished surface, its prominent distal condyles, and its finished supracondylar process covered with rugosities for muscular insertions, which is a sign of advanced maturity in *Dimetrodon* (Brinkman, 1988). Other features of the femur suggest nevertheless that the holotypic individual was still growing. The articular surfaces of the distal condyles are unfinished, for instance. This is also the case of its proximal head, whose surface is not only unfinished, but also distinctly concave, as expected in very immature individuals (ex. *Ophiacodon* and *Dimetrodon*, Brinkman, 1988). Although this seems to contradict the advanced ossification of the other structures of the femur, caseids apparently retained a proximal cartilage cap throughout their life (Olson, 1968).

Regarding the pedal elements, the articular surfaces of the tarsal (Fig. 14B) are concave and covered with unfinished bone except for the well-ossified dorsal facet. In the phalanges, the articular surfaces are made of unfinished (Fig. 15D) or unfinished to spongious bone (Figs. 15B-C). These features also suggest a relative immaturity for the holotype of *Lalieudorhynchus gandi* gen. nov. et sp. nov.

Conclusion. The holotypic skeleton of *Lalieudorhynchus* corresponds to a late juvenile-early adult individual. A mix of both juvenile and adult features was already observed on other large caseid specimens (Stovall *et al.*, 1966; Reisz *et al.*, 2011). The retention of immature traits in mature individuals underlines the possible role of developmental heterochronies in caseid evolution. Juveniles grew rapidly and adults much more slowly (Ricqlès, 1974; Shelton and Sander, 2014). Delaying skeletal maturity would have enabled caseids to attain very large sizes by having an extended period of growth, as already exemplified by *Cotylorhynchus* and *Alierasaurus*. The coexistence of immature and mature features may have been the result of a compromise between evolutionary constraints in the largest caseids, such as the necessity to grow sustainably and to support a heavy weight.

LIFESTYLE

Lambertz *et al.* (2016), based on morphological and histological features, suggest a predominantly aquatic lifestyle for *Alierasaurus* and *Cotylorhynchus*. This hypothesis, which is also supported by a physiological work of Similowski (2017), could also explain the herein described immature osteology. Potential paedomorphic traits may be linked with aquatic habits, as seen in temnospondyls (e.g., Steyer *et al.*, 2004), plesiosaurs and spinosaurids (e.g., Waskow and Mateus, 2017). The presence of a fully aquatic tupilakosaurid temnospondyl in the same locality (Werneburg *et al.*, 2007), together with its sedimentary facies, indicates at least the ephemeral availability of water bodies in the paleoenvironment of *Lalieudorhynchus*.

Preliminary to additional histological sampling, the dorsal rib UM-LIE 03b was cut approximately 10 cm distal to the

vertebral articulation and prepared for thin section (Fig. 10H) in order to describe its microstructure. The rib exhibits a very highly osteoporotic-like structure, in fact to a greater degree than that found in the ribs of *Cotylorhynchus* and *Alierasaurus* (Lambertz *et al.*, 2016: fig. 5; C. Shelton, pers. comm. 2019). The presence of extended spongiosa (porous structure), a reduced cortex lacking recognizable growth marks, and the absence of a distinct medulla suggest a predominantly aquatic lifestyle (e.g., Steyer *et al.*, 2004), although converse patterns are also common among nearshore forms (Houssaye, 2009).

Recent morphometric analyses support a terrestrial lifestyle for *Cotylorhynchus* (Núñez Demarco *et al.*, 2018). The mode of life of the formerly hypothetized aquatic *Ophiacodon* is questionable (Felice and Angielczyk, 2014), whereas *Lystrosaurus* is considered to be highly terrestrial, despite of misleading microcanatomical patterns (Botha, 2020): its rib histology strongly differs from that of *Lalieudorhynchus* (Botha, 2020: fig. 10 C), as both differ from highly adapted nearshore swimmers (Houssaye, 2009). As swimming abilities might indeed have been restricted in early synapsids, bottom-walking and/or foraging seem probable regarding the lifestyle of large caseids. Broad and flattened, somewhat *Desmostylus*-like phalanges (Gingerich, 2005) indeed suggest a foraging lifestyle.

Lalieudorhynchus may have spent much time onshore: the terrestrial plant fossils found near its skeleton suggest that it may indeed browse onshore. It could be speculated whether aquatic and onshore habits followed a certain day-night rhythm, like in living hippopotamids. On the other hand, aquatic plants show a lower potential for preservation, causing an unknown taphonomical bias.

The new osteohistological data support the previous hypothesis of a semi-aquatic lifestyle in at least a variety of large caseids. Our sedimentological and palaeontological findings underpin this supposed environmental setting for *Lalieudorhynchus* (Fig. 18). Interestingly, Gand (1989: fig. 2B) had first presented this hypothesis according to questionable swimming tracks. This semi-aquatic hypothesis is in accordance with a shift to lowland dominance of caseids during the Kungurian (Reisz and Fröbisch, 2014) that underlines a general dependence from water. Moreover, our data suggest that derived, large caseids show a phylogenetic niche conservatism throughout their temporal range (see below). Future investigations should test whether or not the supposed

Figure 18. Life restoration of *Lalieudorhynchus gandi* gen. nov. et sp. nov. in its possible environment based on sedimentological and taphonomical analyses of the type locality, of the La Lieude Formation, and preliminary osteohistological observations. Associated aquatic tupilakosaurid temnospondyl (bottom left) described by Werneburg et al. (2007). Estimated water depth about 2 meters (see text), algae are possible (not preserved). Artwork by FS.

hippopotamid-like lifestyle decreased direct competition with other, contemporary herbivores. Our observations question the traditional hypothesis of fully terrestrial caseids and thereby support an ongoing debate, like similarly regarding the aquatic habits of Pareiasauridae (Kriloff *et al.*, 2008; Boitsova *et al.*, 2019).

PHYLOGENETIC ANALYSIS: CASEID INTERRELATIONSHIPS

The unique anatomy of the caseid described herein justifies the erection of a new genus. In order to test the generic validity and phylogenetic affinities of *Lalieudorhynchus gandi* gen. nov. et sp. nov. with other caseids, a phylogenetic analysis has been carried out. Romano and Nicosia (2015) provided the first comprehensive and broad analysis of caseid interrelationships. Unfortunately, various test versions with this template resulted in inconsistent positions of certain taxonomic units. Since no consensus could be gained, including methodical adaptations (Brocklehurst *et al.*, 2016b; Romano *et al.*, 2017a, b), we chosed to modifiy the dataset in order to reduce phylogenetic noise.

Concerning the taxonomic units, we concentrated on herbivorous caseids. From its description and illustrations (Olson, 1954), "*Casea*" *halselli* was deleted because it is a problematic taxon of uncertain, possibly sphenacomorph affinity.

Romano and Nicosia (2015) listed 312 morphometric characters. It is expected, however, that this number of proportional data would cause some noise during the analyses, particularly since numerous cross checks of phrased characters result in biometrical redundancy. Moreover, functional aspects and interrelationships are ignored. In consequence, these morphometric characters reveal the predominance of a mosaic pattern instead of conspicuous trends among derived caseids. As the morphometric characters support the distinctness of *Lalieudorhynchus*, including clear distinctness from any species previously assigned to *Cotylorhynchus*, they are commented on in the following, although not used for the cladistic analysis.

There are 165 qualitative (discrete) characters (#313 to 477 of Romano and Nicosia, 2015) used for the cladistic analysis and applied to 17 taxonomic units (see matrix). These characters were not completely revised, but commented with some needed corrections regarding certain taxonomic units. In the original version, 24 out of 62 postcranial characters became uninformative for the present sample.

Morphometric characters applied to *Lalieudorhynchus*:

char. 1-10: unknown

char. 11: ratio of probable ilium narrowing to its height: around 0.4 → closest to *Casea* and *Ennatosaurus*, then *Caseopsis*, differing from *Cotylorhynchus-Angelosaurus* and others with higher ratios

char. 12: ratio of probable ilium narrowing to itsdorsal width: around 0.7 → middle to the range of *Cotylorynchus* spp. and the even wider range of *Angelosaurus* spp.

char. 13: ratio of probable ilium dorsal width to possible acetabulum position: around 0.9, if correctly interpreted → close match with *Angelosaurus*; interestingly, no species of *Cotylorhynchus* was scored by Romano and Nicosia (2015), but should be seemingly higher, according to Stovall *et al.* (1966)

char. 14: ratio of probable ilium height to its dorsal width: around 1.5 → considering the incomplete condition of the preserved ilium, this ratio could be markedly lower, however a close match with *Ennatosaurus* is seen, followed by *Cotylorhynchus* spp.

char. 15: ratio glenoid width to scapulocoracoid total height: around 0.35 → within the narrow spectrum of various caseids

char. 16, 19, 20, 22: left out for morphometrical uncertainties regarding how the posterior extension of the coracoid is defined in the measurements

char. 17: ratio scapular narrowing to scapular dorsal width: around 0.6 → exceeding the known caseid range from ca 0.7 in *Angelosaurus romeri* to ca. 1.1 in "*Cotylorhynchus" hancocki*

char. 18: ratio scapulacoracoid width to scapulocoracoid height: 0.75 → within the spectrum of *Cotylorhynchus*; *Angelosaurus* appears similar according to Romano and Nicosia (2015: App. S6, Pl. 3)

char. 21: ratio scapula dorsal width to scapulocoracoid total height: higher than 0.55 → matches *Angelosaurus romeri* more than *Cotylorhynchus* spp.

char. 23: ratio femoral proximal width to femur length: around 0.37 → best matches with *Ruthenosaurus* and *Cotylorhynchus bransoni*, followed by *Casea* and *Cotylorhynchus romeri*, well distinguished from *Angelosaurus*, *Trichasaurus* and *Caseopsis*

char. 24: ratio femoral distal width to femur length: around 0.37 → close to *Ruthenosaurus*, followed by *Casea* and *Cotylorhynchus* spp., well distinguished from *Angelosaurus* as well as "*Cotylorhynchus" hancocki*

char. 25: ratio femoral shaft narrowing to femur length: around 0.18 → right within a narrow range of caseids, although distinct from *Casea*, *Trichasaurus*, and "*Cotylorhynchus" hancocki*

char. 26: ratio width of anterior femoral condyle to femur length: around 0.18 (uncertain orientation of measurement) → within narrow range of most caseids, well distinguished from *Trichasaurus*, *Ruthenosaurus* and *Angelosaurus dolani*

char. 27: position of fourth trochanter (ratio): uncertain point for measurement → due to the far distal position, the only match would be *Angelosaurus greeni*, followed by *A. romeri*; in this char. 27 (and redundant in char. 31), *Ruthenosaurus* is left out, but distinct from *Lalieudorhynchus* by a markedly proximal fourth trochanter

char. 28: ratio femoral proximal width to femoral distal width: around 1 → closest between *Cotylorhynchus romeri* and *Angelosaurus* spp.

char. 29: ratio femur shaft narrowing to femoral proximal width: redundant information from ratios already included; ratio around 0.5 matches with *Cotylorhynchus* and *Ruthenosaurus*

char. 30: ratio width of posterior femoral condyle to proximal width of femur: around 0.56 → matches *Cotylorhynchus* (not "*Cotylorhanchus" hancocki*) and *Angelosaurus* (not *A. greeni*)

char. 31: ratio position of fourth trochanter to femur proximal width: uncertain point for measurement → due to the far distal position of the trochanter, the closest match would be *Angelosaurus greeni*, although redundant with char. 27

char. 32: ratio femoral shaft narrowing to femur distal width: redundant information from ratios already included; ratio around 0.45 is between that of "*Cotylorhynchus"* (not *C. romeri*), less similar to *Ruthenosaurus* and *Angelosaurus* (not *A. greeni*)

char. 33: left out for both redundant information and undefined

point of measurement for position of fourth trochanter

char. 34, 35: left out due to redundancy with above ratios

char. 36: ratio width of anterior femoral condyle to width of posterior femoral condyle: uncertain due to undefined orientation of measurement; ratio around 0.83 is closest to that of *Trichasaurus*, followed by *Caseopsis*

char. 37-312: unknown in *Lalieudorhynchus*

char. 478-482 (Romano *et al.*, 2017a: app.2): unknown in *Lalieudorhynchus.*

Discrete morphological characters:

char. 313-415: unknown in *Lalieudorhynchus* (cranial)

char. 416-419: unknown in *Lalieudorhynchus*

char. 420: keel characteristic of sphenacodontids → uninformative for ingroup

char. 421: unknown → difficult to prove in disarticulated skeletons

char. 422-425: uninformative for ingroup

char. 426: plane and widely spaced prezygapophyses occur in *Casea* and *Trichasaurus* (plesiomorphic condition, if possibly confirmed for *Oromycter*); concave and contacting prezygapophyses are scored for all species assigned to *Cotylorhynchus*, two of *Angelosaurus*, and *Ruthenosaurus*; *Alierasaurus* is scored as unknown. *Lalieudorhynchus* is considered to reflect the apomorphic condition, but lacks the concavity in its prezygapophysial facts. The closely spaced prezygapophyses are reconstructed for dorsal vertebrae, with resemblance to the narrow processes in caudals

char. 427: widely spaced postzygapophyses are shared by *Casea*, *Trichasaurus*, *Cotylorhynchus romeri*, *Ennatosaurus*, *Ruthenosaurus*, *Angelosaurus dolani* and *A. greeni*. Narrow postzagapophyses are present in "*Cotylorhynchus" bransoni* and *hancocki*, and also in *Lalieudorhynchus*. *Alierasaurus* is scored as unknown

char. 428: the hyposphene is missing in all caseids but "*Cotylorhynchus" hancocki* and *Lalieudorhynchus* (dorsals to caudals)

char. 429: long diapophyses are common to caseids → uninformative for ingroup

char. 430: anteriorly placed diapophyses are absent in *Casea*, but present in *Trichasaurus* and more derived caseids → largely uninformative for more derived caseids

char. 431: laterally expanded spine tips are absent in *Casea*, but present in more derived caseids including "*Casea*" *nicholsi*, *Ruthenosaurus*, *Ennatosaurus*, species assigned to *Cotylorhynchus* and *Angelosaurus*, as well as *Alierasaurus*. In all of the preserved spines throughout the column of *Lalieudorhynchus*, the tip is narrow, with the possible exception of one sacral. This condition represents an autapomorphy.

char. 432: Of the taxa included in former analyses, only *Dimetrodon* and *Edaphosaurus* exhibit hyperelongated spines. The erroneous coding of *Ruthenosaurus* with "2" is not defined, thus corrected. → unsuitable for ingroup.

char. 433: curved ribs are common among caseids → uninformative for ingroup

char. 434: the (mostly) low rib tubercle is cup-shaped in *Cotylorhynchus romeri*, *Angelosaurus romeri*, *Alierasaurus*, *Ruthenosaurus* and *Lalieudorhynchus*; this structure is absent in *Ennatosaurus* and *Casea*

char. 435: the first sacral rib of *Ruthenosaurus* was scored as being enlarged, which was corrected as it does not match its published description (Reisz *et al.*, 2011), though differing from *Lalieudorhynchus* in details of the shape. Similar-sized sacral ribs are typical of all caseids, with the exception of *Casea* (LeBlanc and Reisz, 2014). → largely uninformative for more derived caseids

char. 436: increased number of sacrals → uninformative for ingroup

char. 437-441: unknown in *Lalieudorhynchus*

char. 442: *Euromycter* and *Ennatosaurus* had been scored as sharing a singular coracoid (like in *Limnoscelis*). Instead, neither Olson (1968) nor Romano *et al.* (2017a, b) confirm this condition in *Ennatosaurus*. For *Euromycter*, only the metacoracoid is preserved (Sigogneau-Russell and Russell, 1974). Therefore, these two scorings were corrected. → uninformative for ingroup

char. 443-444: uninformative for ingroup

char. 445: supraglenoid foramen absent in *Casea* and more derived caseids, with "*Cotylorhynchus" hancocki* being the only exception, based on observations of Benson (2012: Appendix S1, #174); requires confirmation. *Lalieudorhynchus* is now the only other known taxon in which it is the case

char. 446: supraglenoid foramen of "*Cotylorhynchus" hancocki* (char. 445) is scored as placed immediately above the glenoid, like in *Lalieudorhynchus* → uninformative for ingroup

char. 447-448: uninformative for ingroup

char. 449-452: unknown in *Lalieudorhynchus*

char. 453: uninformative for ingroup

char. 454-462: unknown in *Lalieudorhynchus*

char. 463: prominent femoral trochanter is plesiomorphic → uninformative for ingroup

char. 464: uninformative for ingroup

char. 465: posterior intertrochanteric ridge absent in caseids including in *Lalieudorhynchus*) → uninformative for ingroup

char. 466: anterior condyle on distal femur not compressed in *Ruthenosaurus* and *Caseopsis*, otherwise scored as compressed for remaining caseids. In *Lalieudorhynchus*, the flat compression like in *Cotylorhynchus* und *Angelosaurus* is not present. Generally, the character is hard to score since it seems to be rather continuous (Olson, 1968: fig. 20), so *Lalieudorhynchus* is scored as unknown.

char. 467-468: unknown in *Lalieudorhynchus*

char. 469: astragalus is common to amniotes → uninformative for ingroup

char. 470: neck of astragalus is scored as being long in all caseids. This was corrected, as the indeed long condition of *Casea* and *Ennatosaurus* is shared also by *Caseoides* (Olson and Beerbower, 1953: fig. 4), whereas the astragalus neck is short compared to the overall element in all three species assigned to *Cotylorhynchus* and *Angelosaurus dolani* (Stovall *et al.*, 1966. fig. 16; Olson, 1968:fig. 18). The short condition is also scored for *Lalieudorhynchus*.

char. 471-474: unknown in *Lalieudorhynchus*

char. 475: common to caseids → uninformative for ingroup

char. 476: ungual shape of sphenacomorphs → uninformative for ingroup

char. 477: unknown in *Lalieudorhynchus*; useful synapomorphy of the genus *Cotylorhynchus*, now also with *Alierasaurus* (Romano *et al.* 2017a, b).

Our new matrix comprises 165 discrete characters (#313 to 477 of Romano and Nicosia, 2015) and 17 taxa.

Data matrix, reduced version of Romano *et al.*, 2017a (app. 3); recodings are in **bold**:

Casea 11100 12100 11110 ?11?? 00101 0?0?? ?0??? ???0? ?12?? ?0112 00001 00001 10100 00111 10120 0100? 1?0?1 21100 10110 00101 ?0?10 00010 00000 01000 11111 ????? 0010? 01020 ?0000 20010 00010 111?? ??100

Caseopsis ????? ????? ????? ????? ????? ????? ????? ????? ????? ????? ????? 00??? 1?1?0 ????? ????? ????? 1???? ????? ????? ????? ????? ????? ????? ????? 12??? ????? ????? ?1030 0???? ????? 0000? 1???? ??1??

Caseoides ????? 0???? ????? ????? ????? ????? ????? ?100? ????? 000?0 ??**1**?? ??100

"*Casea*" *nicholsi* ?1?0? ????? ????? ????? ????? ????? ????? ????? ????? ??1?? ????? ????? ??1?? ????? ?0??? ????? ????? ????? ????? ????? ???1? ????? ?00?? ?1?10 1?111 ????? ????? ????0 ????? ???10 0???? ?1110 111?0

Trichasaurus ????? ???1? 00?00 ?11?0 ??11? ????? ????? ?10?? 0??00 ????0 0?01? ????? ???0?

Cotylorhynchus romeri 11100 12100 ?1110 12111 00111 00000 00101 00?11 ?2202 001?2 10001 00001 10100 00011 10111 110?0 11?11 21100 11111 00?00 ?0?12 00010 00010 01110 12111 01110 0010? 01030 0?011 11011 00010 ?1**0**00 00101

"*Cotylorhynchus" bransoni* ????? ??1?? ????? ????? ????? ????? ????? ????? ????? ????? ????? 00??1 101?0 ????? ????1 110?? ????? ????? ????? ????? ????? ??010 00011 01110 1?11? 01110 0010? 01030 0?011 110?1 00010 11**0**00 00???

"*Cotylorhynchus"* hancocki ?110? ????0 ????? ?2111 001?1 ????? ????? ????? ?22?? ????? ?001? 00?01 10100 00??1 1011? ????? 1???1 ?11?? 1??1? ?0?0? ???0? ??010 00011 11110 1?111 01110 00010 01030 01011 110?1 00010 11**0**?? 0??01

"*Angelosaurus" romeri* ??1?? ??10? ????? ????? ????? ????? ????? ????? ????? ????? ???0? 00??1 201?0 01??1 10111 110?? ????1 211?? ???1? ????? ????? ??01? 00010 01110 1211? ?1110 0010? 01030 01011 110?? 0001? ????? ??1??

Angelosaurus dolani ????? ???1? 00010 01110 ??11? ????? ????? ?1030 01?11 110?1 00010 ?1**0**?? ???00

"*Angelosaurus" greeni* ????? 0001? ????? ?????

Ruthenosaurus ????? ???2? 00010 0111**0** 12**1**1? ????? 0?1?? ????? ?101? 1???? 00000 ????? ?????

Ennatosaurus 11100 12100 11110 11111 00011 0?000 00102 00011 02002 0011? 00011 00001 20100 ??1?1 111?1 11000 ?1??1 2?100 11111 00100 000?2 0?0?0 0?0?0 ?1??0 1111? ??11**0** 0010? ????0 ??0?? 21?1? ????? ?1100 00?0?

Euromycter 11??0 12100 11110 1111? ?0?11 0000? ?0?01 20001 01202 00112 20001 00001 20100 00111 10121 ?10?1 11011 21100 ?1?11 0?1?? 000?2 0?0?? ????? ????? ????? 0?11**?** ????? ????? ????? ???1? ????? ??11 111??

Oromycter 1???? ??100 ??010 ?1001 00?01 00??? ????? ????? ????? ????? 1001? 00001 00110 ????? ????? ????? ????? ????? ??10 ?1?1? ????? ????? ????? ????? ????? ????? ????? ????? ????? ????? ????? ????? ??100

Alierasaurus ????? ??0?? ?1?10 12??? ????? ????? ????? ????? ????? ????? 1???? ??101

Lalieudorhynchus ????? ??0?? 00011 11100 1211? ????0 00010 0???? 0???? ????? 000?? ?10?? ??1??

Results of phylogenetic analysis:

Our analysis was performed using PAUP* 4.0b10 (Swoford 2001) with iterative tests, starting with a heuristic search that was interrupted after more than 50.000 trees (no ordered characters, no weighting of certain states). Despite of the optimized (noise-reduced) dataset, the strict consensus tree obtained is not completely resolved. The 50%-majority-rule consensus tree proposes the following topology: *Oromycter* + ([unresolved remaining units] + (*Cotylorhynchus romeri* + (*Ruthenosaurus* + *Caseopsis*) + (*Alierasaurus* + (*"Cotylorhynchus" bransoni*. + (*"Cotylorhynchus" hancocki* + *Lalieudorhynchus*)))). In subsequent tests, taxonomic units were deleted stepwise in order of their incompleteness of scored lines: *Angelosaurus greeni* (scored for only 4 characters), *Alierasaurus* (10), *Caseoides* (12), *Caseopsis* (19), and *Trichasaurus* (20). The heuristic tree after deletion of *Angelosaurus greeni* reads as such: *Ennatosaurus* + (*Angelosaurus dolani* + *Angelosaurus romeri* + (*Alierasaurus* + *Cotylorhynchus romeri* + (*Ruthenosaurus* + *Caseopsis*) + (*"Cotylorhynchus" bransoni*. + (*"Cotylorhynchus" hancocki* + *Lalieudorhynchus*)))). The deletion of *Alierasaurus* caused no further changes in the tree topology. After the deletion of *Caseoides*, it was possible to switch from heuristic to branch-and-bound search, without further changes in the topology of the tree (50%-majority-rule consensus of 495 trees). After the deletion of *Caseopsis*, the majority-rule consensus of 945 trees plots *Cotylorhynchus romeri* in a higher position, now occurring as the sister taxon to the clade ("*C." bransoni* + ("*C." hancocki* + *Lalieudorhynchus*)). Moreover, this tree portion is fully resolved in the strict consensus. Finally, after the deletion of *Trichasaurus*, the majority-rule consensus of 105 trees gives: *Oromycter* + (*Casea* + ("*Casea*" *nicholsi* + (*Euromycter* + (*Ennatosaurus* + (*Ruthenosaurus* + *Angelosaurus dolani* + *Angelosaurus romeri* + (*Cotylorhynchus romeri*. + (*"Cotylorhynchus" bransoni* + (*"Cotylorhynchus" hancocki*. + *Lalieudorhynchus*)))))))).

The additional deletion of *Ruthenosaurus* did not change the topology. When including *Alierasaurus* again, the majority-rule consensus of 115 trees ends with: *Cotylorhynchus romeri* + (*"Cotylorhynchus" bransoni* + *Alierasaurus* + (*"Cotylorhynchus" hancocki* + *Lalieudorhynchus*)). The stepwise deletion of less known taxonomic units continuously increased the resolution of the tree consensuses, without any

wildcard taxon. This underlines that discrete characters reveal signals of true phyletic trends, though basing on only few steps. In contrast to that, the morphometric characters are of minor contribution, since our results largely resemble those of the cited previous analyses. Nonetheless, this analysis remains preliminary pending a detailed redecriptions of species like those assigned to *Angelosaurus*. In the light of incomparable and missing information, the calculation of additional robustness values would not support our state-of-the-art understanding of caseid phylogeny. For reliably character histories and a robust phylogenetic resolution, more appropriate and specific characters are needed, regarding all major parts of the skeleton. So far, cladistics often base on cranial characters to a disproportional degree. For example, scoring widened phalanges as a discrete character would support a closer relationship between *Euromycter* and *Cotylorhynchus* than with "*Casea*" *nicholsi* (e.g., Spindler *et al.*, 2016: fig. 7F). Moreover, the juvenile status of most of the material of *Ennatosaurus* deserves further investigation.

The tree hypothesis resulting from our analysis (Fig. 19) suggests a close relationship of *Lalieudorhynchus gandi* gen. nov. et sp. nov. with "*Cotylorhynchus*" *hancocki*, as seen in the above diagnosis. The synapomorphies of this clade are the unique presence of a hyposphene (character 428), as well as the presence and position of the supraglenoid foramen (characters 445, 446). Along with "*Cotylorhynchus*" *bransoni*, this apical clade is unequivocally characterized by closely spaced postzygapophyses (character 427). Nonetheless, both morphological and morphometrical characters (see comments listed above) strongly question the conspecifity of these forms. A striking trait is the presence of narrow dorsal and sacral neural spine tips, found only in *Casea* and *Lalieudorhynchus* (character 431).

Species groups assigned to *Cotylorhynchus* and partly those assigned to *Angelosaurus* appear to plot in tree positions not too far from each other, therefore suggest narrower relationships than found by previous workers (Romano and Nicosia, 2015; Brocklehurst *et al.*, 2016b). In fact, these genera may not even be monophyletic, because they have not always been recovered as such in recent analyses (e.g., Benson, 2012; Brocklehurst *et al.*, 2016a; Brocklehurst and Fröbisch, 2017; Berman *et al.*, 2020). These taxa deserve detailed revisions to tests their possible conspecifity. For now, we prefer to restrict the use of these two genera to their type species in this study.

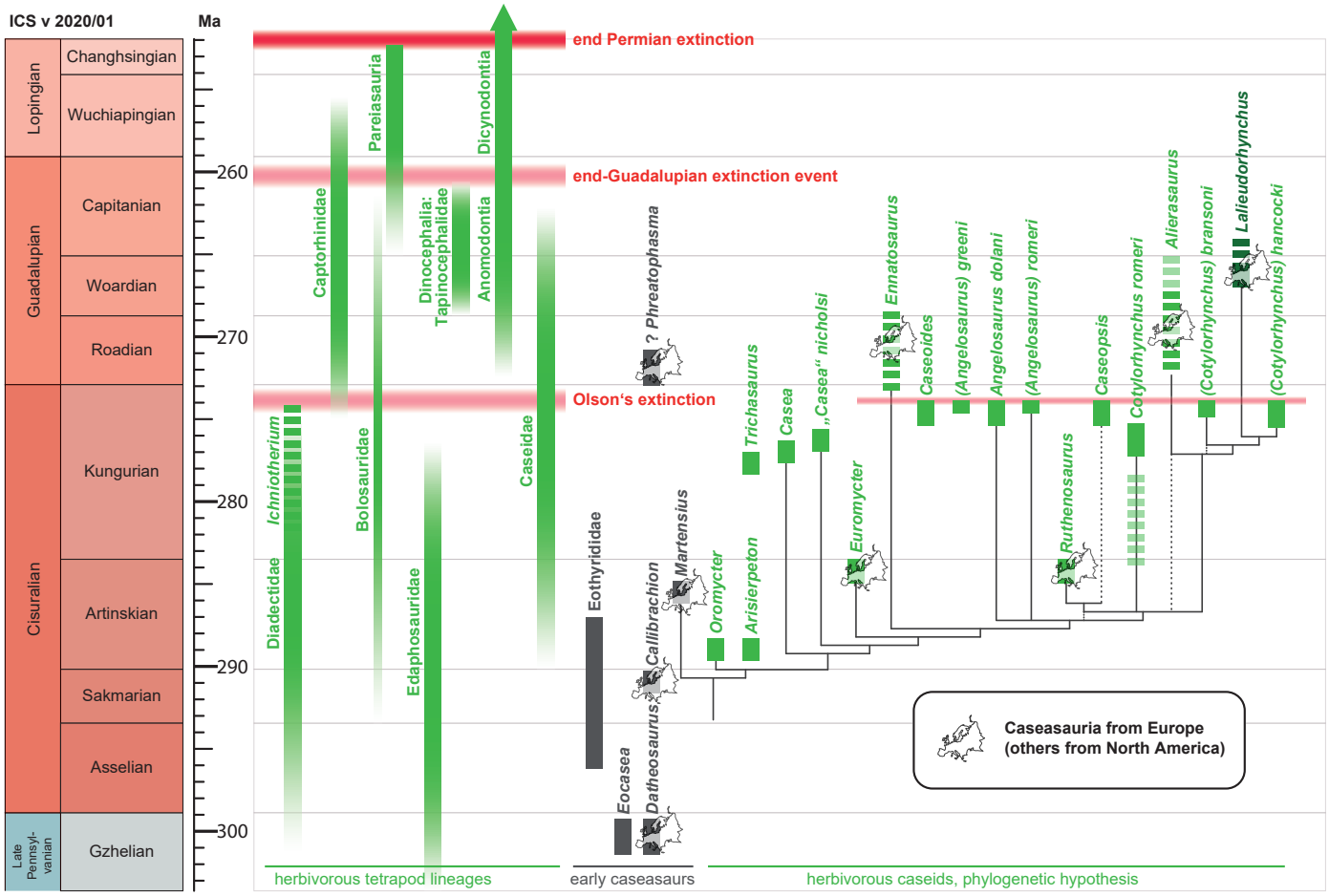

Figure 19. Stratigraphic range of Palaeozoic high-fiber herbivorous tetrapods (left) and time-calibrated phylogenetic hypothesis for Caseidae (right). Early, carnivorous representatives added for outgroup information; uncertain tree positions of Caseidae lack branching. The caseids appear as a clade of large herbivores that persist after the Olson's extinction (ranges and phylogenetic positions from Reisz and Fröbisch, 2014; Brocklehurst and Fröbisch, 2017; Lucas, 2018a; Lucas and Golubev 2019; Schneider et al. 2020; and our study). Dotted taxon bars mean less precise stratigraphic range. Dotted tree lines stand for uncertain or alternative relationships.

EVOLUTIONARY HISTORY OF CASEIDAE

Based on the tree obtained by our phylogenetical analysis, along with temporal ranges of other Palaeozoic herbivores (Fig. 19), we tentatively discuss the evolutionary history of the Caseidae.

Early caseasaurs are very rare, leaving their spatial origin unknown. The Pennsylvanian caseid *Eocasea* and the Cisuralian eothyridids *Eothyris*, *Oedaleops* and *Vaughnictis* are from North America. The Pennsylvanian caseid *Datheosaurus* is from Europe. The Cisuralian basal and faunivorous caseids *Callibrachion*, *Martensius* and possibly *Phreatophasma* are known from Europe. It is possible, though basing on patchy sampling, that the North American eothyridids and the European early caseids represent ecological equivalents. The presence of faunal provinces, however, is challenged by the first appearance of herbivorous caseids in North America during the Artinskian (*Oromycter* and *Arisierpeton* from the same fauna, Reisz 2005, 2019). The record of both faunivorous and herbivorous early caseids in rare inland (*Martensius*) and upland localities (*Oromycter*, *Arisierpeton*) suggests that this trophic diversification took place in the extra-basinal realm.

Large herbivorous caseids were supposed to invade into or radiate in lowland habitats as late as the Kungurian, as suggested by Reisz and Fröbisch (2014). This temporal gap is bridged by the stratigraphical re-evaluation of the caseids from the Rodez Basin, *Euromycter* and *Ruthenosaurus* (this study). These two genera are distantly related, confirming that the increased diversification of caseids dates back to the Artinskian. This was paralleled by a considerable selection toward a larger size (Reisz and Fröbisch, 2014; Brocklehurst and Brink, 2017). The long ghost lineage towards *Casea* bears the possibility of an increased autapomorphic nature. Therefore, *Euromycter* might be called a more fitting approximation for the ancestral morphology of large, *Cotylorhynchus*-like caseids.

Figure 19 also shows a gap in the caseid record during the early Kungurian, with multiple ghost lineages. An older Kungurian or even Artinskian age for *Cotylorhynchus* has also been assumed but not demonstrated so far (S. Lucas, pers. comm. 2019). As late Kungurian caseids (*Caseoides*, *Caseopsis*, forms assigned to *Angelosaurus* and to *Cotylorhynchus*, as well as *Casea* partim.) are of similar tree positions like the late Artinskian forms, this gap does not hide a major ecological transition within this clade. The early Kungurian hiatus in the caseid record may reflect a climatic and sedimentological bias in the recorded basins (see fig. 2 in Schneider *et al.*, 2020). Moreover, instead of reconstructing ecological or biogeographical signals, we expect Lagerstätten effects implied by the obvious geographical grouping of the stratigraphical record (European herbivorous caseids all from the late Artinskian or Guadalupian; North American finds strictly alternate with them, being from the early Artinskian or late Kungurian).

In the late Kungurian, caseids appear as the predominant and most diverse tetrapod herbivores (Brocklehurst, 2020). This could be linked to specific climatic conditions, such as increased aridity, and by this possibly reflects biome shift patterns (Spindler, 2019: fig. 6). This diverse episode in caseid evolution may represent a partial guild succession induced by the decline of two older herbivore communities, the swamp-related faunas with edaphosaurids and the seemingly more tolerant diadectid faunas. Diadectidae are ichnologically reported until the Kungurian-Roadian boundary (see Schneider *et al.*, 2020, fig. 19), with uncertain diet of the trackmakers background. For a rejection of the diadectid status of the Lopingian *Alveusdectes* see Spindler *et al.* (2019).

Altogether, the renewed stratigraphical evaluation (Fig. 19) suggests a Cisuralian radiation, contrary to previous hypotheses which suggested a rather Guadalupian radiation (Reisz, 1986; Brocklehurst and Fröbisch, 2017). To some extent, the Olson's gap issue around the Kungurian-Roadian transition may mask this. The nature of Olson's gap is subject to a recent debate (Brocklehurst *et al.* 2017; Olroyd and Sidor, 2017; Brocklehurst 2018; Lucas and Golubev, 2019), now strongly supported to represent an extinction event rather than a real hiatus (Brocklehurst, 2020). The caseid diversity largely declined during Olson's extinction, as far as visible under the alluded Lagerstätten effects. The Guadalupian caseids *Ennatosaurus*, *Alierasaurus* and *Lalieudorhynchus* imply that two or three lineages (depending on the tree resolution) persisted beyond this end-Kungurian extinction event.

Apart from the markedly smaller bolosaurid parareptiles, caseids are the only herbivorous tetrapods that survived Olson's extinction, as well as Captorhinidae, which evolved definite herbivorous forms during this phase. Larger captorhinid eureptiles may partially have replaced the diadectid and caseid predominance (Brocklehurst and Brink, 2017; Reisz and Fröbisch, 2014: fig. 4), with so far unknown biogeographic differentiation. During the Guadalupian, caseids may have occupied different ecological niches than those of other herbivorous clades such as moradisaurine captorhinids, early anomodonts (including early dicynodonts) and tapinocephalid dinocephalians. Most of these herbivores have also undergone a turnover during the less understood end-Guadalupian extinction event, during which dinocephalians became extinct (Lucas, 2009, Day *et al.*, 2015; Lucas in Schneider *et al.*, 2019: p.28). From the revised record, the Caseidae disappeared prior to that, around the earliest Capitanian. Previously, Lopingian *Chelichnus* tracks had been assigned to caseid trackmakers (Silva *et al.*, 2012), but they were later demonstrated to belong to therapsids (Krapovickas *et al.*, 2015). Subsequent to the last occurrence of caseids, pareiasaurs and dicynodonts rose as the new predominant large herbivorous tetrapods, while dinocephalians likewise declined (Olroyd and Sidor, 2017).

The here time-calibrated tree hypothesis for caseid interrelationships has been compared to the stratigraphic range of Paleozoic tetrapod herbivore clades (Fig. 19) to propose a history of this ecological guild. The rise of the caseids during the Kungurian and their decline during the middle Guadalupian are indeed rather simultaneous to the rise and decline of other comparable herbivores. Furthermore, during the presumed caseid heyday around the Kungurian-Roadian transition, moradisaurine captorhinids represented the only contemporary herbivores of greater body sizes. Despite differences in their latitudinal distributions, specific food sources and niche availability, or resilience against aridification, caseids appear to have taken part in an evolution of episodic herbivore assemblages. Interestingly, plant diversity exhibits a significant co-evolution with herbivores, as certain crises occurred in both groups (Brocklehurst *et al.*, 2020). Although being at least partially aquatic, caseids are no exceptional component of their assemblages. Instead, they were normal representatives of the megaherbivorous guild, interlinked with the evolution of other Paleozoic herbivores in terms of competition and replacement. This, in turn, suggests that much of their diet was browsed onshore.

Regarding the paleobiogeography, the majority of derived caseids comes from the paleo-equatorial belt. However, the occurrence of *Ennatosaurus* in Russia opens the expectation of Gondwanan finds, although no caseid has yet been reported from the well-sampled Karoo System basin or the growing number of other African localities. Despite a possible Lagerstätten effect, which may mask the true stratigraphic extinction, caseids may have survived in Europe thanks to regional differences, similar to those found during the Carboniferous-Permian transition (Pardo *et al.*, 2019) or the end-Guadalupian extinction event (Olroyd and Sidor, 2017).

CONCLUSIONS

The Lodève Basin in Southern France is besides the Nurra region of Sardinia (Italy) one of the rare areas in Europe where fossiliferous late Cisuralian and Guadalupian sediments are exposed: the Guadalupian wet red beds of the French La Lieude Formation and of the Italian Cala del Vino Formation were deposited in the Permian paleo-equatorial belt under subhumid to semiarid conditions (biome 2 of Ziegler, 1990) as indicated by facies architectures, vegetation, and paleosols. Large caseids were evolving in these environments.

The new caseid *Lalieudorhynchus gandi* gen. nov. et sp. nov. is defined by five apomorphies: a transverse section of the sacral and anterior caudal neural spines with a very thin keel-like process anteriorly, a slender dorsal tip of the dorsal and caudal spines, a narrow distal end of the first sacral rib, a fossa on triceps process of metacoracoid, and a very large distal tarsal 1 of same width than the astragalus, with nearly all sides being shallowly concave.

Lalieudorhynchus is closely related to the robust and large "*Cotylorhynchus" hancocki* with which it shares the same supraglenoid foramen, a process-like bulged anteromedian margin of the scapula, a greatly dorsally elongated neural spine of the first sacral and first caudal vertebrae, a large pronounced internal trochanter, and an astragalus that is nearly as broad as long.

Our anatomical and histological observations suggest that this caseid may have spent time underwater. Yet our sedimentological analysis, together with the associated flora, suggests it may have browsed outside water. The mixture of mature and immature ontogenetical characters is consistent with a possible semi-aquatic lifestyle.

The radiation of large herbivorous caseids started during the Artinskian. Contrary to previous hypotheses, most of these *Cotylorhynchus*-type caseids are from the late Kungurian, prior to Olson's gap or extinction.

The genus *Lalieudorhynchus* (Woardian-Capitanian) is the stratigraphically youngest caseid. Along with *Ennatosaurus* and *Alierasaurus*, it confirmes a caseid persistence during the Guadalupian, at least in Europe where they represent the only megaherbivores bridging from the Cisuralian to the Guadalupian.

AUTHORS' CONTRIBUTIONS

RW carried out documentation, anatomical description, figures and diagnosis of the new taxon, with great input on the discussion. FS was responsible for phylogeny and writing up the evolutionary history as well as conclusions on the living environment up to the artwork. JF analyzed the ontogenetic stage, partly anatomy, contributed the age discussions, realized the table and provided important input on the phylogeny. JSS wrote the abstract, the introduction, most of the bone histology, and provided important input on the entire manuscript. MVL supported the excavations and were included to geological background analyses and discussion. JWS delivered the geological background and stratigraphy including sedimentology and taphonomy, as well as important input on the entire discussion.

ACKNOWLEDGMENTS

This publication is dedicated to Georges Gand (UB) and to the memory of Jacques Garric (ex Compagnie Générale des Matières nucléaires) who realized intensive researches in the Lodève Basin in the framework of the Convention for Study of the Permian of the Lodève and Saint-Affrique Basins (Gand *et al.*, 2000). We thank the Ollier's family (the regretted Simone, her son Pierre and nephews) for their field authorizations and hospitality. Our excavation team thank Gaz de France, the Direction Régionale de l'Environnement, the Direction Départementale de l'Agriculture et de la Forêt, and the Service Territorial de l'Architecture et du Patrimoine for their field authorizations in this protected area. We thank the Municipality of Brénas for its help, M. Lacoste, Maryse and François Alysse for their support. We thank Frank Körner (now Lausitz Energie Bergbau AG, Cottbus, Germany) who greatly improves the knowledge on the Permian Lodève Basin in the frame of his PhD research (DFG-Schn PhD-project 408/7), and who discovered both femora and a large rib of this caseid. We thank the excavation team of international students and colleagues from the FG, UM, MNHN, who worked hard during the 2004-2009 excavations, especially Jan Brückner and Berit Legler, who measured together with JWS sections 1 and 2, Olivier Béthoux and Damien Germain (both MNHN), Josep Fortuny (Institut Català de Paleontologia), Sophie Hervet (ex Rhinopolis Association), Michel Lopez (UM), Jean Lapeyrie and Stéphane Fouchet (both Musée de Lodève). Georg Sommer (NHMS) and Suzanne Jiquel (UM) are also thanked for the very careful preparation of the skeleton. Michael Magnus is thanked for the preparation of the thin section of a rib and Ilja Kogan for the photographs of this thin section (both FG). Birgit Gaitzsch helped with sedimentological interpretations and made together with Nailia Rizatdinova the photography of the juvenile triopsid (both FG). We thank Robert R. Reisz (University of Toronto) for first suggestions on the first-discovered elements of this new caseid and Christen Shelton (New Jersey State Museum) for fruitful discussions regarding caseid histology, ontogeny, and evolution. Bill DiMichelle (NMNH Smithsonian Institution, Washington), Jean Galtier (UM), and Hans Kerp (University of Münster) helped with the determination of plant remains. Michel Lopez (UM), Lily Pfeifer (University of Oklahoma), Spencer G. Lucas (New Mexico Museum of Natural History), Lorenzo Marchetti (Museum für Naturkunde Berlin), Aussonio Ronchi (University of Pavia), and Sebastian Voigt (Urweltmuseum GEOSKOP Thallichtenberg) are thanked for fruitful discussions and English improvements. Steffen Trümper and Sebastian Germann (both FG) helped with computer graphics. JWS gratefully acknowledges the financial support provided by the German Research Foundation (DFG) by the grants DFG-Schn 408/7, and DFG-Schn 408/22 as well as the Russian Government for a subsidy allocated to Kazan Federal University for the state assignment

no. 5.2192.2017/4.6. JSS and JF were supported by regular credits from the CNRS (UMR5143, UMR7207) granted by the Ministère de l'Enseignement supérieur et de la Recherche. MVL thank the UM and the Paleontological Department of the Institut des Sciences de l'Évolution (UM, CNRS, IRD and EPHE) for substantial supports and the Master PPP (UM) which allowed excavation's internships. This publication contributes to the tasks of the "Nonmarine–Marine Correlation Working Group" of the Subcommissions on Carboniferous Stratigraphy (SCCS), Permian Stratigraphy (SPS), and Triassic Stratigraphy (STS). The authors thank the anonymous reviewers for their constructive work.

BIBLIOGRAPHY

Barthel, M., 2009. Die Rotliegendflora des Thüringer Waldes. Veröffentlichungen Naturhistorisches Museum Schleusingen, Sonderveröffentlichung 2009, 163 pp.

Behrensmeyer, A. K., 1991. Terrestrial Vertebrate Accumulations. In: Allison, P.A., Briggs, D. E. G., Taphonomy. Releasing the Data Locked in the Fossil Record. Topics in Geobiology, Volume 9, Plenum Press, New York, London, 291-335. https://doi.org/10.1007/978-1-4899-5034-5_6

Benson, R. B. J., 2012. Interrelationships of basal synapsids: cranial and postcranial morphological partitions suggest different topologies. Journal of Systematic Palaeontology 10, 601-624. https://doi.org/10.1080/14772019.2011.631042

Berman, D. S., Henrici, A. C., Sumida, S. S., Martens, T., Pelletier, V., 2014. First European record of a varanodontine (Synapsida: Varanopidae): Member of a unique Early Permian upland paleoecosystem, Tambach Basin, central Germany. In: Early Evolutionary History of the Synapsida, eds. C. F. Kammerer, K. D. Angielczyk, J. Fröbisch, 69-86. New York: Springer. (Vertebrate Paleobiology and Paleoanthropology Series). https://doi.org/10.1007/978-94-007-6841-3_5

Berman, D. S., Maddin, H. C., Henrici, A. C., Sumida, S. S., Scott, D., Reisz, R. R., 2020. New primitive caseid (Synapsida, Caseasauria) from the early Permian of Germany. Annals of Carnegie Museum 86 (1), 43-75. https://doi.org/10.2992/007.086.0103

Boitsova, E. A., Skutschas, P. P., Sennikov, A. G., Golubev, V. K., Masuytin, V. V., Masuytina, O. A., 2019. Bone histology of two pareiasaurs from Russia (*Deltavjatia rossica* and *Scutosaurus karpinskii*) with implications for pareiasaurian palaeobiology. Biological Journal of the Linnean Society, 128, 289-310. https://doi.org/10.1093/biolinnean/blz094

Botha, J., 2020. The paleobiology and paleoecology of South African *Lystrosaurus*. PeerJ 8, e10408. https://doi.org/10.7717/peerj.10408

Bourges, P., Rolando, J.-P., Souquet, P., 1987. Le Permien de la partie occidentale du détroit de Rodez (France) : systèmes de dépôt, dynamique du bassin. Annales de la Société géologique du Nord 106, 173-182.

Bourquin, S., Bercovici, A., López-Gómez, J., Diez, J. B., Broutin, J., Ronchi, A., Durand, M., Arché, A., Linol, B., Amour, F., 2011. The Permian–Triassic transition and the onset of Mesozoic sedimentation at the northwestern peri-Tethyan domain scale: Palaeogeographic maps and geodynamic implications. Palaeogeography, Palaeoclimatology, Palaeoecology 299 (1–2), 265-280. https://doi.org/10.1016/j.palaeo.2010.11.007

Brinkman, D., 1988. Size-independent criteria for estimating relative age in *Ophiacodon* and *Dimetrodon* (Reptilia, Pelycosauria) from the Admiral and Lower Belle Plains Formations of West-Central Texas. Journal of Vertebrate Paleontology 8, 172-180. https://doi.org/10.1080/02724634.1988.10011695

Brochu, C. A., 1996. Closure of neurocentral sutures during crocodilian ontogeny: implications for maturity assessment in fossil archosaurs. Journal of Vertebrate Paleontology 16, 49-62. https://doi.org/10.1080/02724634.1996.10011283

Brocklehurst, N., 2018. An examination of the impact of Olson's extinction on tetrapods from Texas. PeerJ 6, e4767. https://doi.org/10.7717/peerj.4767

Brocklehurst, N., 2020. Olson's Gap or Olson's Extinction? A Bayesian tipdating approach to resolving stratigraphic uncertainty. Proc. R. Soc. B 287, 20200154. https://doi.org/10.1098/rspb.2020.0154

Brocklehurst, N., Brink, K. S. 2017. Selection towards larger body size in both herbivorous and carnivorous synapsids during the Carboniferous. FACETS 2, 68-84. https://doi.org/10.1139/facets-2016-0046

Brocklehurst, N., Fröbisch, J. 2017. A re-examination of the enigmatic Russian tetrapod *Phreatophasma aenigmaticum* and its evolutionary implications. Fossil Record 20, 87-93. https://doi.org/10.5194/fr-20-87-2017

Brocklehurst, N., Reisz, R. R., Fernandez, V., Fröbisch, J., 2016a. A re-description of '*Mycterosaurus' smithae*, an Early Permian eothyridid, and its impact on the phylogeny of pelycosaurian-grade synapsids. PLoS ONE 11(6), e0156810. https://doi.org/10.1371/journal.pone.0156810

Brocklehurst, N., Romano, M., Fröbisch, J., 2016b. Principal component analysis as an alternative treatment for morphometric characters: phylogeny of caseids as a case study. Palaeontology 2016, 1-10. https://doi.org/10.1111/pala.12264

Brocklehurst, N., Day, M. O., Rubidge, B. S., Fröbisch, J., 2017. Olson's Extinction and the latitudinal biodiversity gradient of tetrapods in the Permian. Proc. R. Soc. B 284, 20170231. https://doi.org/10.1098/rspb.2017.0231

Brocklehurst, N., Kammerer, C. F., Benson, R. J., 2020. The origin of tetrapod herbivory: effects on local plant diversity. Proc. R. Soc. B 287, 20200124. https://doi.org/10.1098/rspb.2020.0124

Buatois, L. A., Màngano, M. G., 1995. The paleoenvironmental and paleoecological significance of the lacustrine *Mermia* ichnofacies: an archetypical subaqueous nonmarine trace fossil assemblage. Ichnos 4, 151-161. https://doi.org/10.1080/10420949509380122

Campione, N. E., Reisz, R. R., 2010. *Varanops brevirostris* (Eupelycosauria: Varanopidae) from the Lower Permian of Texas, with discussion of varanopid morphology and interrelationships. Journal of Vertebrate Paleontology 30, 724-746. https://doi.org/10.1080/02724631003762914

Châteaneuf, J.-J., Farjanel, G., 1989. Synthèse géologique des bassins permiens français. Mémoires du Bureau de Recherches Géologiques et Minières 128, 1-288.

Citton, P., Ronchi, A., Maganuco, S., Caratelli, M., Nicosia, U., Sacchi, E., Romano, M., 2019. First tetrapod footprints from the Permian of Sardinia and their palaeontological and stratigraphical significance. Geological Journal 54(4), 2084-2098. https://doi.org/10.1002/gj.3285

Conrad, G., Odin, B., 1984. Le bassin permien de Lodève (Hérault), Livret-guide de l'excursion. Laboratoire de Sédimentologie, Université d'Aix-Marseille. 5ème Congrès européen de Sédimentologie, Marseille, 9-11 avril 1984. Université d'Aix-Marseille, Marseille (59 pp.).

Currie, P. J., 1981. *Hovasaurus boulei*, an aquatic eosuchian from the Upper Permian of Madagascar. Palaeontologia Africana 24, 99-168.

Day, M. O., Ramezani, J., Bowring, S. A., Sadler, P. M., Erwin, D. H., Abdala, F., Rubidge, B. S., 2015. When and how did the terrestrial mid-Permian mass extinction occur? Evidence from the tetrapod record of the Karoo Basin, South Africa. Proceedings of the Royal Society B 282 (1811), 1-8. https://doi.org/10.1098/rspb.2015.0834

Diego-Orozco, A., Chen, Y., Henry, B., Becq-Giraudon, J. F., 2002. Paleomagnetic results from the Permian Rodez Basin implications: the Late Variscan tectonics in the southern French Massif Central. Geodinamica Acta 15 (4), 249-260. https://doi.org/10.1080/09853111.2002.10510757

Doubinger, J., 1974. Études palynologiques dans l'Autunien. Review

of Palaeobotany and Palynology 17 (1-2), 21-38. https://doi.org/10.1016/0034-6667(74)90089-X

Doubinger, J., Heyler D., 1959. Note paléontologique sur le Permien de Lodève et de Bourbon-l'Archambault. Bulletin de la Société Géologique de France S7-I (3), 304-311. https://doi.org/10.2113/gssgfbull.S7-I.3.304

Doubinger, J., Odin, B., Conrad G., 1987. Les associations sporopolliniques du Permien continental du bassin de Lodève (Hérault, France). Caractérisation de l'Autunien supérieur, du «Saxonien» et du Thuringien. Annales de la Société Géologique du Nord 106, 103-109.

Efremov, J. A., 1956. American elements in the fauna of Permian reptiles of the USSR. Doklady Akademii Nauk SSSR 111, 1091-1094.

Evans, M. E. 2012. Magnetostratigraphy of the Lodève Basin, France: implications for the Permo-Carboniferous reversed superchron and the geocentric axial dipole. Studia Geophysica et Geodaetica 56 (3), 725-734. https://doi.org/10.1007/s11200-010-0082-y

Evans, M. E., Pavlov, V., Veselovsky, R., Fetisova, A., 2014. Late Permian paleomagnetic results from the Lodève, Le Luc, and Bas-Argens Basins (southern France): magnetostratigraphy and geomagnetic field morphology. Physics of Earth and Planetary Interiors 237, 18-24. https://doi.org/10.1016/j.pepi.2014.09.002

Faure, M., Lardeaux, J. M., Ledru, P., 2009. A review of the pre-Permian geology of the Variscan French Massif Central. Comptes Rendus Geoscience 341, 202-213. https://doi.org/10.1016/j.crte.2008.12.001

Felice, R. N., Angielczyk, K. D., 2014. Was *Ophiacodon* (Synapsida, Eupelycosauria) a swimmer? A test using vertebral dimensions. In: Early Evolutionary History of the Synapsida, Vertebrate Paleobiology and Paleoanthropology, eds. C. F. Kammerer, K. D. Angielczyk, J. Fröbisch (Dordrecht: Springer), 25-50. https://doi.org/10.1007/978-94-007-6841-3_3

Galtier, J., Broutin, J., 2008. Floras from red beds of the Permian Basin of Lodève (Southern France). Journal of Iberian Geology 34(1), 57-72.

Gand, G., 1986. Interprétations paléontologique et paléoécologique de quatre niveaux à traces de vertébrés observés dans l'Autunien du Lodévois (Hérault). Géologie de la France, 2, 155-176.

Gand, G., 1987. Les traces de vertébrés tétrapodes du Permien français. Professorial thesis, Université de Bourgogne, Centre des Sciences de la Terre, Dijon, 341pp.

Gand, G., 1989. Essai de reconstitution paléoenvironnementale et paléoécologique d'une partie du nord du bassin de Lodève (Hérault) au Permien inférieur. Géologie de la France (4), 17-30.

Gand, G., 1993. La palichnofaune de vertébrés tétrapodes du bassin permien de Saint-Affrique (Aveyron): comparaisons et conséquences stratigraphiques. Géologie de la France 1, 41-56.

Gand, G., Durand, M., 2006. Tetrapod footprint ichno-associations from French Permian basins. Comparisons with other Euramerican ichnofaunas. In: Lucas, S. G., Cassinis, G., Schneider, J. W. (Eds.), Non-Marine Permian Biostratigraphy and Biochronology. Geological Society of London, Special Publications 265 (1), 157-177. https://doi.org/10.1144/GSL.SP.2006.265.01.07

Gand, G., Haubold, H., 1984. Traces de vertébrés du Permien du Bassin de Saint-Affrique (description, datation, comparaison avec celle du bassin de Lodève). Géologie Méditerranéenne 11 (4), 321-351. https://doi.org/10.3406/geolm.1984.1333

Gand, G., Garric, J., Lapeyrie J., 2000. Convention d'étude du Permien des bassins de Lodève et Saint-Affrique. Bulletin de la Société d'Histoire naturelle d'Autun, 171, 6-16.

Gand, G., Garric, J., Demathieu, G., Ellenberger, P., 2000. La palichnofaune de vertébrés tétrapodes du Permien supérieur du bassin de Lodève (Languedoc, France). Palaeovertebrata, 29 (1), 1-82.

Gebhardt, U., Schneider, J., 1985. *Stomochara* aus den Mansfelder Schichten (Stefan) der Saalesenke und der erste sichere Nachweis von CharaceenThalli im Paläozoikum. Freiberger Forschungshefte C 400, 37-43.

Gingerich, P. D., 2005. Aquatic Adaptation and Swimming Mode Inferred from Skeletal Proportions in the Miocene Desmostylian *Desmostylus*. Journal of Mammalian Evolution 12, 183-194. https://doi.org/10.1007/s10914-005-5719-1

Girondot, M., Laurin, M., 2003. Bone profiler: a tool to quantify, model and statistically compare bone sections compactness profiles. Journal of Vertebrate Paleontology 23(2), 458-461. https://doi.org/10.1671/0272-4634(2003)023[0458:BPATTQ]2.0.CO;2

Haldan, M. M., Langereis, C. G., Biggin, A. J., Dekkers, M. J., Evans, M. E., 2009. A comparison of detailed equatorial red bed records of secular variation during the Permo-Carboniferous Reversed Superchron. Geophysical Journal International 177 (3), 834-848. https://doi.org/10.1111/j.1365-246X.2009.04124.x

Holmes, R. B., 1977. The osteology and musculature of the pectoral limb of small captorhinids. Journal of Morphology 152, 101-140. https://doi.org/10.1002/jmor.1051520107

Holmes R. B., 2003. The hind limb of *Captorhinus aguti* and the step cycle of basal amniotes. Canadian Journal of Earth Sciences 2003, 40, 515-526. https://doi.org/10.1139/e02-039

Hounslow, M. W., Balabanov, Y. P., 2018. A geomagnetic polarity timescale for the Permian, calibrated to stage boundaries. Geological Society, London, Special Publications 450, 61-103. https://doi.org/10.1144/SP450.8

Houssaye, A., 2009. "Pachyostosis" in aquatic amniotes: a review. Integrative Zoology 4, 325- 340. https://doi.org/10.1111/j.1749-4877.2009.00146.x

Hübner, N., Körner, F., Schneider, J., 2011. Tectonics, climate and facies of the Saint Affrique Basin and correlation with the Lodève Basin (Permian, Southern France). Z. dt. Ges. Geowiss. 162, 157-170. https://doi.org/10.1127/1860-1804/2011/0162-0157

Irmis, R. B., 2007. Axial skeleton ontogeny in the Parasuchia (Archosauria: Pseudosuchia) and its implications for ontogenetic determination in archosaurs. Journal of Vertebrate Paleontology 27, 350-361. https://doi.org/10.1671/0272-4634(2007)27[350:ASOITP]2.0.CO;2

Ivakhnenko, M. F., 1990. Elements of the Early Permian tetrapod faunal assemblages of Eastern Europe. Paleontological Journal 1990, 104-112.

Körner, F., 2006. Klima- und Sedimentationsmuster des peri-tethyalen, kontinentalen Perms – interdisziplinäre Studien an red beds des Lodève Beckens (S-Frankreich). PhD thesis, TU Bergakademie Freiberg, 261 pp.

Körner, F., Schneider, J. W., Hoernes, S., Gand, G., Kleeberg, R., 2003. Climate and continental sedimentation in the Permian of the Lodève Basin (southern France). Bollettino della Società Geologica Italiana, Volume Speciale 2, 185-191.

Krapovickas, V., Marsicano, C. A., Mancuso, A. C., de la Fuente, M. S., Ottone E. G., 2015. Tetrapod and invertebrate trace fossils from aeolian deposits of the lower Permian of central-western Argentina, Historical Biology, 27, 7, 827-842. https://doi.org/10.1080/08912963.2014.904857

Kriloff, A., Germain, D., Canoville, A., Vincent, P., Sache, M., Laurin, M., 2008. Evolution of bone microanatomy of the tetrapod tibia and its use in palaeobiological inference. J. Evol. Biol. 21, 807-826. https://doi.org/10.1111/j.1420-9101.2008.01512.x

Krings, M., Klavins, S. D., Barthel, M., Lausberg, S., Serbet, R., Taylor, T. N., Taylor, E. L., 2007. *Perissothallus*, a new genus for Late Pennsylvanian-Early Permian noncalcareous algae conventionally assigned to *Schizopteris* (aphleboid foliage). Botanical Journal of the Linnean Society 153, 477-488. https://doi.org/10.1111/j.1095-8339.2007.00616.x

Lambertz, M., Shelton, C. D., Spindler, F., Perry, S. F., 2016. A caseian point for the evolution of a diaphragm homologue among the earliest synapsids. Annals of the New York Academy of Sciences 1385(1), 3-20. https://doi.org/10.1111/nyas.13264

Langston, W. J., Reisz, R. R., 1981. *Aerosaurus wellesi*, new species, a varanopseid mammal-like reptile (Synapsida: Pelycosauria) from the Lower Permian of New Mexico. Journal of Vertebrate Paleontology 1, 73-96. https://doi.org/10.1080/02724634.1981.10011881

Laurin, M., Reisz, R. R., 1995. A reevaluation of early amniote phylogeny. Zoological Journal of the Linnean Society 113, 165-223. https://doi.org/10.1111/j.1096-3642.1995.tb00932.x

LeBlanc, A. R. H., Reisz, R. R., 2014. New postcranial material of the early caseid *Casea broilii* Williston, 1910 (Synapsida: Caseidae) with a review of the evolution of the sacrum in Paleozoic non-mammalian synapsids. PLoS ONE 9 (12), e115734. https://doi.org/10.1371/journal.pone.0115734

Legler, B., Schneider, J., Gand, G., Körner, F., 2004. Playa and sabkha from northern Germany and Southern France. Workshop, IGCP 469 Central European Meeting „Freiberg 2004“, Freiberg University, 64-82.

Lopez, M., 1992. Dynamique du passage d'un appareil terrigène à une plate-forme carbonatée en domaine semi-aride : Le Trias de Lodève, Sud de la France. PhD dissertation, Université de Montpellier II, 403 pp.

Lopez, M., Gand, G., Garric, J., Galtier, J., 2005. Playa environments in the Lodève Permian Basin and the Triassic cover (Languedoc-France). Excursion, 10-12 may 2005, Association des Sédimentologistes français, 54 pp.

Lopez, M., Gand, G., Garric, J., Körner, F., Schneider, J., 2008. The playa environements of the Lodève Permian Basin (Languedoc-France). Journal of Iberian Geology 34(1), 29-56.

Lucas, S. G., 2009. Timing and magnitude of tetrapod extinctions across thePermo-Triassic boundary. Journal of Asian Earth Sciences 36 (6), 491-502. https://doi.org/10.1016/j.jseaes.2008.11.016

Lucas, S. G., 2018a. Permian tetrapod biochronology, correlation and evolutionary events. In: Lucas, S. G., Shen, S. Z. (eds.), The Permian Timescale. Geological Society of London, Special Publications 450, 405-444. https://doi.org/10.1144/SP450.12

Lucas, S. G., 2018b. Permian charophytes: distribution and biostratigraphy. Permophiles 66, 20-25.

Lucas, S. G., 2019. An ichnological perspective on some major events of Paleozoic tetrapod evolution. Bollettino della Società Paleontologica Italiana 58 (3), 223-266.

Lucas, S. G., Golubev, V. K., 2019. Age and duration of Olson's Gap, a global hiatus in the Permian tetrapod fossil record. Permophiles 67, 20-23.

Machette, M. N., 1985. Calcic soils of the southwestern United States. In: Weide, D. L., Faber, M. L. (Eds.), Soils and Quaternary Geology of the Southwestern United States, Geol. Soc. Am. Spec. Pap., 1-21. https://doi.org/10.1130/SPE203-p1

Maddin, H. C., Sidor, C. A., Reisz, R. R., 2008. Cranial anatomy of *Ennatosaurus tecton* (Synapsida: Caseidae) from the Middle Permian of Russia and the evolutionary relationships of Caseidae. Journal of Vertebrate Paleontology 28, 160-180. https://doi.org/10.1671/0272-4634(2008)28[160:CAOETS]2.0.CO;2

Marchetti, L., Klein, H., Buchwitz, M., Ronchi, A., Smith, R. M., De Klerk, W. J., Sciscio, L., Groenewald, G. H., 2019. Permian–Triassic vertebrate footprints from South Africa: ichnotaxonomy, producers and biostratigraphy through two major faunal crises. Gondwana Research 72, 139-168. https://doi.org/10.1016/j.gr.2019.03.009

Michel, L. A., Tabor, N. J., Montañez, I. P., Schmitz, M. D. Davydov, V. I., 2015a. Chronostratigraphy and paleoclimatology of the Lodève Basin, France: Evidence for a pan-tropical aridification event across the Carboniferous–Permian boundary. Palaeogeography, Palaeoclimatology, Palaeoecology 430, 118-131. https://doi.org/10.1016/j.palaeo.2015.03.020

Michel, L. A., Tabor, N. J., Montañez, I. P., Schmitz, M. D. Davydov, V. I., 2015b. Reply to the comment on "Chronostratigraphy and paleoclimatology of the Lodève Basin, France: Evidence for a pan-tropical aridification event across the Carboniferous-Permian boundary" by Michel et al., (2015). Palaeogeography, Palaeoclimatology, Palaeoecology 430, 118-131. https://doi.org/10.1016/j.palaeo.2015.03.020

Modesto, S. P., Reisz, R. R., 1992. Restudy of Permo-Carboniferous synapsid *Edaphosaurus novomexicanus* Williston and Case, the oldest known herbivorous amniote. Canadian Journal of Earth Sciences 29, 2653-2662. https://doi.org/10.1139/e92-210

Núñez Demarco, P., Meneghel, M., Laurin, M., Piñeiro, G., 2018. Was *Mesosaurus* a fully aquatic reptile? Frontiers in Ecology and Evolution, 6. https://doi.org/10.3389/fevo.2018.00109

Odin, B., 1986. Les formations permiennes, Autunien supérieur à Thuringien, du «bassin» de Lodève (Hérault, France). PhD thesis, Université Aix-Marseille III., 392 pp.

Odin, B., Conrad, G., Stapf, K., 1987. Les aspects de la sédimentation permienne continentale et détritique à Lodève (Hérault, France) : le rôle de la tectonique synsédimentaire et de la subsidence dans la dynamique du bassin. Géologie Alpine 13, 39-46.

Olroyd, S.L., Sidor, C. A., 2017. A review of the Guadalupian (middle Permian) global tetrapod fossil record. Earth Science Reviews 171, 583-597. https://doi.org/10.1016/j.earscirev.2017.07.001

Olson, E. C., 1954. Fauna of the Vale and Choza: 7. Pelycosauria: Family Caseidae. Fieldiana 17(10), 193-204. https://doi.org/10.5962/bhl.title.3457

Olson, E. C., 1962. Late Permian terrestrial vertebrates, U.S.A. and U.S.S.R. American Philosophical Society Transaction, new series 52, 1-224. https://doi.org/10.2307/1005904

Olson, E. C., 1968. The family Caseidae. Fieldiana: Geology 17, 225-349. https://doi.org/10.2307/583246

Olson, E. C., Barghusen, H., 1962. Permian Vertebrates from Oklahoma and Texas. Part I.-Vertebrates from the Flowerpot Formation, Permian of Oklahoma. - Oklahoma Geological Survey, Circular 59, 1-48.

Olson, E. C., Beerbower, J.R., Jr., 1953. The San Angelo Formation, Permian of Texas, and its vertebrates. Journal of Geology 61, 381-423. https://doi.org/10.1086/626109

Osborn, H. F., 1903. The reptilian subclasses Diapsida and Synapsida and the early history of the Diaptosauria. Memoirs of the American Museum of Natural History 1, 449-507.

Pardo, J. D., Small, B. J., Milner, A. R., Huttenlocker, A. K., 2019. Carboniferous–Permian climate change constrained early land vertebrate radiations. Nature Ecology & Evolution 3, 200-206. https://doi.org/10.1038/s41559-018-0776-z

Pellenard, P., Gand, G., Schmitz, M., Galtier, J., Broutin, B., Stéyer, J.S., 2017. High-precision U-Pb zircon ages for explosive volcanism calibrating the NW European continental Autunian stratotype. Gondwana Research 51, 118-136. https://doi.org/10.1016/j.gr.2017.07.014

Pfeifer, L. S., Soreghan, G. S., Pochat, S., Van Den Driessche, J., Thomson, S.N. 2016. Permian exhumation of the Montagne Noire core complex recorded in the Graissessac-Lodève Basin, France. Basin Research 30 (Suppl.1), 1-14. https://doi.org/10.1111/bre.12197

Pfeifer, L., Soreghan, G. S., Pochat, S., Van Den Driessche, J., 2020. Loess in eastern equatorial Pangea archives a dusty atmosphere and possible upland glaciation. The Geological Society of America Bulletin 133, 379-392. https://doi.org/10.1130/B35590.1

Pochat, S., Van Den Driessche, J., 2011. Filling sequence in Late Paleozoic continental basins: a chimera of climate change? A new light shed given by the Graissessac–Lodève Basin (SE France). Palaeogeography, Palaeoclimatology, Palaeoecology 302, 170-186. https://doi.org/10.1016/j.palaeo.2011.01.006

Pochat, S., Van Den Driessche, J., 2015. Comment on "Chronostratigraphy and paleoclimatology of the Lodève Basin, France: evidence for a pan-tropical aridification event across the Carboniferous–Permian boundary." by Michel, L. A., Tabor, N. J., Montanez, I. P., Schmitz, M. D., Davydov, V. I., 2015. Palaeogeography, Palaeoclimatology, Palaeoecology 430, 118-131. https://doi.org/10.1016/j.palaeo.2015.03.020

Reisz, R. R., 1981. A diapsid reptile from the Pennsylvanian of Kansas.

University of Kansas. Museum of Natural History, Special Publication 7, 1-74. https://doi.org/10.5962/bhl.title.8440

Reisz, R. R., 1986. Pelycosauria. Handbuch der Paläoherpetologie, 17A, 102 pp. Gustav Fischer Verlag, Stuttgart.

Reisz, R. R., 2005. *Oromycter*, a new caseid from the Lower Permian of Oklahoma. Journal of

Vertebrate Paleontology 25(4), 905-910. https://doi.org/10.1671/0272-4634(2005)025[0905:OANCFT]2.0.CO;2

Reisz, R. R., Maddin, H. C., Fröbisch, J., Falconnet, J., 2011. A new large caseid from the Permian of Rodez (France), including a reappraisal of "*Casea*" *rutena*. Geodiversitas 33, 227-246. https://doi.org/10.5252/g2011n2a2

Reisz, R. R., 2019. A small caseid synapsid, *Arisierpeton simplex* gen. et sp. nov., from the early Permian of Oklahoma, with a discussion of synapsid diversity at the classic Richards Spur locality. PeerJ 7: e6615. https://doi.org/10.7717/peerj.6615

Reisz, R. R., Fröbisch, J., 2014. The Oldest Caseid Synapsid from the Late Pennsylvanian of Kansas, and the Evolution of Herbivory in Terrestrial Vertebrates. PLoS ONE 9(4), e94518. https://doi.org/10.1371/journal.pone.0094518

Ricqlès, A. de, 1974. Recherches paléohistologiques sur les os longs des tétrapodes. IV: Éothériodontes et pélycosaures. Annales de Paléontologie (Vertébrés) 60, 1-39.

Rolando, J. P., Doubinger, J., Bourges, P., Legrand, X., 1988. Identification de l'Autunien supérieur, du Saxonien et du Thuringien inférieur dans le bassin de Saint-Affrique (Aveyron, France). Corrélations séquentielles et chronostratigraphiques avec le bassin de Lodève (Hérault) et de Rodez (Aveyron). Comptes Rendus hebdomadaires des Séances de la l'Académie des Sciences, Série II 307 (2), 1459-1464.

Romano, M., Nicosia, U., 2014. *Alierasaurus ronchii*, gen. et sp. nov., a caseid from the Permian of Sardinia, Italy. Journal of Vertebrate Paleontology 34, 900-913. https://doi.org/10.1080/02724634.2014.837056

Romano, M., Nicosia. U., 2015. Cladistic analysis of Caseidae (Caseasauria, Synapsida): using the gap-weighting method to include taxa based on incomplete specimens. Palaeontology, 1-22. https://doi.org/10.1111/pala.12197

Romano, M., Ronchi, A., Maganuco, S., Nicosia, U., 2017a. New material of *Alierasaurus ronchii* (Synapsida, Caseidae) from the Permian of Sardinia (Italy), and its phylogenetic affinities. Palaeontologia Electronica 20.2.26A, 1-27. https://doi.org/10.26879/684

Romano, M., Brocklehurst, N., Fröbisch, J., 2017b. The postcranial skeleton of *Ennatosaurus tecton* (Synapsida, Caseidae). Journal of Systematic Palaeontology 16 (13), 1097-1122. https://doi.org/10.1080/14772019.2017.1367729

Romano, M., Citton, P., Nicosia, U., 2015. Corroborating trackmaker identification through footprint functional analysis: the case study of *Ichniotherium* and *Dimetropus*. Lethaia 49 (1), 102-116. https://doi.org/10.1111/let.12136

Romano, M., Citton, P., Maganuco, S., Sacchi, E., Caratelli, M., Ronchi, A., Nicosia U., 2018. New basal synapsid discovery at the Permian outcrop of Torrre del Porticciolo (Alghero, Italy). Geological Journal, 1-13, Wiley.

Romer, A. S., 1922. The locomotor apparatus of certain primitive and mammal-like reptiles. Bulletin of the American Museum of Natural History 46, 517-606.

Romer, A. S., Price. L. I., 1940. Review of the Pelycosauria. Geological Society of America Special Papers 28, 1-538. https://doi.org/10.1130/SPE28-p1

Romer, A. S., Parson, T.S., 1983. Vergleichende Anatomie der Wirbeltiere. 1-624, Paul Parey, Hamburg, Berlin.

Ronchi, A., Sacchi, E., Romano, M. Nicosia, U., 2011. A huge caseid pelycosaur from north-western Sardinia and its bearing on European Permian stratigraphy and palaeobiogeography. Acta Palaeontologica Polonica 56, 723-738. https://doi.org/10.4202/app.2010.0087

Roscher, M., Schneider, J. W., 2006. Early Pennsylvanian to Late Permian climatic development of central Europe in a regional and global context. In: Lucas, S. G., Cassinis, G., Schneider, J. W. (eds.), Non-Marine Permian Biostratigraphy and Biochronology. Geological Society of London, Special Publications 265 (1), 95-136. https://doi.org/10.1144/GSL.SP.2006.265.01.05

Sacchi, E., Cifelli, R., Citton, P., Nicosia, U., Romano, M., 2014. *Dimetropus osageorum* n. isp. from the Early Permian of Oklahoma (USA): A Trace and its Trackmaker. Ichnos 21, 3, 175-192. https://doi.org/10.1080/10420940.2014.933070

Schiller, W., 2002. Magnetostratigraphie im oberen Perm des Lodève Beckens, Hérault, Südfrankreich. Diploma thesis, dep. of Geo- und Environmental-sciences, section Geophysics, Ludwig-Maximilians Universität München, 104 pp.

Schneider, J. W., Körner, F., Roscher, M., Kroner, U., 2006. Permian climate development in the northern peri-Tethys area The Lodève Basin, French Massif Central, compared in a European and global context. Palaeogeography, Palaeoclimatology, Palaeoecology 240, 161-183.

Schneider, J. W., Rössler, R., Gaitzsch, B., 1995. Time lines of the Late Variscan volcanism - a holostratigraphic synthesis. Zentralblatt für Geologie und Paläontologie, Teil I, 5/6, 477-490. https://doi.org/10.1016/j.palaeo.2006.03.057

Schneider, J. W., Lucas, S. G., Werneburg, R., Rößler, R., 2010. Euramerican Late Pennsylvanian / Early Permian arthropleurid/tetrapod associations – implications for the habitat and paleobiology of the largest terrestrial arthropod. In Lucas, S. G., Schneider, J. W. Spielmann, J. A., eds., Carboniferous-Permian transition in Canõn del Cobre, northern New Mexico, New Mexico Museum of Natural History and Science, Bulletin 49, 49-70.

Schneider, J. W., Voigt, S., Lucas, S. G. Rößler, R., 2015. Late Palaeozoic wet red beds – dry red beds: How to distinguish them. XVIII International Congress on the Carboniferous and Permian, August 11–15, 2015, Kazan, Russia, Abstracts Volume, 169.

Schneider, J. W., Lucas, S. G., Scholze, F., Voigt, S., Marchetti, L., Klein, H., Opluštil, S., Werneburg, R., Golubev, V. K., Barrick, J. E., Nemyrovska, T., Ronchi, A., Day, M. O., Silantiev, V. V., Rößler, R., Saber, H., Linnemann, U., Zharinova, V., Shen, S. Z., 2020. Late Paleozoic-early Mesozoic continental biostratigraphy – Links to the Standard Global Chronostratigraphic Scale. Paleoworld 531, 186-238. https://doi.org/10.1016/j.palwor.2019.09.001

Sennikov, A. G., Golubev, V. K., 2017. Sequence of Permian tetrapod faunas of Eastern Europe and the Permian–Triassic ecological crisis. Paleontological Journal 51, 600-611. https://doi.org/10.1134/S0031030117060077

Shelton, C. D., Sander. P. M., 2013. Comparison of postcranial bone histology of carnivorous and herbivorous pelycosaur groups. The Second International Symposium on Paleohistology, Bozeman, July 18-20, 2013, 2, 73.

Sigogneau-Russell, D., Russell, D. E., 1974. Étude du premier caséidé (Reptilia, Pelycosauria) d'Europe occidentale. Bulletin du Muséum national d'histoire naturelle, 3e série, Sciences de la Terre 230, 145-216.

Silva, R. C., Sedor, F. A., Fernandes, A. C. S., 2012. Fossil footprints from the Late Permian of Brazil: An example of hidden biodiversity. J. South Am. Earth Sci. 38, 31-43. https://doi.org/10.1016/j.jsames.2012.05.001

Similowski, T., 2017. Early evolution of the diaphragm in caseids: the diaphragm as an adaptation to mixed aquatic-terrestrial lifestyle. Respiratory Physiology and Neurobiology 243, 115-116. https://doi.org/10.1016/j.resp.2017.03.011

Spindler, F., 2019. Re-evaluation of an early sphenacodontian synapsid from the Lower Permian of England. Earth and Environmental Science Transactions of the Royal Society of Edinburgh, 1-11. https://doi.org/10.1017/S175569101900015X

Spindler, F., Falconnet, J., Fröbisch, J. 2016. *Callibrachion* and *Datheosaurus*, two historical and previously mistaken basal caseasaurian synapsids from Europe. Acta Palaeontologica Polonica 61 (3), 597-616. https://doi.org/10.4202/app.00221.2015

Spindler, F., Werneburg, R., Schneider, J. W., 2019. A new mesenosaurine from the lower Permian of Germany and the postcrania of *Mesenosaurus*: implications for early amniote comparative osteology. PalZ 93, 303-344. https://doi.org/10.1007/s12542-018-0439-z

Steyer, J.-S. 2000. Are European Paleozoic amphibians good stratigraphical markers? Bulletin de la Société Géologique de France 171(1), 127-135.

Steyer, J.-S., Escuillié, F., Pouillon, J.-M., Broutin, J., Debriette, P., Freytet, P., Gand, G., Poplin, C., Rage, J.-C., Rival, J., Schneider, J. W., Stamberg, S., Werneburg, R., Cuny, G., 2000. New data on the flora and fauna from the ?uppermost Carboniferous-Lower Permian of Buxières-les-Mines, Bourbon-l'Archambault Basin (Allier, France). A preliminary report. Bulletin de la Société Géologique de France 171(2), 239-249. https://doi.org/10.2113/171.2.239

Steyer, J.-S., Laurin, M., Castanet, J., Ricqlès A. de, 2004. First histological and skeletochronological data on temnospondyl growth: palaeoecological and palaeoclimatological implications. Palaeogeography, Palaeoclimatology, Palaeoecology 206, 193-201. https://doi.org/10.1016/j.palaeo.2004.01.003

Steyer J. S., Peecook B. R., Arbez T., Nesbitt S. J., Tolan S., Stocker M. R, Smith R. M. H., Angielczyk K., Sidor C. A., 2021. New data on the Triassic temnospondyls from the Karoo rift basins of Tanzania and Zambia. Geodiversitas 43, 365-376. https://doi.org/10.5252/geodiversitas2021v43a12

Stovall, J. W., Price, L. I., Romer, A. S., 1966. The postcranial skeleton of the giant Permian pelycosaur *Cotylorhynchus romeri*. Bulletin of the Museum of Comparative Zoology 135, 1-30.

Sumida, S. S., Pelletier, V., Berman, D. S., 2014. New information on the basal pelycosaurian-grade synapsid *Oedaleops*; 7–23, In: Kammerer, C. F., Angielczyk, K. D., Fröbisch, J. (eds.), Early evolutionary history of the Synapsida. Vertebrate Paleobiology and Paleoanthropology Series, Springer, Dordrecht. https://doi.org/10.1007/978-94-007-6841-3_2

Swoford, D. L., 2001. PAUP*: Phylogenetic Analysis Using Parsimony. Sunderland, MA, Sinauer Associates.

Vetter, P., 1968. Géologie et paléontologie des bassins houillers de Decazeville, de Figeac et du Détroit de Rodez. Tome 2. Études paléontologiques. Houillères du bassin d'Aquitaine, Albi, 196 pp.

Vickaryous, M. K., Hall, B. K., 2006. Homology of the reptilian coracoid and a reappraisal of the evolution and development of the amniote pectoral apparatus. Journal of Anatomy 208, 263-285. https://doi.org/10.1111/j.1469-7580.2006.00542.x

Waskow, K., Mateus, O., 2017. Dorsal rib histology of dinosaurs and a crocodylomorph from western Portugal: Skeletochronological implications on age determination and life history traits. Comptes Rendus Palevol 16, 425-439. https://doi.org/10.1016/j.crpv.2017.01.003

Werneburg, R., Steyer, J.-S., Sommer, G., Gand, G., Schneider, J. W., Vianey-Liaud, M., 2007. The earliest tupilakosaurid amphibian with diplospondylous vertebrae from the Late Permian of southern France. Journal of Vertebrate Paleontology, 27(1), 26-30. https://doi.org/10.1671/0272-4634(2007)27[26:TETAWD]2.0.CO;2

Werneburg, R., Štamberg, S., Steyer J.-S., 2020. A new stereospondylomorph from the Lower Permian of the Czech Krkonose Piedmont Basin and the redescription of *Intasuchus silvicola* from the Lower Permian of Russia (Temnospondyli, Amphibia). Fossil Imprint 76 (2), 217-242, Prague. https://doi.org/10.37520/fi.2020.019

Williston, S. W., 1910. New Permian reptiles: rhachitomous vertebrae. Journal of Geology 18, 585-600. https://doi.org/10.1086/621786

Williston, S. W., 1911a. American Permian Vertebrates. University of Chicago Press, Chicago, 145 pp. https://doi.org/10.5962/bhl.title.54741

Williston, S. W., 1911b. A new family of reptiles from the Permian of New Mexico. American Journal of Science, Fourth Series 31, 378-398. https://doi.org/10.2475/ajs.s4-31.185.378

Williston, S. W., 1911c. Permian reptiles. Science 33, 631-632. https://doi.org/10.1126/science.33.851.631

Williston, S. W., 1912. Primitive reptiles. Journal of Morphology 23, 637-666. https://doi.org/10.1002/jmor.1050230404

Williston, S. W., Case, E. C., 1913. Description of a nearly complete skeleton of *Ophiacodon* Marsh. Carnegie Institution of Washington Publication 181, 37-59.

Ziegler, A. M., 1990. Phytogeographic patterns and continental configurations during the Permian Period. In: McKerrow, W. S., Scotese, C. R. (eds.) Palaeozoic Palaeogeography and Biogeography. Geological Society, London, Memoir 12, 363-379. https://doi.org/10.1144/GSL.MEM.1990.012.01.35